UNIVERSITÀ DEGLI STUDI DI MILANO

FACOLTÀ DI SCIENZE E TECNOLOGIE

Corso di Laurea triennale in Fisica

DIPARTIMENTO DI FISICA

''ALDO PONTREMOLI''

Resummation of QCD large infrared logarithms for Thrust distribution in Electron-Positron Annihilation

Supervisor: Giancarlo Ferrera

Co-supervisor: Wan-Li Ju

Author:

Jiahao Miao

Matr. Nr. 986136

ACADEMIC YEAR 2023-2024

Abstract

This thesis focuses on the Thrust event-shape distribution in electron-positron annihilation, a classical precision collider observable which can be measured very accurately and provides an ideal proving ground for testing our understanding of strong interactions. Our particular focus lies on the back-to-back region, where we employ all-order resummation techniques to address logarithmically enhanced contributions within QCD perturbation theory. Our calculations extend the pioneering work of Catani et al [1] in this field, aiming to achieve next-to-next-to-next-to-leading logarithmic (N^3LL) accuracy and then consistently match with the known fixed-order results up to next-to-next-to-leading order (NNLO).

Our approach involves calculating the resummation coefficients in Laplace space where natural exponentiation of the logarithmic contributions occurs, perform the inverse Laplace transform analytically up to N^4LL accuracy to obtain the resummed distribution in thrust space and then match the resummed expression to the fixed-order NNLO calculations at large values of τ using the R-matching scheme. We compare each step with experimental results, even though the experimental data are measured on hadron level while our prediction is calculated at parton level. Non-perturbative effects affecting the peak Thrust distribution are not included; a phenomenological model describing hadronization effects would enhance the agreement with experimental data, aiding in the extraction of the strong coupling constant α_s. The results presented in this thesis are a step towards achieving a more precise theoretical prediction for the Thrust distribution in e^+e^- annihilation and a more precise extraction of the strong coupling constant α_s, which is essential for the precision tests of the Standard Model and the search for new physics at the LHC.

Contents

Chapter 1

Introduction

In this thesis, we focus on a specific aspect of theoretical high-energy physics and collider physics: the resummation of QCD large logarithms for the Thrust event-shape distribution in electron-positron (e^+e^-) collisions.

High energy physics, often synonymous of particle physics, and collider physics are crucial because they explores the most basic constituents of matter and helps us understand three of the four fundamental forces of nature: the strong, weak, and electromagnetic forces. Collider experiments test the predictions of the Standard Model of particle physics, the most successful theory of particle and interactions to date. Through high precision theoretical prediction and experimental measurements, it is possible to test the limits of the Standard Model, search for new physics beyond it and gain a better understanding of the fundamental forces.

One key parameter of the Standard Model is the strong coupling constant α_s, which measures the strength of the strong force. Precise measurements of α_s is crucial for accurate predictions in Quantum Chromodynamics (QCD), the theory of the strong force, as all calculations in QCD depends on it.

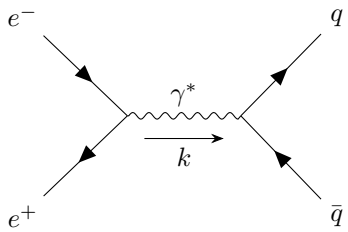

Figure 1: Tree-level Feynman diagram of electron-positron annihilation producing a virtual photon that decays into a quark-antiquark pair.

One example of a process studied in high-energy physics is electron-positron annihilation, as shown in fig. 1. Electron-positron annihilation has been extensively studied, particularly during the operation of the Large Electron-Positron Collider (LEP) at CERN from 1989 to 2000. LEP provided an optimal environment for precision studies in high-energy physics. Unlike hadron colliders, which are complicated by strongly interacting initial states, LEP enabled extremely accurate measurements of Standard Model quantities such as the Z-boson mass. These results tightly constrain beyond-the-Standard Model physics. Precision data from LEP is also used in Quantum Chromodynamics (QCD) studies to determine the strong coupling constant, α_s.

When high-energy particles collide, quarks and gluons are produced in the interactions. Due to a phenomenon called *color confinement*, these quarks and gluons cannot exist freely and thus hadronize, forming jets of particles. A jet is a collimated stream of hadrons (such as protons, pions, and kaons) that originates from the hadronization of a single quark or gluon.

In electron-positron annihilation, the electron and positron interact electromagnetically through the exchange of a virtual photon, which mediates the electromagnetic interaction, virtual refers to the fact that the photon is off-shell, meaning it does not satisfy the mass-shell condition $E = pc$ for a real photon with mass $m = 0$. This virtual photon can then decay into a quark-antiquark pair in another electromagnetic process, conserving the electrical and color charge of the initial state, as well as the four-momentum.

The quark-antiquark pair produced interacts through both the strong force and the electromagnetic force, as they possess both electric charge and color charge. They can radiate gluons via the strong force and photons via the electromagnetic force. This radiation process continues, creating a cascade of particles known as a *parton shower*. The parton shower eventually hadronizes into jets when the particles are no longer energetic enough to radiate further, and the final state particles can be revealed by the detectors, with their momenta measured to study the underlying processes.

As is typical in physics, the equations governing these interactions are highly complex so that finding exact solutions is nearly impossible. Therefore, functions of interest are often expanded perturbatively, meaning they are expressed as a power series in a small parameter.

For the electromagnetic interaction, this small parameter is the fine structure constant (or electromagnetic coupling constant) $\alpha_{em} \sim \frac{1}{137}$.

For interactions involving the strong force, it is natural to use the aforementioned strong coupling constant, α_s. This key parameter becomes small at high energies (or equivalently, short distances) due to the phenomen known as *asymptotic freedom* of QCD.

Extraction of α_s can be achieved from comparing precise QCD prediction such as the thrust event-shape distribution against experimental data.

1.1 Thrust variable

Thrust T is defined as:

$$T = \max_{\vec{n}} \frac{\sum_i |\vec{p}_i \cdot \vec{n}|}{\sum_i |\vec{p}_i|} \stackrel{\text{def}}{=} 1 - \tau, \tag{1}$$

where the sum is over all final state particles and $\vec{n}$ is a unit vector that points in the direction which maximizes the magnitude of T.

In practice, the sum may be carried over the detected particles only. The thrust distribution represents the probability of observing a given value of T in e^+e^- annihilation, *i.e* the probability of observing a configuration of momenta in the final state whose thrust calculated with eq. (1) is T.

It can be seen from this definition that the thrust is an infrared and collinear safe quantity, that is, it is insensitive to the emission of zero momentum particles and to the splitting of one particle into two collinear ones.

In fact, contribution from soft particles with $\vec{p_i} \to 0$ drop out, and collinear splitting of a parton with momenta $\vec{p}$ into two partons of momenta $(1-\lambda)\vec{p}$ and $\lambda\vec{p}$ does not change the thrust:

$$|(1-\lambda)\vec{p_i} \cdot \vec{n}| + |\lambda\vec{p_i} \cdot \vec{n}| = (1-\lambda)|\vec{p_i} \cdot \vec{n}| + \lambda|\vec{p_i} \cdot \vec{n}| = |\vec{p_i} \cdot \vec{n}|,$$
$$|(1-\lambda)\vec{p_i}| + |\lambda\vec{p_i}| = (1-\lambda)|\vec{p_i}| + \lambda|\vec{p_i}| = |\vec{p_i}|.$$

Formally, infrared-safe observables are the one which do not distinguish between (n+1)-partons and n-partons in the soft/collinear limit, *i.e*, are insensitive to what happens at long-distance (non-perturbative) scales.

Infrared safe observables are important in the context of perturbative QCD, because they allow for a meaningful comparison between theory and experiment.

A significant challenge in achieving precise theoretical predictions from QCD lies in the complexity of the relevant fixed-order calculations. While the next-to-leading-order (NLO) results for event shapes have been known since 1980 [2], the relevant next-to-next-leading order (NNLO) calculations were completed only in 2007 [3].

From fig. 2, it is evident that the NNLO prediction agrees well with the data, except in the region near $T = 0.5$ (spherical final state) and $T = 1$ (pencil-like final state).

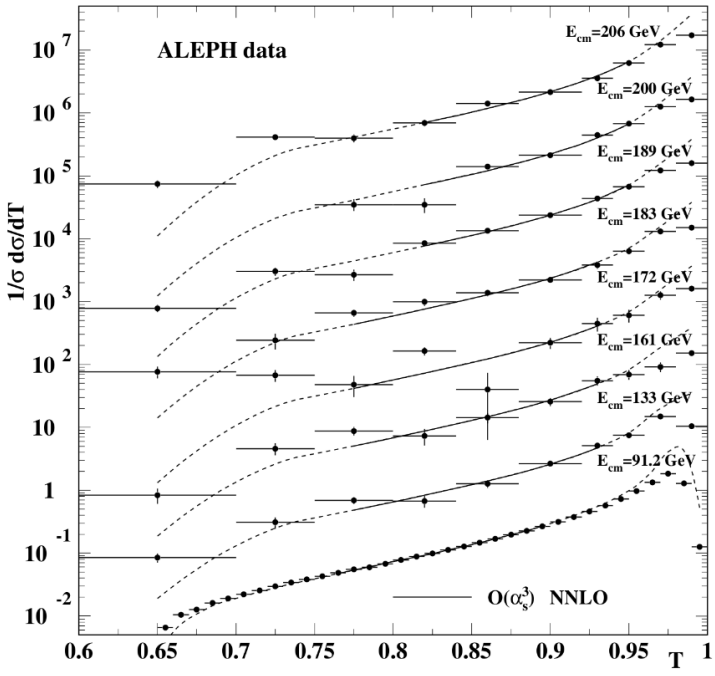

Figure 2: Distributions measured by ALEPH, after correction for backgrounds and detector effects of thrust at energies between 91.2 and 206 GeV together with NNLO QCD predictions. The error bars correspond to statistical uncertainties. The plotted distributions are scaled by arbitrary factors for presentation. Image taken from [4].

This is because thrust distribution for $T \simeq 1$ is dominated by two-jet configurations, *i.e.* the final state particles consist of two partons emitted back-to-back like fig. 1. In contrast, the tail of the distribution near $T = 0.5$ is dominated by multijet final states.

To improve the agreement between theory and experiment, we'll need higher fixed order calculations (challenging task), but this will only improve the agreement in the tail region, to also improve the agreement in the dijet region we need to use resummation techniques.

1.1.1 Thrust distribution

The cross section is defined as the probability of observing a final state with a given thrust value τ and Thrust distribution is expressed in three ways: as a differential cross section, as a cumulative distribution and as its Laplace transform.

$$\sigma(\tau) = \frac{1}{\sigma_0}\frac{\mathrm{d}\sigma}{\mathrm{d}\tau}, \tag{2}$$

$$R_T(\tau) = \int_0^\tau \mathrm{d}\tau' \, \frac{1}{\sigma_0}\frac{\mathrm{d}\sigma}{\mathrm{d}\tau'}, \tag{3}$$

$$\tilde{\sigma}(\nu) = \int_0^\infty \mathrm{d}\tau \, e^{-\nu\tau}\frac{\mathrm{d}\sigma}{\mathrm{d}\tau}. \tag{4}$$

It can be seen that a two-particle final state has fixed $T = 1$ because of momentum conservation, in fact at the zeroth order of the fixed order this corresponds to a delta distribution for the differential cross section, as shown in eq. (7), consequently the thrust distribution receives its first non-trivial contribution from three-particle final states.

The upper limit of τ or lower limit on T depends on the number of final-state partons. Knowing the lower limit of T is important because it allows us to normalize correctly the fixed-order cross section. Neglecting masses, for three particles, $\tau_{max} = 1/3$, corresponding to a symmetric trigonal-planar configuration (Figure 3). For four particles the minimum thrust corresponds to final-state momenta forming the vertices of a regular tetrahedron (Figure 4), each making an angle $\cos^{-1}(1/\sqrt{3})$ with respect to the thrust axis. Thus $\tau_{max} = 1 - \frac{1}{\sqrt{3}} \approx 0.42265$ in this case. For more than four particles, as far as we know there's no known value of τ_{max} in literature, it's only known that τ_{max} approaches $1/2$ from below as the number of particles increases. For $N = 5$ the maximum value of τ was previously estimated to be $\tau_{max} = 0.4275$ by checking at what bin the cross sections is 0 for NNLO Monte Carlo (MC) calculation of the fixed-order cross sections [5]. We also have another estimate of τ_{max} for $N = 5$ from the tables in [6] of NNLO thrust cross section whose bins end at $\tau = 0.445$. The numerical NNLO calculation of the thrust distribution can only give an estimate to the upper limit of τ, limited by the number of events used in the MC calculation, the smallness of the cross section in the kimematical limit and some small, but non zero, resolution parameters which are always present in numerical calculation at higher-orders

We have used a stochastic optimization algorithm to find the lower limit of T for $N = 5$ and found a configuration which gives $\tau_{max} = 0.4539536$ for $N = 5$ (Figure 5).

Finding the lower limit of T is non trivial as it involves a double optimization problem. Given a configuration of N parton momenta one needs to find the direction of the thrust axis which maximizes the value of eq. (1) and then find the minimum value of T by varying the momenta of the partons and repeating the process of finding the thrust axis.

A quick way to calculate the thrust axis $\vec{n}$ for small number N of partons in the final state is described in Appendix A of [6], where the optimization problem of finding the unit vector which maximizes a certain

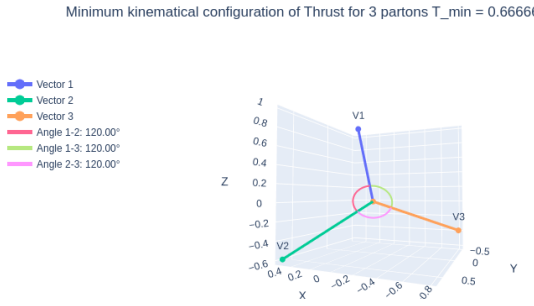

Figure 3: Configuration of final state momenta of three partons that maximizes τ, forming a trigonal-planar configuration.

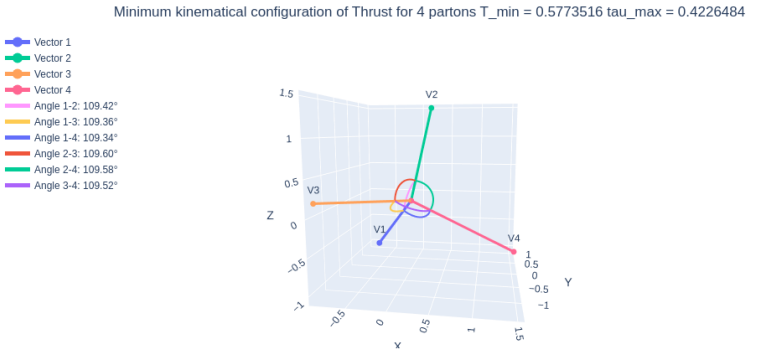

Figure 4: Configuration of final state momenta of four partons that maximizes τ, forming a tetrahedral configuration.

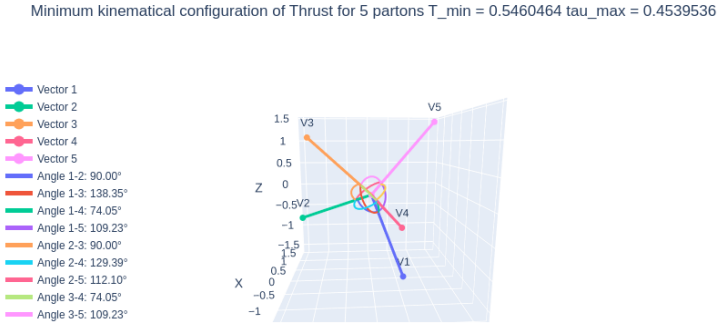

Figure 5: Configuration of final state momenta of five partons that maximizes τ.

Table 1: The maximum kinematically allowed value of τ as a function of the number of partons N in the final state. They should be interpreted as lower limits to the maximum value of τ since a stochastic algorithm is not guaranteed to find the absolute minimum.

N	3	4	5	6	7	8
τ_{max}	$\frac{1}{3}$	1 - $\frac{1}{\sqrt{3}}$	0.4539536	0.4616661	0.4716270	0.4737373
N	9	10	11	12	13	14
τ_{max}	0.4782286	0.4802864	0.4816904	0.4840608	0.4836307	0.4842613

configuration of final state partons is reduced to a simple loop over $2^{N-1}-1$ configurations of signs $\{s_1,\ldots,s_N\}$ which satisfies the constraint

$$\vec{p}_j\cdot\vec{n} = s_j|\vec{p}_j\cdot\vec{n}|, \tag{5}$$

where $\vec{p}_j$ is the momenta of the j-th parton.

To see why the Thrust axis can be found by this method, suppose the constraint eq. (5) is satisfied. Then the thrust can be written as:

$$T = \max_{\vec{n}}\frac{\sum_j|\vec{p}_j\cdot\vec{n}|}{\sum_j|\vec{p}_j|} = \max_{\vec{n}}\frac{\sum_j s_j\vec{p}_j\cdot\vec{n}}{\sum_j|\vec{p}_j|} = \max_{\vec{n}}\frac{\vec{P}\cdot\vec{n}}{\sum_i|\vec{p}_i|}, \tag{6}$$

where $\vec{P}=\sum_j s_j\vec{p_i}$. It is clear that the thrust axis is the direction of the vector $\vec{n}=\frac{\vec{P}}{|P|}$ and can be found by checking which of the $2^{N-1}-1$ configurations of signs $\{s_1,\ldots,s_N\}$ satisfies the constraint eq. (5) for all $j=1,\cdots,N$ and among them choose the one which maximizes the value of eq. (1). There are in total 2^N configurations of signs $s_1,\cdots,s_N$, but we have to exclude the one where all the signs are equal because it violates momentum conservation, and also thrust is invariant under the transformation $\vec{n}\to-\vec{n}$.

We have implemented this algorithm in C++ to calculate the value of Thrust eq. (1) given a set of N momenta. We then used metaheuristic optimization algorithms (Genetic Algorithm (GA) and Particle Swarm Optimization (PSO)), to find the maximum value of τ (or minimum of T) for a given number N of partons by perturbing repeatedly the initially randomly generated momenta of the partons, always respecting the constraint of momentum conservation, and calculating the thrust for each configuration. The results for the first few N are shown in table 1, then the problem becomes computationally expensive because the evaluation of the thrust scales as $O(2^N)$.

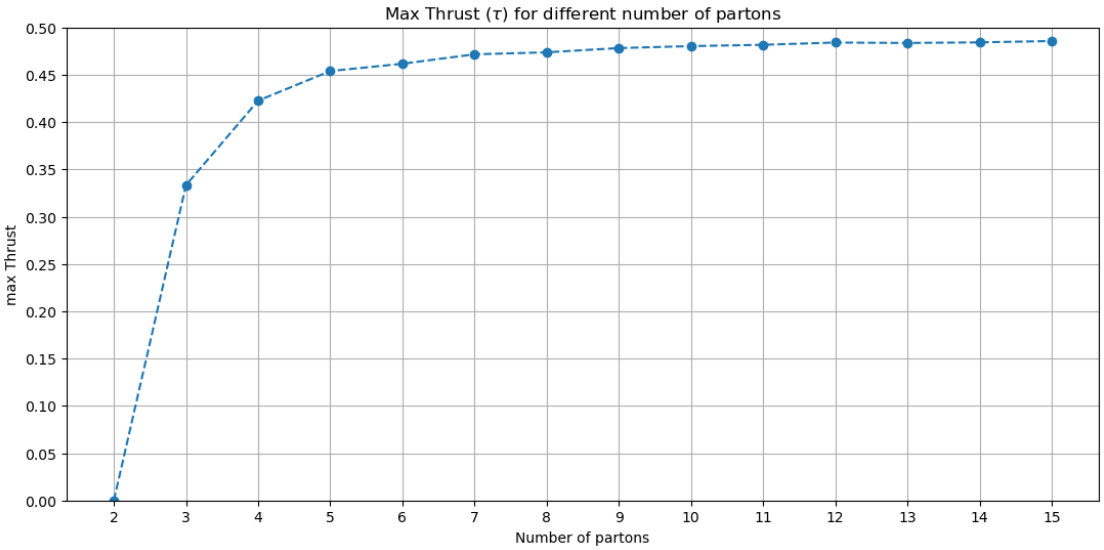

Figure 6: The maximum kinematically allowed value of τ as a function of the number of partons N in the final state. The value of τ_{max} approaches $1/2$ from below as the number of partons increases.

At small values of τ, higher order terms enhanced by powers of $\ln(\tau)$ dominates the thrust distribution. In this kinematical region the real expansion parameter is the large effective coupling $\alpha_s \ln^2(\tau)$ and therefore any finite-order perturbative calculation cannot give an accurate evaluation of the cross section.

For example, at leading order in perturbation theory the thrust distribution has the form:

$$\frac{1}{\sigma_0}\frac{\mathrm{d}\sigma}{\mathrm{d}\tau} = \delta(\tau) + \frac{2\alpha_s}{3\pi}\left[\frac{-4\ln\tau - 3}{\tau} + \dots\right]_+, \tag{7}$$

where σ_0 is the born cross section, the ellipsis denotes terms that are regular as $\tau \to 0$ and the subscript $+$ denotes the plus distribution, which is defined as:

$$\left[\frac{-4\ln\tau - 3}{\tau}\right]_+ = \lim_{\epsilon\to 0}\left[\left(\frac{-4\ln\tau - 3}{\tau}\right)\theta(\tau-\epsilon) + \delta(\tau-\epsilon)\int_1^\tau \mathrm{d}\tau'\left(\frac{-4\ln\tau' - 3}{\tau'}\right)\right]. \tag{8}$$

Upon integration over τ, we obtain the cumulative distribution:

$$\begin{aligned} R_T(\tau) &= \int_0^\tau \mathrm{d}\tau' \frac{1}{\sigma_0}\frac{\mathrm{d}\sigma}{\mathrm{d}\tau'} \\ &= 1 + \frac{2\alpha_s}{3\pi} + \lim_{\epsilon\to 0}\left[\int_\epsilon^\tau \mathrm{d}\tau'\left(\frac{-4\ln\tau' - 3}{\tau'} + \dots\right) + \int_1^\epsilon \mathrm{d}\tau'\left(\frac{-4\ln\tau' - 3}{\tau'} + \dots\right)\right] \\ &= 1 + \frac{2\alpha_s}{3\pi}\left[-2\ln^2\tau - 3\ln\tau + \dots\right]. \end{aligned} \tag{9}$$

Double logarithmic terms of the form $\alpha_s^n \ln^{2n} \tau$ plagues the fixed order expansion in the strong coupling. In the dijet region, higher order terms are as important as lower order ones, necessitating resummation to achieve reliable predictions.

1.1.2 Fixed Order Cross Section

The fixed-order thrust differential distribution has been calculated to leading order analytically and to NLO and NNLO numerically, as mentioned earlier. At a centre-of-mass energy Q and for a renormalization scale μ, the differential cross section takes the form:

$$\frac{1}{\sigma_0}\frac{\mathrm{d}\sigma}{\mathrm{d}\tau}(\tau, Q) = \delta(\tau) + \frac{\alpha_s(\mu)}{2\pi}\frac{\mathrm{d}A}{\mathrm{d}\tau}(\tau) + \left(\frac{\alpha_s(\mu)}{2\pi}\right)^2 \frac{\mathrm{d}B}{\mathrm{d}\tau}\left(\tau, \frac{\mu}{Q}\right) + \left(\frac{\alpha_s(\mu)}{2\pi}\right)^3 \frac{\mathrm{d}C}{\mathrm{d}\tau}\left(\tau, \frac{\mu}{Q}\right) + \mathcal{O}\big(\alpha_s^4\big), \tag{10}$$

where the complete leading order expression for the thrust distribution reads [2]:

$$\frac{\mathrm{d}A}{\mathrm{d}\tau} = \mathrm{C}_F \left(9\tau - \frac{3}{\tau} + \left(-6 + \frac{4}{(1-\tau)\tau}\right)\ln\left(\frac{1-2\tau}{\tau}\right) + 6\right), \tag{11}$$

with $C_F = \frac{4}{3}$ the Casimir of the fundamental representation of SU(3). As mentioned earlier, this expansion becomes unreliable near the dijet limit $\tau \to 0$ due to the presence of large logarithms. Resummation of these terms to all orders in α_s is necessary to obtain a reliable prediction.

The cumulant distribution has the following fixed-order expansion:

$$R_T(\tau) = 1 + A(\tau)\frac{\alpha_s(\mu)}{2\pi} + B(\tau,\mu)\frac{\alpha_s(\mu)}{2\pi}^2 + C(\tau,\mu)\frac{\alpha_s(\mu)}{2\pi}^3 + \mathcal{O}\big(\alpha_s^4\big), \tag{12}$$

the fixed-order coefficient A, B and C can be obtained by integrating the differential cross section eq. (11) to all order and imposing the normalization condition $R(\tau_{max}) = 1$, where τ_{max} is the maximum kinetically allowed value of τ. At leading order ($e^+e^- \to q\bar{q}g$) $\tau_{max} = \frac{1}{3}$, at Next-to-Leading Order is $\tau_{max} = 1 - \frac{1}{\sqrt{3}}$ and from NNLO onwards τ_{max} needs to be estimated numerically table 1.

At leading order we have:

$$\begin{aligned} A(\tau) = \int_0^\tau \mathrm{d}\tau' \frac{\mathrm{d}A}{\mathrm{d}\tau'} = C_F\Big(&\frac{9\tau^2}{2} - 2\ln^2(1-\tau) - 2\ln^2(\tau) + 6\tau(\ln(\tau)+1) \\ &+ 4\ln(1-\tau)\ln(\tau) - 3\ln(\tau) + 3(1-2\tau)\ln(1-2\tau) \\ &- 4\mathrm{Li}_2\left(\frac{\tau}{1-\tau}\right)\Big). \end{aligned} \tag{13}$$

For NLO and NNLO calculations, we use the numerical results from Table 1 in [6], interpolating the data to obtain the fixed-order coefficients B and C.

We plot the fixed-order results for the thrust distribution in fig. 7 and compare it with data from OPAL [7], DELPHI [8], [9], ALEPH [10], [11], L3 [12] experiments at LEP, as well as the SLD experiment [13] at SLAC. The fixed-order predictions show good agreement with the data in the middle region of τ.

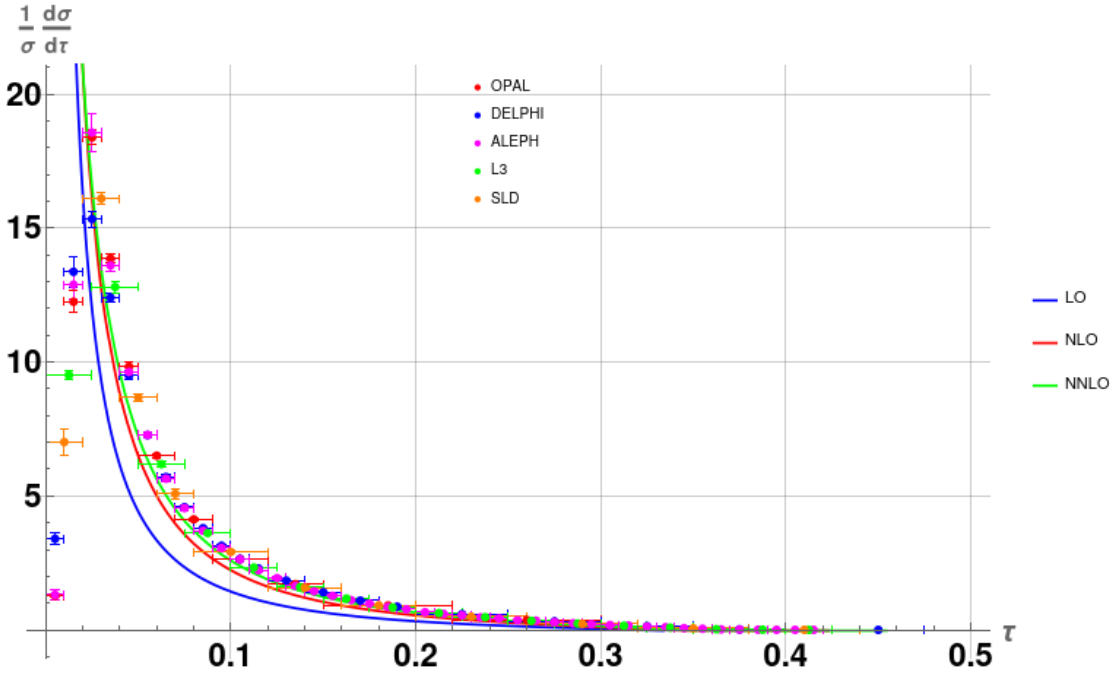

Figure 7: Fixed-order predictions for the thrust distribution at leading order (LO), next-to-leading order (NLO) and next-to-next-to-leading order (NNLO) compared with data from LEP and SLD experiments.

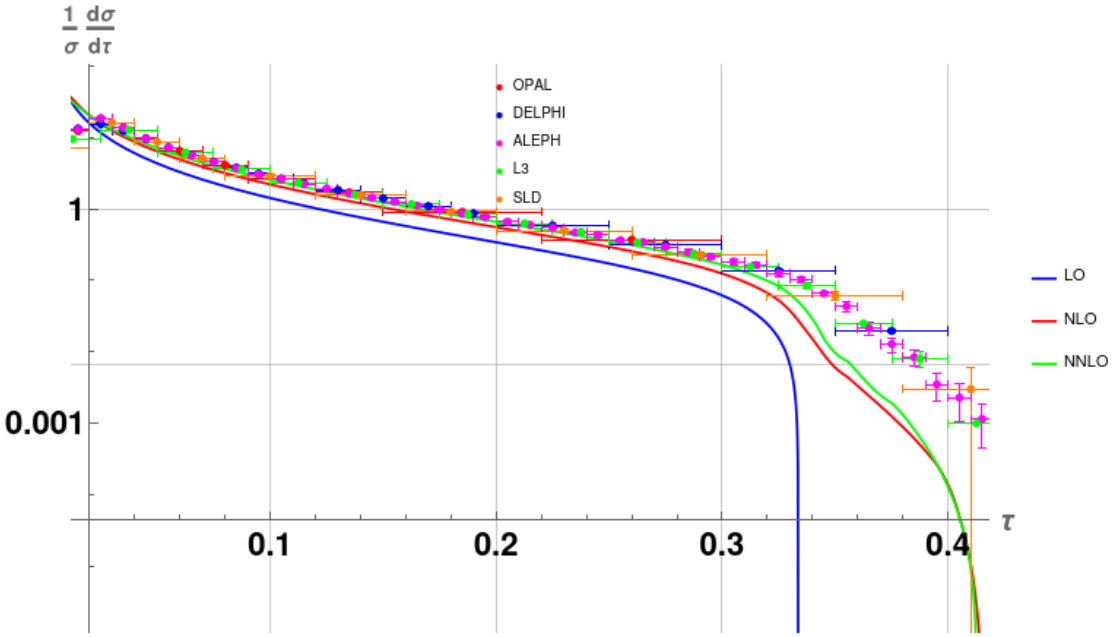

Figure 8: Log plot of the fixed-order predictions for the thrust distribution at leading order (LO), next-to-leading order (NLO) and next-to-next-to-leading order (NNLO) in the tail region.

Chapter 2

Resummation formalism

2.1 Soft-gluon effects in QCD cross sections

Soft-gluon effects and the soft-gluon exponentiation are reviewed in [14] and [15], here we summarize the physical motivation and main ideas of the resummation of soft gluon effects in QCD.

The finite energy resolution in any particle detector implies that the physical cross sections, those experimentally measured, inherently incorporate all contributions from arbitrarily soft particles produced in the final state. In other words, because we lack the ability to precisely resolve the energy of soft particles, we are unable to distinguish between their presence or absence in our calculations (see fig. 9). Consequently, we must account for the sum over all possible final states.

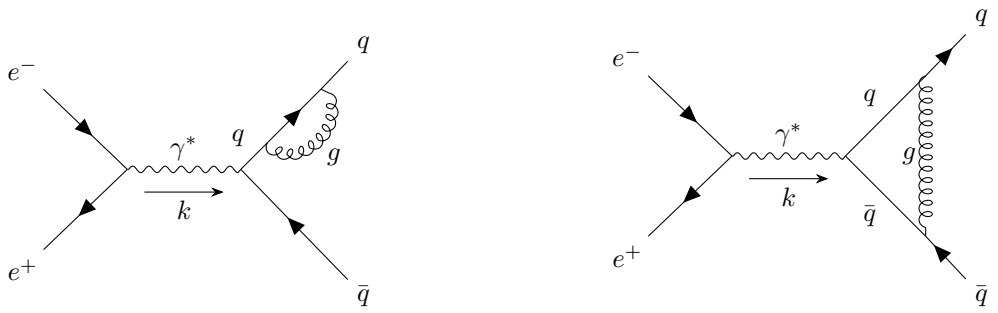

Figure 9: Examples of one loop Feynman diagrams whose final state is identical to the Tree level diagram in fig. 1

This inclusiveness is essential in QCD calculations. Higher order perturbative contributions due to *virtual* gluons are infrared divergent and the divergences are exactly cancelled by radiation of undetected

real gluons. In particular kinematic configurations, *e.g* Thrust in the dijet limit $T \to 1$, real and virtual contributions are highly unbalanced, because the emission of real radiation is inhibited by kinematic constraints, spoiling the cancellation mechanism. As a result, soft gluon contribution to QCD cross sections can still be either large or singular.

In these cases, the cancellation of infrared divergences bequeaths higher order contributions of the form:

$$G_{nm}\alpha_s^n \ln^m \frac{1}{\tau}, \quad \text{with } m \leq 2n, \tag{14}$$

that can become large, $\alpha_s \ln^2 \frac{1}{\tau} \gtrsim 1$, even if the QCD coupling α_s is in the perturbative regime $\alpha_s \ll 1$. These logarithmically enhanced terms in eq. (14) are certainly relevant near the dijet limit $\tau \to 0$. In these cases, the theoretical predictions can be improved by evaluating soft gluon contributions to high orders and possibly resumming to all of them in α_s [5], [16].

The resummation of large logarithms in event shape distributions was described by Catani, Trentadue, Turnock, and Webber (CTTW) [1].

The physical basis for all-order resummation of soft-gluon contributions to QCD cross sections are dynamics and kinematics factorizations. The first factorization follows from gauge invariance and unitarity while the second factorization strongly depends on the observable to be computed.

In the appropriate soft limit, if the phase-space for this observable can be written in a factorized way, then resummation is feasible in the form of a generalized exponentiation [17]. However even when phase-space factorization is achievable, it does not always occur in the space where the physical observable x is defined.

Thrust is a good example of this situation, in fact, the thrust distribution admits a factorization in Laplace space, where the observable is the Laplace transform of the thrust distribution.

2.2 CTTW formalism

According to general theorems [18],[19],[20], the cumulant cross section $R_T(\tau)$ eq. (3) has a power series expansion in $\alpha_s(Q^2)$ of the form:

$$R_T(\tau) = C\big(\alpha_s\big(Q^2\big)\big)\Sigma\big(\tau, \alpha_s\big(Q^2\big)\big) + D\big(\tau, \alpha_s\big(Q^2\big)\big), \tag{15}$$

where

$$C(\alpha_s) = 1 + \sum_{n=1}^{\infty} C_n \bar{\alpha}_s^n, \tag{16}$$

$$\Sigma(\tau, \alpha_s) = \exp\left[\sum_{n=1}^{\infty} \bar{\alpha}_s^n \sum_{m=1}^{2n} G_{nm} \ln^m \frac{1}{\tau}\right], \tag{17}$$

$$D(\tau, \alpha_s) = \sum_{n=1}^{\infty} \bar{\alpha}_s^n D_n(\tau). \tag{18}$$

Here the C_n and G_{nm} are constants and $\bar{\alpha}_s = \frac{\alpha_s}{2\pi}$, while $D_n(\tau)$ is the non-singular part of the fixed-order expansion of $R_T(\tau)$ eq. (12).

Thus at small τ (large thrust) it becomes morst important to resum the series of large logarithms in $\Sigma(\tau, \alpha_s)$. These are normally classified as *leading* logarithms when $n < m \leq 2n$, *next-to-leading* when $m = n$ and *subdominant* logarithms when $m < n$.

The cumulant cross section $R(\tau)$ in the small τ region, in general, can be written in an exponential form as : (neglecting the $D(\tau, \alpha_s)$ term)

$$R_T(\tau) \simeq \left(1 + \sum_{n=1}^{\infty} C_n \bar{\alpha_s}^n\right) \exp\left[L g_1(\lambda) + g_2(\lambda) + g_3(\lambda)\alpha_s + g_4(\lambda)\alpha_s^2 + g_5(\lambda)\alpha_s^3 + \mathcal{O}\left(\alpha_s^4\right)\right], \tag{19}$$

where $L = \ln \frac{1}{\tau}$ and $\lambda = \alpha_s b_0 L$. The function g_1 encodes all the leading logarithms, the function g_2 resums all next-to-leading logarithms and so on.

The last equation gives a better prediction of the thrust distribution in the two-jet region, but fails to describe the multijet region $\tau \to \tau_{max}$, where non-singular pieces of the fixed-order prediction become important. To achieve a reliable description of the observable over a broader kinematical range the two expressions eq. (12) and eq. (15) have to be matched, taking care of double counting of logarithms appearing in both expressions.

Expanding eq. (15) in powers of α_s we have:

$$R(\tau) = 1 + R^{(1)}(\tau)\bar{\alpha}_s + R^{(2)}(\tau)\bar{\alpha}_s^2 + R^{(3)}(\tau)\bar{\alpha}_s^3 + \ldots, \tag{20}$$

where

$$R^{(n)}(\tau) = \sum_{m=1}^{2n} R_{nm} \ln^m \frac{1}{\tau} + D_n(\tau), \tag{21}$$

and the first three terms given by:

$$
\begin{aligned}
R^{(1)}(\tau) &= C_1 + G_{12}\ln^2\frac{1}{\tau} + G_{11}\ln\frac{1}{\tau} + D_1(\tau),\\
R^{(2)}(\tau) &= C_2 + \frac{1}{2}G_{12}^2\ln^4\frac{1}{\tau} + (G_{11}G_{12}+G_{23})\ln^3\frac{1}{\tau}\\
&\quad + \ln^2\frac{1}{\tau}\Big(C_1G_{12} + \frac{G_{11}^2}{2} + G_{22}\Big) + \ln\frac{1}{\tau}\Big(C_1G_{11}+G_{21}\Big)\\
&\quad + D_2(\tau),\\
R^{(3)}(\tau) &= C_3 + \frac{1}{6}G_{12}^3\ln^6\frac{1}{\tau} + \left(\frac{1}{2}G_{11}G_{12}^2 + G_{23}G_{12}\right)\ln^5\frac{1}{\tau}\\
&\quad + \ln^4\frac{1}{\tau}\left(\frac{1}{2}C_1G_{12}^2 + \frac{1}{2}G_{12}G_{11}^2 + G_{23}G_{11} + G_{12}G_{22} + G_{34}\right)\\
&\quad + \ln^3\frac{1}{\tau}\left(C_1G_{12}G_{11} + C_1G_{23} + \frac{G_{11}^3}{6} + G_{22}G_{11} + G_{12}G_{21} + G_{33}\right)\\
&\quad + \ln^2\frac{1}{\tau}\left(\frac{1}{2}C_1G_{11}^2 + C_2G_{12} + C_1G_{22} + G_{21}G_{11} + G_{32}\right)\\
&\quad + \ln\frac{1}{\tau}\left(C_2G_{11} + C_1G_{21} + G_{31}\right) + D_3(\tau).
\end{aligned}
\tag{22}
$$

To see how the resummation works, we can write the contributions to the cross section in a tabular form:

Table 2: Fixed-order and Resummed expansion contributions to the thrust event shape cross section.

		LL	NLL	NNLL	N^{3}LL	N^{4}LL	$\cdots$
LO	$\bar{\alpha}_s^1$	R_{12}	R_{11}	$C_1 + D_1(\tau)$	-	-	-
NLO	$\bar{\alpha}_s^2$	R_{23}	R_{22}	R_{21}	$C_2 + D_2(\tau)$	-	-
NNLO	$\bar{\alpha}_s^3$	R_{34}	R_{33}	R_{32}	R_{31}	$C_3 + D_3(\tau)$	-
N^{3}LO	$\bar{\alpha}_s^4$	R_{45}	R_{44}	R_{43}	R_{42}	R_{41}	$\cdots$
	$\vdots$	$\vdots$	$\vdots$	$\vdots$	$\vdots$	$\vdots$	$\ddots$

Normally, in perturbation theory, the fixed-order expansion of the cross section is expanded in powers of α_s, line by line in the table above thereby taking all α_s terms first (the so called *leading* order, LO), then all α_s^2 terms (the *next-to-leading* order, NLO) and so on. However, for small τ one has that $\alpha_s L \sim 1$ with $L = \ln\frac{1}{\tau}$, therefore by only taking the first line one does not take into account all other terms in the first column which are all of the same magnitude. In order to have a better prediction of the cross section in the small τ region, one needs to sum all the terms in the first column first (the *leading logarithms*, LL), then all the terms in the second column (the *next-to-leading logarithms*, NLL) and so on.

This is achieved by knowing the resummation coefficients g_i in eq. (19). In fact by expanding $\ln\frac{1}{\tau}g_1(\lambda)$

in α_s we get all the coefficients G_{nn+1}, expanding $g_2(\lambda)$ yields the coefficients G_{nn}, expading $\alpha_s g_3(\lambda)$ yields G_{nn-1} and so on.

The difference between the logarithmic part and the full fixed-order series at different orders is given by the remainder function $D(\tau, \alpha_s)$:

$$\begin{aligned} D_1(\tau) &= A(\tau) - R^{(1)}(\tau), \\ D_2(\tau) &= B(\tau) - R^{(2)}(\tau), \\ D_3(\tau) &= C(\tau) - R^{(3)}(\tau), \end{aligned} \tag{23}$$

which contains the non-logarithmic part of the fixed-order contribution and vanish for $\tau \to 0$.

However, in order to calculate the resummation coefficients $g_i(\lambda)$, whose expansion in α_s yields the G_{nm} coefficients, we need to perform an inverse transformation from Laplace space to real space. This necessity arises because the factorization is carried out in Laplace space. As demonstrated in [1], the problem of resummation can be recast in the form of an integral equation in Laplace space eq. (24), whose solution directly provides the exponent function.

$$\ln \tilde{J}^q_\nu(Q^2) = \int_0^1 \frac{\mathrm{d}u}{u}\Big(e^{-u\nu Q^2} - 1\Big)\left[\int_{u^2Q^2}^{uQ^2} \frac{1}{q^2} A\big(\alpha_s(q^2)\big)\mathrm{d}q^2 + \frac{1}{2} B\big(\alpha_s(uQ^2)\big)\right], \tag{24}$$

where $\tilde{J}^q_\nu(Q^2)$ is the Laplace transform of the quark jet mass distribution, a quantity related to the thrust distribution.

We'll see explicitly in the next chapter that resolving the above integral gives the exponent:

$$\mathcal{F}(\alpha_s, \ln N) = L f_1(\lambda) + f_2(\lambda) + f_3(\lambda)\alpha_s + f_4(\lambda)\alpha_s^2 + f_5(\lambda)\alpha_s^3 + \mathcal{O}\big(\alpha_s^4\big), \tag{25}$$

where $L = \ln N = \ln\big(\nu Q^2\big)$ and $\lambda = \alpha_s b_0 L$. We require the functions $f_i(\lambda)$ to be omogeneous,*i.e* $f_i(0) = 0$, so that at N^{n}LL we can write:

$$f_{n+1}(\lambda) = \sum_{k \geq n} \tilde{G}_{k,k+1-n} \alpha_s^k L^{k+1-n}. \tag{26}$$

This requirement is automatically satisfied if we choose as variable $L = \ln\Big(\frac{N}{N_0}\Big)$ where $N_0 = e^{-\gamma_E}$, $\gamma_E = 0.5772\ldots$ being the Euler-Mascheroni constant. With the latter choice the terms proportional to γ_E and its powers disappear. The advantage of the variable N is that the total rate is directly reproduced by setting $N = 1$, while in the variable $n = N/N_0$ it's when $N = N_0$. These two choices differ only by terms of higher order in γ_E. In literature the variable N is more common and in order to compare

with other results we'll use the variable N, we can recover the results in the variable n by simply setting $\gamma_E = 0$.

In the presentation of CTTW, N^{k}LL accuracy means how many terms g_i in the exponent of eq. (19) are known.

Chapter 3

Resummed Calculations for Thrust

We now turn to one of the many results of the present work: the calculation of the resummation coefficients $f_i(\lambda)$ of the Sudakov form factor $\exp\{\mathcal{F}\}$. To compute the $f_i(\lambda)$ functions, equation eq. (24) is used, which requires knowledge of the μ-dependence of the QCD running coupling $\alpha_s(\mu)$. We therefore proceed firstly to calculate the running coupling $\alpha_s(\mu)$ from LO up to N^{4}LO because the QCD β-function is known up to five loops [21]. We then use the obtained results to calculate the $f_i(\lambda)$ functions up to $i = 5$.

3.1 QCD running coupling

A surpring effect of the renormalization procedure is that, after renormalization, the coupling "constants" are not constant at all, but depend on the energy.

One way to understand this is the following: Classically, the Coulomb potential between two sources is then given by $V = \frac{\alpha}{r}$, characterized by a universal coefficient – the coupling constant α, which quantifies the force between two static bodies of unit "charge" at distance r, *i.e.*, the electric charge for QED, the color charge for QCD, the weak isospin for the weak force, or the mass for gravity. Consequently, the coupling α is defined as being proportional to the elementary charge squared, *e.g.*, $\alpha_{em} \equiv \frac{e^2}{4\pi}$ where e is the elementary electric charge, or $\alpha_s \equiv \frac{g^2}{4\pi}$ where g is the elementary gauge field coupling in QCD. In the non-relativistic limit of QCD, $\frac{1}{r}$ is the coordinate-space representation for the propagator of the gluon (force carrier) at leading-order in perturbation theory: in momentum space, the analogous propagator is proportional to $\frac{1}{q^2}$, where q is the boson 4-momentum ($Q^2 = -q^2 > 0$).

For sources interacting weakly, the one-boson exchange representation of interactions is a good approximation. However, when interactions become strong, higher orders in perturbation theory become

noticeable and the $\frac{1}{r}$ law no longer stands. In such cases, it makes good physics sense to fold the extra r-dependence into the coupling, which thereby becomes r, or equivalently Q^2, dependent.

Another way to view this is that the running of the coupling is due to vacuum polarization. The vacuum is not empty, but is filled with virtual particles that are constantly created and annihilated which can interact with the propagating particles, leading to a modification of the interaction strength.

While in QED, the extra r-dependence comes only from the vacuum polarization. In QCD, α_s receives contributions from the vacuum polarization and from gluon self-interactions since the gluon has a color charge.

The two couplings have opposite trends: the QED coupling increases with energy and the theory could eventually become strongly coupled at extremely high energies, whereas the opposite happens for the QCD coupling as it is large at low energies and decreases with energy. This property of being weakly coupled at high energies is known as *asymptotic freedom* and it means that perturbative calculations in QCD can be used at high energies where α_s becomes small enough that a power expansion is meaningful.

In the framework of perturbative QCD (*pQCD*), predictions for observables are expressed in terms of the renormalized coupling $\alpha = \alpha(\mu^2)$, a function of an unphysical renormalization scale μ_R. The coupling satisfies the following renormalization group equation (RGE):

$$\mu^2 \frac{d\alpha}{d\mu^2} = \beta(\alpha) = -\left(b_0\alpha^2 + b_1\alpha^3 + b_2\alpha^4 + \ldots\right), \tag{27}$$

where b_0 is the 1-loop β-function coefficient, b_1 is the 2-loop coefficient, b_2 is the 3-loop coefficient. $C_A = 3$ and $C_F = \frac{4}{3}$ are the Casimir operators of the adjoint and fundamental representations of $SU(3)$, $T_R = \frac{1}{2}$ is the trace normalization, n_f is the number of active quark flavors.

It is not possible to solve eq. (27) as it is for two reasons: only the first few b_n coefficients are known (up to b_4); the exact equation becomes more and more complicated as more terms of the series are included, making it impossible to obtain an analytic solution.

In order to solve both problems, the equation is solved in the following way: at first only b_0 is included and the obtained solution is called α_{LO} , as it will only contain a term proportional to α ; then also b_1 is included and only terms up to the second order in α are kept to obtain α_{NLO} ; this same procedure is used to obtain α_{NNLO} , $\alpha_{\text{N}^3\text{LO}}$, $\alpha_{\text{N}^4\text{LO}}$. There will be a complication in calculating α_{NLO} and higher orders which will be explained and resolved in the following sections.

3.1.1 One-loop running coupling and higher order corrections

The one-loop running coupling α_{LO} is obtained by solving the RGE eq. (27) with only the first term of the β-function:

$$\mu^2 \frac{d\alpha}{d\mu^2} = -b_0 \alpha^2. \tag{28}$$

This equation can be solved by separation of variables and imposing the boundary condition $\alpha(Q^2) = \alpha_s$:

$$\int_{\alpha(Q^2)}^{\alpha(\mu^2)} \frac{\mathrm{d}\alpha}{\alpha^2} = \int_{Q^2}^{\mu^2} -b_0 \frac{\mathrm{d}\mu^2}{\mu^2}, \tag{29}$$

and one obtains:

$$\alpha_{\mathrm{LO}}(\mu^2) = \frac{\alpha_s}{1 + b_0 \alpha_s \log\left(\frac{\mu^2}{Q^2}\right)}, \tag{30}$$

in which one can observe the decreasing with energy trend of the running coupling (asymptotic freedom).

It is useful to define the variable $\lambda_\mu = b_0 \alpha_s \log\left(\frac{\mu^2}{Q^2}\right)$ so that:

$$\alpha_{\mathrm{LO}}(\mu^2) = \frac{\alpha_s}{1 + \lambda_\mu}. \tag{31}$$

In order to obtain the two-loop running coupling α_{NLO}, we need to solve the RGE with the first two terms of the β-function eq. (27):

$$\mu^2 \frac{d\alpha}{d\mu^2} = -b_0 \alpha^2 - b_1 \alpha^3, \tag{32}$$

but this equation is not solvable in a straightforward way as the one-loop equation, we have to use the perturbative approach. We can rewrite the equation as:

$$\frac{d\alpha}{d\mu^2} = -\frac{b_0 \alpha^2}{\mu^2}(1 - \frac{b_1}{b_0}\alpha), \tag{33}$$

and expand the α term in the parenthesis as:

$$\alpha = \alpha_{\mathrm{LO}} + \delta\alpha, \tag{34}$$

where α_{LO} is the one-loop running coupling and $\delta\alpha$ contains the higher order correction, one obtains:

$$\frac{d\alpha}{d\mu^2} = -\frac{b_0\alpha^2}{\mu^2}(1 - \frac{b_1}{b_0}\alpha_{LO} - \frac{b_1}{b_0}\delta\alpha). \tag{35}$$

Observe that in parenthesis, by keeping 1 gave us the one-loop running coupling, by keeping $\frac{b_1}{b_0}\alpha_{LO}$ we can obtain the first order corrections and $\delta\alpha$ are needed for higher order corrections. The equation to solve is then:

$$\int_{\alpha_s}^{\alpha(\mu^2)} -\frac{\mathrm{d}\alpha}{\alpha^2} = \int_{Q^2}^{\mu^2} -b_0\frac{\mathrm{d}\mu^2}{\mu^2}(1 - \frac{b_1}{b_0}\alpha_{LO}(\mu^2)). \tag{36}$$

Using *Mathematica* [22] to solve this equation, we obtain the two-loop running coupling:

$$\alpha_{\mathrm{NLO}}(\mu^2) = \frac{\alpha_s}{1 + \lambda_\mu + \alpha_s\frac{b_1}{b_0}\log(1 + \lambda_\mu)}, \tag{37}$$

in which the expansion in powers of α_s is not explicit. One can expand in powers of α_s by keeping λ_μ fixed and only keeping terms up to $\mathcal{O}\big(\alpha_s^2\big)$ by doing so one obtains:

$$\alpha_{\mathrm{NLO}}\big(\mu^2\big) = \alpha_{\mathrm{LO}}\big(\mu^2\big) - \frac{b_1}{b_0}\alpha_{LO}^2\big(\mu^2\big)\log(1 + \lambda_\mu) + \mathcal{O}(\alpha_s^2). \tag{38}$$

We found the correction:

$$\delta\alpha_{\mathrm{NLO}}\big(\mu^2\big) = -\frac{b_1}{b_0}\alpha_{\mathrm{LO}}^2\big(\mu^2\big)\log(1 + \lambda_\mu). \tag{39}$$

By repeating the same procedure, one can obtain the three-loop running coupling α_{NNLO} and so on.

In order to calculate higher order corrections, one need to be careful of the powers of α needed for the desired order, and the contributions to various orders of α_s may not be immediately apparent, but they are straightforward to compute. Expand the running coupling in powers of α_s as:

$$\alpha = \alpha_{\mathrm{LO}} + \delta\alpha_{\mathrm{NLO}} + \delta\alpha_{\mathrm{NNLO}} + \delta\alpha_{\mathrm{N^3LO}} + \delta\alpha_{\mathrm{N^4LO}} + \ldots, \tag{40}$$

with $\delta\alpha_{\mathrm{NLO}} = \mathcal{O}(\alpha_s)$, $\delta\alpha_{\mathrm{NLO}} = \mathcal{O}\big(\alpha_s^2\big)$, $\delta\alpha_{\mathrm{NNLO}} = \mathcal{O}(\alpha_s^3)$, $\delta\alpha_{\mathrm{N^3LO}} = \mathcal{O}(\alpha_s^4)$, $\delta\alpha_{\mathrm{N^4LO}} = \mathcal{O}(\alpha_s^5)$, and so on.

We present these contributions in the following table:

For the three-loop running coupling, the equation to solve is:

$$\mu^2\frac{d\alpha}{d\mu^2} = -b_0\alpha^2(1 - \frac{b_1}{b_0}\alpha - \frac{b_2}{b_0}\alpha^2). \tag{41}$$

One can substitute the expansion of $\alpha = \alpha_{\mathrm{LO}} + \delta\alpha_{\mathrm{NLO}} + \mathcal{O}\big(\alpha_s^2\big)$ in powers of α_s and retain only terms up to $\mathcal{O}\big(\alpha_s^2\big)$, with this prescription the equation to solve is:

Table 3: Contributions to different powers of α_s.

Power	$\mathcal{O}(\alpha_s)$	$\mathcal{O}(\alpha_s^2)$	$\mathcal{O}(\alpha_s^3)$	$\mathcal{O}(\alpha_s^4)$	$\mathcal{O}(\alpha_s^5)$
α	$\alpha_{\rm LO}$	$\delta\alpha_{\rm NLO}$	$\delta\alpha_{\rm NNLO}$	$\delta\alpha_{\rm N^3LO}$	$\delta\alpha_{\rm N^4LO}$
α^2		$\alpha_{\rm LO}^2$	$2\alpha_{\rm LO}\delta\alpha_{\rm NLO}$	$\delta\alpha_{\rm NLO}^2 + 2\alpha_{\rm LO}\delta\alpha_{\rm NNLO}$	$2\alpha_{\rm LO}\delta\alpha_{\rm N^3LO} + 3\alpha_{\rm LO}\delta\alpha_{\rm NLO}^2$
α^3			$\alpha_{\rm LO}^3$	$3\alpha_{\rm LO}^2\delta\alpha_{\rm NLO}$	$3\alpha_{\rm LO}^2\delta\alpha_{\rm NNLO} + 3\alpha_{\rm LO}\delta\alpha_{\rm NLO}^2$
α^4				$\alpha_{\rm LO}^4$	$4\alpha_{\rm LO}^3\delta\alpha_{\rm NLO}$
α^5					$\alpha_{\rm LO}^5$

$$\int_{\alpha_s}^{\alpha(\mu^2)} -\frac{\mathrm{d}\alpha}{\alpha^2} = \int_{Q^2}^{\mu^2} -b_0\frac{\mathrm{d}\mu^2}{\mu^2}(1 - \frac{b_1}{b_0}\alpha_{\rm NLO}(\mu^2) - \frac{b_2}{b_0}\alpha_{LO}^2(\mu^2)), \tag{42}$$

solving the above integral yields the three-loop running coupling α_{NNLO}:

$$\alpha_{\rm NNLO}(\mu^2) = \alpha_{\rm LO}\big(\mu^2\big) + \delta\alpha_{\rm NLO}\big(\mu^2\big) + \delta\alpha_{\rm NNLO}\big(\mu^2\big), \tag{43}$$

with

$$\delta\alpha_{\rm NNLO}\big(\mu^2\big) = \frac{\alpha_{\rm LO}^3\big(\mu^2\big)}{b_0^2}\left(b_1^2\lambda_\mu - b_0b_2\lambda_\mu + b_1^2\log^2(1+\lambda_\mu) - b_1^2\log(1+\lambda_\mu)\right). \tag{44}$$

Similarly, one can obtain the four-loop running coupling α_{N^3LO} and five-loop running coupling α_{N^4LO}

$$\alpha_{\rm N^3LO}(\mu^2) = \alpha_{\rm LO}\big(\mu^2\big) + \delta\alpha_{\rm NLO}\big(\mu^2\big) + \delta\alpha_{\rm NNLO}\big(\mu^2\big) + \delta\alpha_{\rm N^3LO}\big(\mu^2\big), \tag{45}$$

$$\begin{aligned}\delta\alpha_{\rm N^3LO}\big(\mu^2\big) = \frac{\alpha_{\rm LO}^4\big(\mu^2\big)}{2b_0^3}\Big(&-\left(b_1^3 - 2b_0b_2b_1 + b_0^2b_3\right)\lambda_\mu^2 \\ &- \left(2b_0^2b_3 - 2b_0b_1b_2\right)\lambda_\mu - 2b_1^3\log^3\left(\lambda_\mu+1\right) + 5b_1^3\log^2\left(1+\lambda_\mu\right) \\ &+ \left(2b_0b_1b_2\left(2\lambda_\mu - 1\right) - 4b_1^3\lambda_\mu\right)\log\left(1+\lambda_\mu\right)\Big),\end{aligned} \tag{46}$$

$$\alpha_{\rm N^4LO}(\mu^2) = \alpha_{\rm LO}\big(\mu^2\big) + \delta\alpha_{\rm NLO}\big(\mu^2\big) + \delta\alpha_{\rm NNLO}\big(\mu^2\big) + \delta\alpha_{\rm N^3LO}\big(\mu^2\big) + \delta\alpha_{\rm N^4LO}\big(\mu^2\big), \tag{47}$$

$$
\begin{aligned}
\delta\alpha_{\mathrm{N^4LO}} = \frac{\alpha_{\mathrm{LO}}^5}{6b_0^4}\Big(& \left(2b_1^4 - 6b_0b_2b_1^2 + 4b_0^2b_3b_1 + 2b_0^2b_2^2 - 2b_0^3b_4\right)\lambda_\mu^3 \\
& + \left(9b_1^4 - 24b_0b_2b_1^2 + 9b_0^2b_3b_1 + 12b_0^2b_2^2 - 6b_0^3b_4\right)\lambda_\mu^2 \\
& + \left(6b_0^2b_1b_3 - 6b_0^3b_4\right)\lambda_\mu + 6b_1^4\log^4(1+\lambda_\mu) \\
& - 26b_1^4\log^3(\lambda_\mu+1) + 9\left(\left(2b_1^4 - 2b_0b_1^2b_2\right)\lambda_\mu + b_1^4 + 2b_0b_2b_1^2\right)\log^2(1+\lambda_\mu) \\
& + \left(6b_1\left(b_1^3 - 2b_0b_2b_1 + b_0^2b_3\right)\lambda_\mu^2 + 6b_1\left(-3b_1^3 + b_0b_2b_1 + 2b_0^2b_3\right)\lambda_\mu\right. \\
& \left. - 6b_1b_3b_0^2\right)\log(1+\lambda_\mu)\Big).
\end{aligned}
\tag{48}
$$

The plot of the running coupling α_s as a function of the energy scale $(xm_z)^2$ for different orders of perturbation theory, where $m_z = 91.18$ GeV is the mass of the Z boson, is shown in fig. 10. The global average value of the strong coupling constant is $\alpha_s(m_z^2) = 0.1179 \pm 0.0009$ [23]. For the plots $\alpha_s(m_z^2) = 0.118$ is used.

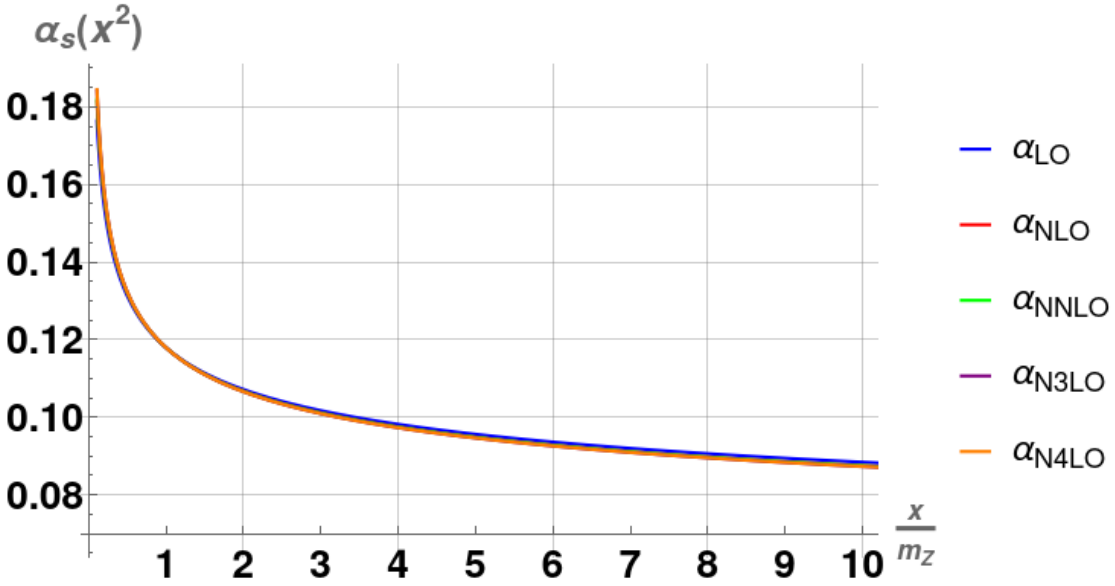

Figure 10: Energy dependence of the strong coupling α_s

In fig. 11 wee see that at low energies the running coupling α_s is large and diverges at a finite energy (the so called Landau pole), this is a sign of the non-perturbative nature of QCD at low energies.

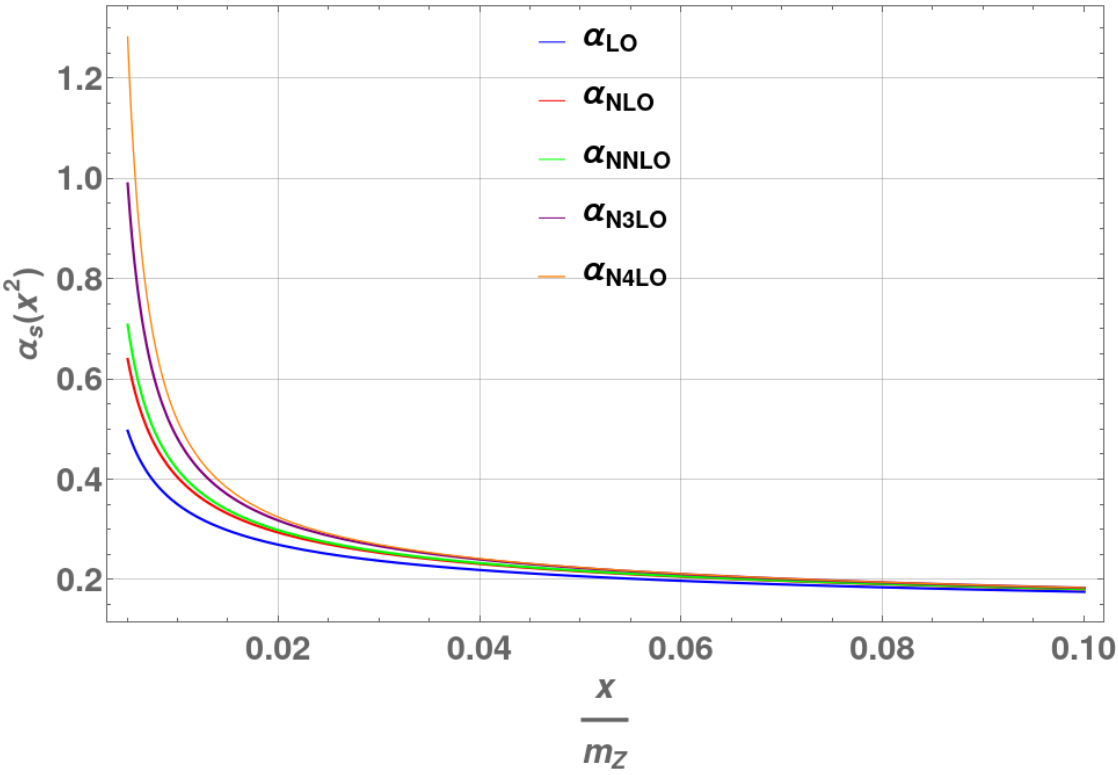

Figure 11: Zoom-in at low energies of the strong running coupling α_s at different orders

3.2 Calculating the resummation coefficients

In this section we discuss the calculation of the resummation coefficients $f_i(\lambda)$ for the thrust distribution.

In the article by Catani, Turnock, Webber and Trentadue [16], it was observed that for a final state configuration corresponding to a large value of thrust , eq. (1) can be approximated by

$$\tau = 1 - T \approx \frac{k_1^2 + k_2^2}{Q^2}, \tag{49}$$

where k_1^2 and k_2^2 are the squared invariant masses of two back-to-back jets and Q^2 is the energy of the center of mass. Thus the key to the evaluation of the thrust distributions is its relation to the quark jet mass distribution $J^q(Q^2, k^2)$, also denoted as $J^q_{k^2}(Q^2)$, which represents the probability of finding a jet originating from quarks, with an invariant mass-squared k^2, produced in collisions with a center-of-mass energy Q^2.

Then the thrust distribution $R_T(\tau, \alpha_s(Q^2))$ eq. (3) takes the form of a convolution of two jet mass distributions $J(Q^2, k_1^2)$ and $J(Q^2, k_2^2)$

$$R_T(\tau, \alpha_s(Q^2)) \underset{\tau \ll 1}{=} \int_0^\infty \mathrm{d}k_1^2 \int_0^\infty \mathrm{d}k_2^2 J^q_{k_1^2}(Q^2) J^q_{k_2^2}(Q^2) \Theta\left(\tau - \frac{k_1^2 + k_2^2}{Q^2}\right), \tag{50}$$

Introducing the Laplace transform of the jet mass distribution:

$$\tilde{J}^q_\nu(Q^2) = \int_0^\infty J^q(Q^2, k^2) e^{-\nu k^2} \mathrm{d}k^2, \tag{51}$$

where ν is the conjugate variable to k^2 in Laplace space,

and the integral representation of the Heaviside step function:

$$\Theta\left(\tau - \frac{k_1^2 + k_2^2}{Q^2}\right) = \frac{1}{2\pi i} \int_{C-i\infty}^{C+i\infty} \frac{\mathrm{d}N}{N} e^{N\tau} e^{-N\frac{k_1^2+k_2^2}{Q^2}}, \tag{52}$$

where $N = \nu Q^2$.

By substituting eq. (52) into eq. (50) and setting $N = \nu Q^2$ we obtain:

$$\begin{aligned} R_T(\tau) &= \int_{C-i\infty}^{C+i\infty} \frac{\mathrm{d}N}{N} \frac{e^{N\tau}}{2\pi i} \left[\int_0^\infty \mathrm{d}k_1^2 e^{-\nu k_1^2} J^q_{k_1^2}(Q^2)\right] \left[\int_0^\infty \mathrm{d}k_2^2 e^{-\nu k_2^2} J^q_{k_2^2}(Q^2)\right] \\ &= \frac{1}{2\pi i} \int_{C-i\infty}^{C+i\infty} e^{N\tau} \left[\tilde{J}^q_\nu(Q^2)\right]^2 \frac{\mathrm{d}N}{N}, \end{aligned} \tag{53}$$

where C is a real positive constant to the right of all singularities of the integrand $\tilde{J}_\nu(Q^2)$ in the complex ν plane.

An integral representation for the Laplace transform $\tilde{J}_\nu(Q^2)$ is given by [1]:

$$\ln \tilde{J}^q_\nu(Q^2) = \int_0^1 \frac{\mathrm{d}u}{u}\Big(e^{-u\nu Q^2} - 1\Big)\left[\int_{u^2Q^2}^{uQ^2} \frac{1}{q^2} A\big(\alpha_s(q^2)\big)\mathrm{d}q^2 + \frac{1}{2}B\big(\alpha_s(uQ^2)\big)\right], \tag{54}$$

with

$$A(\alpha_s) = \sum_{n=1}^{\infty} A_n \Big(\frac{\alpha_s}{\pi}\Big)^n, \qquad\qquad B(\alpha_s) = \sum_{n=1}^{\infty} B_n \Big(\frac{\alpha_s}{\pi}\Big)^n.$$

Function $A(\alpha_s)$ is associated with the cusp anomalous dimension and governs the exponentiation of the leading logarithms (LL). It captures the resummation of the soft and collinear gluon emissions that dominate in the limit of large thrust values.

Function $B(\alpha_S)$ includes the next-to-leading logarithmic (NLL) corrections and accounts for subleading contributions from hard collinear emissions. It typically involves the non-cusp part of the anomalous dimensions and running of the coupling constant.

The integral as it is cannot be integrated since it involves the Landau pole where $\alpha_s(q^2)$ diverges. The u integration may be performed using the prescription discussed in Appendix A of [24] and readapting the formula to the case of Laplace transform instead of Mellin transform.

This method is a generalization of the prescription to NLL accuracy in [1]

$$e^{-u\nu Q^2} - 1 \simeq -\Theta(u - v) \quad \text{with } v = \frac{N_0}{N} \quad , \tag{55}$$

where $N_0 = e^{-\gamma_E}$.

In appendix A we show that the prescription to evaluate the large-N Mellin moments of soft-gluon contributins at an arbitrary logarithmic accuracy, can be used for the Laplace transform as well, then we can use this result to express eq. (24) in an alternative representation:

$$\ln \tilde{J}^q_\nu(Q^2) = -\int_{N_0/N}^1 \frac{\mathrm{d}u}{u}\left[\int_{u^2Q^2}^{uQ^2} \frac{1}{q^2} A\big(\alpha_s(q^2)\big)\mathrm{d}q^2 + \frac{1}{2}\tilde{B}\big(\alpha_s(uQ^2)\big)\right] + \ln \tilde{C}\left(\alpha_s(\mu^2), \frac{\mu^2}{Q^2}\right). \tag{56}$$

After performing the integration up to a fixed logarithmic accuracy $N^k LL$ (*i.e* we compute the leading $\alpha_s^n \ln^{n+1} N$, next-to-leading $\alpha_s^n \ln^n N$ and so on to $\alpha_s^n \ln^{n+1-k}$ terms), we find the form factor:

$$\begin{aligned}\ln \tilde{J}^q_\nu(Q^2) = {} & \ln N f_1(\lambda) + f_2(\lambda) + \alpha_s f_3(\lambda) + \alpha_s^2 f_4(\lambda) + \alpha_s^3 f_5(\lambda) + \mathcal{O}\big(\alpha_s^n \ln^{n-4} N\big) \\ & + \ln \tilde{C}\left(\alpha_s(\mu^2), \frac{\mu^2}{Q^2}\right)\end{aligned} \tag{57}$$

From now on we'll always use eq. (56), so we'll drop the ˜ notation for B.

We observe that the N-space formula eq. (56) is finite and uniquely defined up to the very large $N = N_L = \exp\Big(\frac{1}{2\alpha_s b_0}\Big)$, where $\lambda = \frac{1}{2}$, thanks to the prescription above.

3.2.1 resummation functions

To calculate explicit expressions for the first few f_i terms, we first write explicitly the internal integral of eq. (24), for now on let's forget the $\ln \tilde{C}$ term, since it can be absorbed into the definition of A and B:

The q^2 integration also becomes simple if we use the renormalization group equation eq. (27) to change the integration variable to as

$$\begin{aligned}\frac{\mathrm{d}q^2}{q^2} &= -\frac{\mathrm{d}\alpha_s}{b_0\alpha_s^2}\bigg(1 - \frac{b_1}{b_0}\alpha_s + \frac{\big(b_1^2 - b_2 b_0\big)}{b_0^2}\alpha_s^2 + \frac{\big(-b_3 b_0^2 + 2b_2 b_1 b_0 - b_1^3\big)}{b_0^3}\alpha_s^3 \\ &\quad + \frac{\big(-b_4 b_0^3 + 2b_3 b_1 b_0^2 + b_2^2 b_0^2 - 3b_2 b_1^2 b_0 + b_1^4\big)}{b_0^4}\alpha_s^4 + \mathcal{O}\big(\alpha_s^5\big)\bigg) \\ &= -\frac{\mathrm{d}\alpha_s}{b_0\alpha_s^2}(N_0 + N_1\alpha_s + N_2\alpha_s^2 + N_3\alpha_s^3 + N_4\alpha_s^4 + \mathcal{O}\big(\alpha_s^5\big)),\end{aligned} \tag{58}$$

where for convenience's sake we have defined:

$$\begin{aligned}&N_0 = 1, \qquad N_1 = \frac{b_1}{b_0}, \qquad N_2 = \frac{\big(b_1^2 - b_2 b_0\big)}{b_0^2}, \\ &N_3 = \frac{\big(-b_3 b_0^2 + 2b_2 b_1 b_0 - b_1^3\big)}{b_0^3}, \\ &N_4 = \frac{\big(-b_4 b_0^3 + 2b_3 b_1 b_0^2 + b_2^2 b_0^2 - 3b_2 b_1^2 b_0 + b_1^4\big)}{b_0^4}.\end{aligned} \tag{59}$$

Subsequently, the integral in eq. (56) can be expressed as:

$$\begin{aligned}&\int_{\alpha_s(u^2Q^2)}^{\alpha_s(uQ^2)} \frac{\mathrm{d}\alpha_s}{b_0\alpha_s^2}(N_0 + N_1\alpha_s + N_2\alpha_s^2 + N_3\alpha_s^3 + N_4\alpha_s^4)\sum_{n=1}^{\infty} A_n\Big(\frac{\alpha_s}{\pi}\Big)^n \\ &= \int_{\alpha_s(u^2Q^2)}^{\alpha_s(uQ^2)} \frac{\mathrm{d}\alpha_s}{b_0}\bigg(\frac{A_1 N_0}{\pi\alpha_s} + \frac{\pi A_1 N_1 + A_2}{\pi^2} + \frac{\big(\pi A_2 N_1 + \pi^2 A_1 N_2 + A_3\big)}{\pi^3}\alpha_s \\ &+ \frac{\big(\pi A_3 N_1 + \pi^2 A_2 N_2 + \pi^3 A_1 N_3 + A_4\big)}{\pi^4}\alpha_s^2 \\ &+ \frac{\big(\pi A_4 N_1 + \pi^2 A_3 N_2 + \pi^3 A_2 N_3 + \pi^4 A_1 N_4 + A_5\big)}{\pi^5}\alpha_s^3 + \mathcal{O}\big(\alpha_s^4\big)\bigg),\end{aligned} \tag{60}$$

and keeping only terms up to N_0,A_1 and α_s^0 we get contributions to f_1, keeping terms up to N_1,A_2 and α_s^1 yields contributions to f_2 and so on. That's because after integration, we evaluate the integrand at $\alpha_s(u^2Q^2)$ and $\alpha_s(uQ^2)$, where α_s is α_{LO} for f_1, α_{NLO} for f_2 and so on.

And there's an easy way to see why it's like this, in fact it's also possible to do the q^2 integration directly, using eqs. (31), (39), (44), (46) and (48) from section 3.1 and keeping in mind table 3.

$$\int_{u^2Q^2}^{uQ^2} \frac{\mathrm{d}q^2}{q^2} \sum_{n=1}^{\infty} \frac{A_n}{\pi^n} \big(\alpha_{\text{LO}}(q^2) + \delta\alpha_{\text{NLO}}(q^2) + \delta\alpha_{\text{NNLO}}(q^2) + \delta\alpha_{\text{N}^3\text{LO}}(q^2) + \delta\alpha_{\text{N}^4\text{LO}}(q^2) + \ldots\big)^n, \quad (61)$$

now we can see that if we consider terms up to α_s^1 only A_1 contributes and this gives f_1, if we consider terms up to α_s^2 we see A_2 starts to contribute together with $A_1\delta\alpha_{\text{NLO}}$ and this gives f_2 , for f_3 we need to consider terms up to α_s^3 and so on.

For the B-term it's similar. However, since the B-term is "already integrated" in q^2, it contributes one order lower in α_s compared to the A-term. Specifically, B_1 starts to contribute from f_2, B_2 from f_3 and so on.

Now armed with this knowledge we can calculate eq. (56) and find:

$$\ln \tilde{J}_\nu^q(Q^2) = \ln N f_1(\lambda) + f_2(\lambda) + \alpha_s f_3(\lambda) + \alpha_s^2 f_4(\lambda) + \alpha_s^3 f_5(\lambda) + \mathcal{O}\big(\alpha_s^n \ln^{n-4} N\big) + \ln \tilde{C}\big(\alpha_s(\mu^2)\big), \quad (62)$$

where $\lambda = \alpha_s b_0 \ln N$, $N = \nu Q^2$, $\alpha_s = \alpha_s(Q^2)$ and

$$f_1(\lambda) = -\frac{A_1}{2\pi b_0 \lambda}[(1-2\lambda)\ln(1-2\lambda) - 2(1-\lambda)\ln(1-\lambda)], \quad (63)$$

$$\begin{aligned} f_2(\lambda) = &-\frac{A_2}{2\pi^2 b_0^2}[2\ln(1-\lambda) - \ln(1-2\lambda)] + \frac{B_1 \ln(1-\lambda)}{2\pi b_0} + \frac{\gamma_E A_1}{\pi b_0}[\ln(1-2\lambda) - \ln(1-\lambda)] \\ &- \frac{A_1 b_1}{2\pi b_0^3}\left[-\ln^2(1-\lambda) + \frac{1}{2}\ln^2(1-2\lambda) - 2\ln(1-\lambda) + \ln(1-2\lambda)\right], \end{aligned} \quad (64)$$

$$\begin{aligned} f_3(\lambda) = &-\frac{A_3}{2\pi^3 b_0^2(\lambda-1)(2\lambda-1)}\lambda^2 + \frac{B_2}{2\pi^2 b_0(\lambda-1)}\lambda + \frac{B_2\lambda}{2\pi^2 b_0(\lambda-1)} \\ &+ \frac{b_1 A_2}{2\pi^2 b_0^3(\lambda-1)(2\lambda-1)}\left[3\lambda^2 + (1-\lambda)\ln(1-2\lambda) - 2(1-2\lambda)\ln(1-\lambda)\right] \\ &- \frac{\gamma_E A_2 \lambda}{\pi^2 b_0(\lambda-1)(2\lambda-1)} - \frac{B_1 b_1}{2\pi b_0^2(\lambda-1)}[\lambda + \ln(1-\lambda)] + \frac{\gamma_E B_1 \lambda}{2\pi(\lambda-1)} + \frac{\gamma_E^2 A_1 \lambda(2\lambda-3)}{2\pi(\lambda-1)(2\lambda-1)} \end{aligned}$$

$$
\begin{aligned}
&+\frac{b_1\gamma_E A_1}{\pi b_0^2(\lambda-1)(2\lambda-1)}[-\lambda+(1-2\lambda)\ln(1-\lambda)-(1-\lambda)\ln(1-2\lambda)] \\
&-\frac{b_1^2 A_1}{2\pi b_0^4(\lambda-1)(2\lambda-1)}\Big[\big(\lambda^2+(2\lambda-1)\ln(1-\lambda)(2\lambda+\ln(1-\lambda))\big) \\
&+\frac{1}{2}\left((1-\lambda)\ln^2(1-2\lambda)\right)-2(\lambda-1)\lambda\ln(1-2\lambda)\Big] \\
&-\frac{b_0 b_2 A_1}{2\pi b_0^4(\lambda-1)(2\lambda-1)}\left[\lambda^2+(\lambda-1)(2\lambda-1)(2\ln(1-\lambda)+\ln(1-2\lambda))\right],
\end{aligned}
\tag{65}
$$

$$
\begin{aligned}
f_4(\lambda) = &-\frac{A_4\lambda^2\left(2\lambda^2-6\lambda+3\right)}{6\pi^4 b_0^2(\lambda-1)^2(2\lambda-1)^2}+\frac{B_3(\lambda-2)\lambda}{4\pi^3 b_0(\lambda-1)^2}+\frac{b_1 A_3}{12\pi^3 b_0^3(\lambda-1)^2(2\lambda-1)^2}\Big[15\lambda^2 \\
&+10(\lambda-3)\lambda^3+3(\lambda-1)^2\ln(1-2\lambda)-6(1-2\lambda)^2\ln(1-\lambda)\Big] \\
&+\frac{\gamma_E A_3\lambda(3\lambda-2)}{2\pi^3 b_0(\lambda-1)^2(2\lambda-1)^2}+\frac{\gamma_E B_2(\lambda-2)\lambda}{2\pi^2(\lambda-1)^2}-\frac{b_1 B_2\left[\lambda^2-2\lambda-2\ln(1-\lambda)\right]}{4\pi^2 b_0^2(\lambda-1)^2} \\
&+\frac{\gamma_E^2 A_2\lambda\left(4\lambda^3-12\lambda^2+15\lambda-6\right)}{2\pi^2(\lambda-1)^2(2\lambda-1)^2}+\frac{b_1\gamma_E A_2}{2\pi^2 b_0^2(\lambda-1)^2(2\lambda-1)^2}\Big[\lambda(2-3\lambda) \\
&+2(\lambda-1)^2\ln(1-2\lambda)-2(1-2\lambda)^2\ln(1-\lambda)\Big]+\frac{b_2 A_2\lambda^3(4\lambda-3)}{3\pi^2 b_0^3(\lambda-1)^2(2\lambda-1)^2} \\
&-\frac{b_1^2 A_2}{12\pi^2 b_0^4(\lambda-1)^2(2\lambda-1)^2}\Big[\lambda^2\left(22\lambda^2-30\lambda+9\right)+3(\lambda-1)^2\ln^2(1-2\lambda) \\
&+3(\lambda-1)^2\ln(1-2\lambda)-6(1-2\lambda)^2\ln(1-\lambda)(\ln(1-\lambda)+1)\Big] \\
&+\frac{b_0\gamma_E^2 B_1(\lambda-2)\lambda}{4\pi(\lambda-1)^2}+\frac{b_1\gamma_E B_1\ln(1-\lambda)}{2\pi b_0(\lambda-1)^2}+\frac{b_2 B_1\lambda^2}{4\pi b_0^2(\lambda-1)^2} \\
&+\frac{b_1^2 B_1(\lambda-\ln(1-\lambda))(\lambda+\ln(1-\lambda))}{4\pi b_0^3(\lambda-1)^2}+\frac{b_0\gamma_E^3 A_1\lambda\left(12\lambda^3-36\lambda^2+39\lambda-14\right)}{6\pi(\lambda-1)^2(2\lambda-1)^2} \\
&+\frac{b_1\gamma_E^2 A_1}{2\pi b_0(\lambda-1)^2(2\lambda-1)^2}\left[2(\lambda-1)^2\ln(1-2\lambda)-(1-2\lambda)^2\ln(1-\lambda)\right] \\
&-\frac{b_1^2\gamma_E A_1}{2\pi b_0^3 A_1(\lambda-1)^2(2\lambda-1)^2}\left[(4\lambda-3)\lambda^2-(1-2\lambda)^2\ln^2(1-\lambda)+(\lambda-1)^2\ln^2(1-2\lambda)\right] \\
&-\frac{b_1^3 A_1}{12\pi b_0^5(\lambda-1)^2(2\lambda-1)^2}\Big[4(3-4\lambda)\lambda^3+2(1-2\lambda)^2\ln(1-\lambda)\left(\ln^2(1-\lambda)-3\lambda^2\right) \\
&+12(\lambda-1)^2\lambda^2\ln(1-2\lambda)-(\lambda-1)^2\ln^3(1-2\lambda)\Big]+\frac{b_2\gamma_E A_1\lambda^2(4\lambda-3)}{2\pi b_0^2(\lambda-1)^2(2\lambda-1)^2} \\
&\frac{b_1 b_2 A_1}{12\pi b_0^4(\lambda-1)^2(2\lambda-1)^2}\Big[\lambda^2(2\lambda(3-7\lambda)+3)+3\left(8\lambda^2-4\lambda+1\right)(\lambda-1)^2\ln(1-2\lambda) \\
&-6(1-2\lambda)^2(2(\lambda-1)\lambda+1)\ln(1-\lambda)\Big]+-\frac{b_3 A_1}{12\pi b_0^3(\lambda-1)^2(2\lambda-1)^2}\Big[(2(\lambda-3)\lambda+3)\lambda^2 \\
&-6\left(2\lambda^2-3\lambda+1\right)^2\ln(1-\lambda)+3\left(2\lambda^2-3\lambda+1\right)^2\ln(1-2\lambda)\Big],
\end{aligned}
\tag{66}
$$

$$
\begin{aligned}
f_5(\lambda) = &-\frac{A_5\lambda^2\left(4\lambda^4-18\lambda^3+33\lambda^2-24\lambda+6\right)}{12\pi^5 b_0^2(\lambda-1)^3(2\lambda-1)^3}+\frac{B_4\lambda\left(\lambda^2-3\lambda+3\right)}{6\pi^4 b_0(\lambda-1)^3} \\
&-\frac{\gamma_E A_4\lambda\left(7\lambda^2-9\lambda+3\right)}{3\pi^4 b_0(\lambda-1)^3(2\lambda-1)^3}+\frac{b_1 A_4}{36\pi^4 b_0^3(\lambda-1)^3(2\lambda-1)^3}\Big[7\lambda^2(\lambda(\lambda(2\lambda(2\lambda-9)+33)-24) \\
&+6)-6(\lambda-1)^3\ln(1-2\lambda)+12(2\lambda-1)^3\ln(1-\lambda)\Big]+\frac{\gamma_E B_3\lambda\left(\lambda^2-3\lambda+3\right)}{2\pi^3(\lambda-1)^3}+ \\
&\frac{b_1 B_3\left(\lambda^3-3\lambda^2+3\lambda+3\ln(1-\lambda)\right)}{6\pi^3 b_0^2(\lambda-1)^3}+\frac{\gamma_E^2 A_3\lambda\left(8\lambda^5-36\lambda^4+66\lambda^3-69\lambda^2+39\lambda-9\right)}{2\pi^3(\lambda-1)^3(2\lambda-1)^3} \\
&-\frac{b_1\gamma_E A_3}{3\pi^3 b_0^2(\lambda-1)^3(2\lambda-1)^3}\Big[\lambda((9-7\lambda)\lambda-3)+3(\lambda-1)^3\ln(1-2\lambda) \\
&-3(2\lambda-1)^3\ln(1-\lambda)\Big]+\frac{b_2 A_3\lambda^3\left(4\lambda^3-18\lambda^2+19\lambda-6\right)}{4\pi^3 b_0^3(\lambda-1)^3(2\lambda-1)^3}- \\
&\frac{b_1^2 A_3}{36\pi^3 b_0^4(\lambda-1)^3(2\lambda-1)^3}\Big[\lambda^3(\lambda(26\lambda(2\lambda-9)+303)-150)-9(\lambda-1)^3\ln^2(1-2\lambda) \\
&+24\lambda^2-6(\lambda-1)^3\ln(1-2\lambda)+6(2\lambda-1)^3\ln(1-\lambda)(3\ln(1-\lambda)+2)\Big] \\
&+\frac{b_0\gamma_E^2 B_2\lambda\left(\lambda^2-3\lambda+3\right)}{2\pi^2(\lambda-1)^3}-\frac{b_1\gamma_E B_2\ln(1-\lambda)}{\pi^2 b_0(\lambda-1)^3}+\frac{b_1^2 B_2\left(\lambda^3-3\lambda^2+3\ln^2(1-\lambda)\right)}{6\pi^2 b_0^3(\lambda-1)^3} \\
&-\frac{b_2 B_2(\lambda-3)\lambda^2}{6\pi^2 b_0^2(\lambda-1)^3}+\frac{b_0\gamma_E^3 A_2\lambda\left(24\lambda^5-108\lambda^4+198\lambda^3-193\lambda^2+99\lambda-21\right)}{3\pi^2(\lambda-1)^3(2\lambda-1)^3} \\
&+\frac{b_1^2\gamma_E A_2}{3\pi^2 b_0^3(\lambda-1)^3(2\lambda-1)^3}\Big[\lambda^2(\lambda(18\lambda-25)+9)+3(\lambda-1)^3\ln^2(1-2\lambda) \\
&-3(2\lambda-1)^3\ln^2(1-\lambda)\Big]-\frac{b_2\gamma_E A_2\lambda^2\left(18\lambda^2-25\lambda+9\right)}{3\pi^2 b_0^2(\lambda-1)^3(2\lambda-1)^3} \\
&+\frac{b_1^3 A_2}{36\pi^2 b_0^5(\lambda-1)^3(2\lambda-1)^3}\Big[\lambda^2(\lambda(\lambda(2\lambda(50\lambda-171)+339)-114)+6) \\
&-6(\lambda-1)^3\ln^3(1-2\lambda)+12(2\lambda-1)^3\ln(1-\lambda)\left(-3\lambda+\ln^2(1-\lambda)+1\right) \\
&+6(6\lambda-1)(\lambda-1)^3\ln(1-2\lambda)\Big]+\frac{b_3 A_2\lambda^3\left(20\lambda^3-54\lambda^2+45\lambda-12\right)}{12\pi^2 b_0^3(\lambda-1)^3(2\lambda-1)^3} \\
&-\frac{b_1\gamma_E^2 A_2}{\pi^2 b_0(\lambda-1)^3(2\lambda-1)^3}\Big[2(\lambda-1)^3\ln(1-2\lambda)-(2\lambda-1)^3\ln(1-\lambda)\Big] \\
&-\frac{b_2 b_1 A_2}{18\pi^2 b_0^4(\lambda-1)^3(2\lambda-1)^3}\Big[\lambda^2(\lambda(\lambda(4\lambda(20\lambda-63)+237)-75)+3) \\
&+3(6\lambda-1)(\lambda-1)^3\ln(1-2\lambda)-6(2\lambda-1)^3(3\lambda-1)\ln(1-\lambda)\Big] \\
&+\frac{b_0^2\gamma_E^3 B_1\lambda\left(\lambda^2-3\lambda+3\right)}{6\pi(\lambda-1)^3}-\frac{b_1^2\gamma_E B_1\left(\lambda-\ln^2(1-\lambda)+\ln(1-\lambda)\right)}{2\pi b_0^2(\lambda-1)^3}- \\
&\frac{b_1^3 B_1}{12\pi b_0^4(\lambda-1)^3}(\lambda+\ln(1-\lambda))\left(2\lambda^2-3\lambda+2\ln^2(1-\lambda)-2\lambda\ln(1-\lambda)-3\ln(1-\lambda)\right)
\end{aligned}
\tag{67}
$$

$$
+\frac{b_2\gamma_E B_1\lambda}{2\pi b_0(\lambda-1)^3}-\frac{b_3B_1\lambda^2(2\lambda-3)}{12\pi b_0^2(\lambda-1)^3}+\frac{b_1\gamma_E^2B_1\left(\lambda^3-3\lambda^2+3\lambda-2\ln(1-\lambda)\right)}{4\pi(\lambda-1)^3}
$$

$$
+\frac{b_2b_1B_1\lambda\left(2\lambda^2-3\lambda-3\ln(1-\lambda)\right)}{6\pi b_0^3(\lambda-1)^3}+\frac{b_0^2\gamma_E^4A_1}{12\pi(\lambda-1)^3(2\lambda-1)^3}\lambda(2\lambda-3)\Big[28\lambda^4
$$

$$
-84\lambda^3+105\lambda^2-63\lambda+15\Big]+\frac{b_1^3\gamma_EA_1}{6\pi b_0^4(\lambda-1)^3(2\lambda-1)^3}\Big[\lambda^2(4\lambda(3(\lambda-3)\lambda+8)-9)
$$

$$
-2(\lambda-1)^3\ln^3(1-2\lambda)+3(\lambda-1)^3\ln^2(1-2\lambda)+12\lambda(\lambda-1)^3\ln(1-2\lambda)
$$

$$
+(2\lambda-1)^3\ln(1-\lambda)(\ln(1-\lambda)(2\ln(1-\lambda)-3)-6\lambda)\Big]
$$

$$
+\frac{b_1^4A_1}{24\pi b_0^6(\lambda-1)^3(2\lambda-1)^3}\Big[8(\lambda-1)^3\lambda^2(4\lambda-3)\ln(1-2\lambda)
$$

$$
-2(2\lambda-1)^3\ln(1-\lambda)\left(2(2\lambda-3)\lambda^2+\ln(1-\lambda)((\ln(1-\lambda)-2)\ln(1-\lambda)-6\lambda)\right)
$$

$$
+2\lambda^3\left(\lambda\left(-28\lambda^2+54\lambda-33\right)+6\right)+(\lambda-1)^3\ln^4(1-2\lambda)-2(\lambda-1)^3\ln^3(1-2\lambda)-
$$

$$
12(\lambda-1)^3\lambda\ln^2(1-2\lambda)\Big]-\frac{b_2\gamma_E^2A_1\lambda\left(4\lambda^3-6\lambda+3\right)}{2\pi b_0(\lambda-1)^3(2\lambda-1)^3}+\frac{b_3\gamma_E\lambda^2\left(12\lambda^3-36\lambda^2+32\lambda-9\right)}{6\pi b_0^2(\lambda-1)^3(2\lambda-1)^3}
$$

$$
+\frac{b_2^2A_1}{36\pi b_0^4(\lambda-1)^3(2\lambda-1)^3}\Big[\lambda^2(6-\lambda(\lambda(2\lambda(10\lambda+9)-69)+42))
$$

$$
-12\left(2\lambda^2-3\lambda+1\right)^3\ln(1-\lambda)+6\left(2\lambda^2-3\lambda+1\right)^3\ln(1-2\lambda)\Big]
$$

$$
+\frac{b_1^2\gamma_E^2A_1}{2\pi b_0^2(\lambda-1)^3(2\lambda-1)^3}\Big[\lambda\left(4\lambda^3-6\lambda+3\right)+2(\lambda-1)^3\ln^2(1-2\lambda)
$$

$$
-2(\lambda-1)^3\ln(1-2\lambda)-(2\lambda-1)^3(\ln(1-\lambda)-1)\ln(1-\lambda)\Big]
$$

$$
-\frac{b_2b_1^2A_1}{36\pi b_0^5(\lambda-1)^3(2\lambda-1)^3}\Big[\lambda^2(\lambda(\lambda(2(153-82\lambda)\lambda-165)+12)+6)
$$

$$
-18\lambda(\lambda-1)^3\ln^2(1-2\lambda)+6\left(6(1-2\lambda)^2\lambda-1\right)(\lambda-1)^3\ln(1-2\lambda)
$$

$$
-6(2\lambda-1)^3\ln(1-\lambda)\left(6\lambda(\lambda-1)^2-3\lambda\ln(1-\lambda)-2\right)\Big]
$$

$$
+\frac{b_1\gamma_E^3A_1}{6\pi(\lambda-1)^3(2\lambda-1)^3}\Big[24\lambda^6-108\lambda^5+198\lambda^4-193\lambda^3+16\lambda^3\ln(1-\lambda)
$$

$$
-8\lambda^3\ln(1-2\lambda)+99\lambda^2-24\lambda^2\ln(1-\lambda)+24\lambda^2\ln(1-2\lambda)-21\lambda
$$

$$
+12\lambda\ln(1-\lambda)-24\lambda\ln(1-2\lambda)-2\ln(1-\lambda)+8\ln(1-2\lambda)\Big]
$$

$$
-\frac{b_2b_1\gamma_EA_1}{3\pi b_0^3(\lambda-1)^3(2\lambda-1)^3}\lambda\Big[\lambda(4\lambda(3(\lambda-3)\lambda+8)-9)+6(\lambda-1)^3\ln(1-2\lambda)
$$

$$
-3(2\lambda-1)^3\ln(1-\lambda)\Big]+\frac{b_3b_1A_1}{18\pi b_0^4(\lambda-1)^3(2\lambda-1)^3}\Big[\lambda^3(\lambda(4(18-7\lambda)\lambda-51)+6)
$$

$$
+3\lambda^2+3(2\lambda(\lambda(8\lambda-9)+3)-1)(\lambda-1)^3\ln(1-2\lambda)
$$

$$
-3(2\lambda-1)^3(\lambda(\lambda(4\lambda-9)+6)-2)\ln(1-\lambda)\Big]
$$

$$- \frac{b_4 A_1}{36\pi b_0^3(\lambda-1)^3(2\lambda-1)^3}\Big[\lambda^2(\lambda(\lambda(2\lambda(2\lambda-9)+33)-24)+6)$$
$$- 12\left(2\lambda^2-3\lambda+1\right)^3\ln(1-\lambda)+6\left(2\lambda^2-3\lambda+1\right)^3\ln(1-2\lambda)\Big].$$

In eqs. (65) to (67) we have removed some constant terms in order to make them homogeneous, *i.e.* $f_i(0)=0$, those constant can be reabsorbed in the C-term eq. (17).

The functions $f_1(\lambda), f_2(\lambda)$ and $f_3(\lambda)$ were already known in the literature. Our results agree with those in [1], [5], [25] [1]. In [25], the resummation coefficients $f_i(\lambda)$ were derived from a similar integral but instead of Laplace space they're problem factorizes in Mellin space, since in the large N limit the Mellin and Laplace transforms are equivalent appendix A, we obtain their same functional form and thus compare our results. In [5], they applied Soft-Collinear Effective Theory (SCET) theory, in which contributions from Hard (H), Collinear (or Jet, J) and Soft (S) functions are treated separately at their respective scales [26]: the hard scale of the e^-e^+ collision $\mu_H \sim Q$, the invariant mass of the two back-to-back jets eq. (49) $\mu_J^2 \sim k_1^2 + k_2^2 \sim \tau Q^2$ and the soft scale $\mu_S \sim \frac{\mu_J^2}{\mu_H} \sim \tau Q$. These functions are evaluated at their respective scales and then evolved to a common scale μ using renormalization group equations eq. (27). The cross section is then factorized into a convolution of these functions and the resummation coefficients are obtained by performing the Laplace transform of the convolution. The results of [5] are in agreement with our results; in fact their $f_1(\lambda)$ and $f_2(\lambda)$ are the same [2] as the one originally obtained in [1], however $f_3(\lambda)$ has two additional terms, one proportional to $c_s^{(1)}$ and the other to $c_j^{(1)}$ which we absorbed in the coefficients A_3 and B_2.

The functions $f_4(\lambda)$ and $f_5(\lambda)$, as far as we know they never appeared in the literature and are one the main results of the present work.

All the relevant constant can be found in Appendix C. The coefficients A_1, A_2 and B_1 were already known in [1] and were obtained from the one and two loop splitting functions. A_3 and B_2 were obtained by comparing our $f_3(\lambda)$ eq. (65) with the corresponding expression in Soft Collinear Effective Theory (SCET) [5] (Eq(4.17)) by absorbing the jet $c_J^{(1)}$ and soft $c_S^{(1)}$ terms into A_3 and B_2 terms. We also compared our G_{21} (in which B_2 appear) and G_{32} (in which both A_3 and B_2 appear) with the exact expressions of G_{21} and G_{32} in [26] and found perfect agreement.

B_3 was extracted by comparing our G_{31} in Appendix C with the exact expression of G_{31} given by [5].

Lastly A_4, A_5 and B_4 can be obtained by comparing $f_4(\lambda)$ and $f_5(\lambda)$ with the corresponding expression derived from [27] by incorporating the hard form factor of [28] as appropriate, then absorbing

[1] We assume there is a misprint in $f_3(\lambda)$ in [5], the last term proportional $A_1\beta_1^2$ in parethesis should have a plus sign instead of the minus sign.

[2] The results differ by a factor 2 because we are considering the jet mass distribution, while the thrust distributions is the convolution of two jet mass distributions eq. (50).

contribution from the jet and soft functions into A_4, A_5 and B_4.

To obtain the Laplace trasform of the thrust distribution eq. (4), we perform the Laplace transform of the convolution eq. (50). By applying the convolution theorem, we find that it is twice the integral given by eq. (24) that we have just calculated. Therefore, we multiply by 2 the $f_i(\lambda)$ we just obtained eqs. (63) to (67). The plot of J_ν^q is shown in fig. 12.

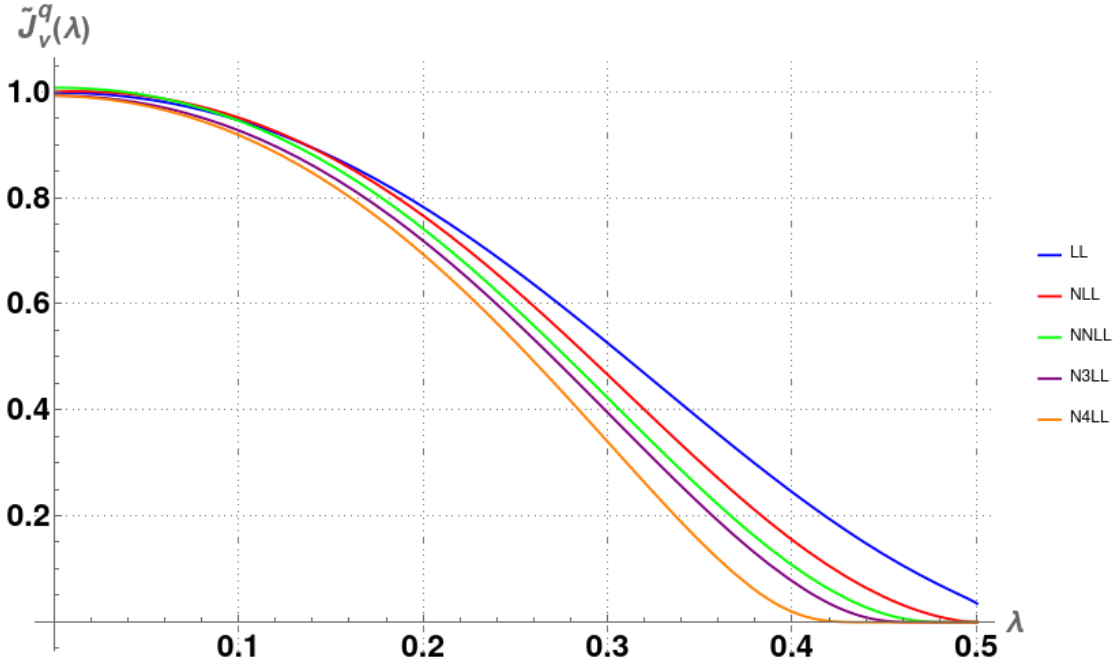

Figure 12: Plot of J_ν^q function defined in eq. (57) at different logarithmin orders.

3.2.2 Renormalization-scale dependence

In this section we consider renormalization-scale dependence of our results. In principle, such scale μ should not appear in the cross sections, as it does not correspond to any fundamental constant or kinematical scale in the problem. The completely resummed perturbative expansion of an observable is indeed formally independent on μ. In practise, truncated perturbative expansions exhibit a residual scale dependence, because of neglected higher orders.

We start with deriving the strong coupling $\alpha_s(Q^2)$ as a function of $\alpha_s(\mu^2)$ and μ^2/Q^2, to do so we expand the explicit eq. (47) in powers of $\alpha_s(\mu^2)$ and obtain:

$$\begin{aligned}\alpha_s(Q^2) = \alpha_s(\mu^2) &+ \alpha_s^2(\mu^2) b_0 \ln\left(\frac{\mu^2}{Q^2}\right) + \alpha_s^3(\mu^2)\left[b_1 \ln\left(\frac{\mu^2}{Q^2}\right) + b_0^2 \ln^2\left(\frac{\mu^2}{Q^2}\right)\right] \\ &+ \alpha_s^4(\mu^2)\left[b_2 \ln\left(\frac{\mu^2}{Q^2}\right) + \frac{5}{2} b_0 b_1 \ln^2\left(\frac{\mu^2}{Q^2}\right) + b_0^3 \ln^3\left(\frac{\mu^2}{Q^2}\right)\right] \\ &+ \alpha_s^5(\mu^2)\left[b_3 \ln\left(\frac{\mu^2}{Q^2}\right) + \left(\frac{3}{2} b_1^2 + 3 b_0 b_2\right) \ln^2\left(\frac{\mu^2}{Q^2}\right)\right. \\ &\left. + \frac{13}{3} b_0^2 b_1 \ln^3\left(\frac{\mu^2}{Q^2}\right) + b_0^4 \ln^4\left(\frac{\mu^2}{Q^2}\right)\right] + \mathcal{O}\big(\alpha_s^6(\mu^2)\big).\end{aligned} \tag{68}$$

For brevity we'll write:

$$\alpha_s(Q^2) = \alpha_s(\mu^2) + c_1 \alpha_s^2(\mu^2) + c_2 \alpha_s^3(\mu^2) + c_3 \alpha_s^4(\mu^2) + c_4 \alpha_s^5(\mu^2) + \mathcal{O}\big(\alpha_s^6(\mu^2)\big), \tag{69}$$

where c_i are the coefficients of the expansion above.

$$\begin{aligned} c_1 &= b_0 \ln\left(\frac{\mu^2}{Q^2}\right), \\ c_2 &= b_1 \ln\left(\frac{\mu^2}{Q^2}\right) + b_0^2 \ln^2\left(\frac{\mu^2}{Q^2}\right), \\ c_3 &= b_2 \ln\left(\frac{\mu^2}{Q^2}\right) + \frac{5}{2} b_0 b_1 \ln^2\left(\frac{\mu^2}{Q^2}\right) + b_0^3 \ln^3\left(\frac{\mu^2}{Q^2}\right), \\ c_4 &= b_3 \ln\left(\frac{\mu^2}{Q^2}\right) + \left(\frac{3}{2} b_1^2 + 3 b_0 b_2\right) \ln^2\left(\frac{\mu^2}{Q^2}\right) + \frac{13}{3} b_0^2 b_1 \ln^3\left(\frac{\mu^2}{Q^2}\right) + b_0^4 \ln^4\left(\frac{\mu^2}{Q^2}\right). \end{aligned} \tag{70}$$

Now we substitute eq. (68) into $\lambda = b_0 \alpha_s(Q^2) L$ and obtain:

$$\lambda(Q^2) = \lambda(\mu^2)\big(1 + c_1 \alpha_s(\mu^2) + c_2 \alpha_s^2(\mu^2) + c_3 \alpha_s^3(\mu^2) + c_4 \alpha_s^4(\mu^2) + \mathcal{O}\big(\alpha_s^5(\mu^2)\big)\big), \tag{71}$$

and formally expand in powers of $\alpha_s(\mu^2)$ all the relevant functions, now $\lambda = \lambda(\mu^2)$:

$$\begin{aligned} Lf_1(Q^2) = Lf_1(\lambda) &+ \frac{c_1}{b_0} \lambda^2 f_1'(\lambda) + \frac{\lambda}{b_0}\left(c_2 \lambda f_1'(\lambda) + \frac{1}{2} c_1^2 \lambda^2 f_1''(\lambda)\right)\alpha_s \\ &+ \frac{\lambda}{b_0}\left(c_3 \lambda f_1'(\lambda) + c_1 c_2 \lambda^2 f_1''(\lambda) + \frac{1}{6} c_1^3 f_1^{(3)}(\lambda)\right)\alpha_s^2 + \frac{\lambda^2}{b_0}\left(c_4 f_1'(\lambda)\right. \\ &\left. + \frac{1}{2} c_2^2 \lambda f_1''(\lambda) + c_1 c_3 \lambda f_1''(\lambda) + \frac{1}{2} c_1^2 c_2 \lambda^2 f_1^{(3)}(\lambda) + \frac{1}{24} c_1^4 \lambda^3 f_1^{(4)}(\lambda)\right)\alpha_s^3, \end{aligned} \tag{72}$$

$$\begin{aligned} f_2(Q^2) = f_2(\lambda) &+ c_1 \lambda f_2'(\lambda)\alpha_s + \left(c_2 \lambda f_2'(\lambda) + \frac{1}{2} c_1^2 \lambda^2 f_2''(\lambda)\right)\alpha_s^2 \\ &+ \left(c_3 \lambda f_2'(\lambda) + c_1 c_2 \lambda^2 f_2''(\lambda) + \frac{1}{6} c_1^3 f_2^{(3)}(\lambda)\right)\alpha_s^3, \end{aligned} \tag{73}$$

$$\alpha_s f_3(Q^2) = \alpha_s f_3(\lambda) + c_1 \lambda f_3'(\lambda)\alpha_s^2 + \left(c_2 \lambda f_3'(\lambda) + \frac{1}{2} c_1^2 \lambda^2 f_3''(\lambda)\right)\alpha_s^3, \tag{74}$$

$$\alpha_s^2 f_4(Q^2) = \alpha_s^2 f_4(\lambda) + c_1 \lambda f_4'(\lambda)\alpha_s^3, \tag{75}$$

$$\alpha_s^3 f_5(Q^2) = \alpha_s^3 f_5(\lambda). \tag{76}$$

As usual, the terms from the expansion proportional to α_s corrects f_3, the terms proportional to α_s^2 corrects f_4 and so on.

So the additional terms in the functions f_i, to partially compensate for the scale change $Q^2 \to \mu^2$, read:

$$\delta f_1\left(\lambda, \frac{\mu^2}{Q^2}\right) = 0, \tag{77}$$

$$\delta f_2\left(\lambda, \frac{\mu^2}{Q^2}\right) = \lambda^2 f_1'(\lambda) \log \frac{\mu^2}{Q^2}, \tag{78}$$

$$\begin{aligned}\delta f_3\left(\lambda, \frac{\mu^2}{Q^2}\right) &= \frac{1}{2} b_0 \lambda^3 f_1''(\lambda) \log^2 \frac{\mu^2}{Q^2} + \lambda^2 \left(b_0 f_1'(\lambda) \log^2 \frac{\mu^2}{Q^2} + \frac{b_1}{b_0} f_1'(\lambda) \log \frac{\mu^2}{Q^2}\right) \\ &+ b_0 \lambda f_2'(\lambda) \log \frac{\mu^2}{Q^2},\end{aligned} \tag{79}$$

$$\begin{aligned}\delta f_4\left(\lambda, \frac{\mu^2}{Q^2}\right) &= \frac{1}{6} b_0^2 \lambda^4 f_1^{(3)}(\lambda) \log^3 \frac{\mu^2}{Q^2} + \lambda^3 \left(b_0^2 f_1''(\lambda) \log^3 \frac{\mu^2}{Q^2} + b_1 f_1''(\lambda) \log^2 \frac{\mu^2}{Q^2}\right) \\ &+ \lambda^2 \left(b_0^2 f_1'(\lambda) \log^3 \frac{\mu^2}{Q^2} + \frac{5}{2} b_1 f_1'(\lambda) \log^2 \frac{\mu^2}{Q^2} + \frac{b_2}{b_0} f_1'(\lambda) \log \frac{\mu^2}{Q^2} + \frac{1}{2} b_0^2 f_2''(\lambda) \log^2 \frac{\mu^2}{Q^2}\right) \\ &+ \lambda \left(b_0^2 f_2'(\lambda) \log^2 \frac{\mu^2}{Q^2} + b_0 f_3'(\lambda) \log \frac{\mu^2}{Q^2} + b_1 f_2'(\lambda) \log \frac{\mu^2}{Q^2}\right),\end{aligned} \tag{80}$$

$$\begin{aligned}\delta f_5\left(\lambda, \frac{\mu^2}{Q^2}\right) &= \frac{1}{24} b_0^3 \lambda^5 f_1^{(4)}(\lambda) \log^4 \frac{\mu^2}{Q^2} + \lambda^4 \left(\frac{1}{2} b_0^3 f_1^{(3)}(\lambda) \log^4 \frac{\mu^2}{Q^2}\right. \\ &\left. + \frac{1}{2} b_0 b_1 f_1^{(3)}(\lambda) \log^3 \frac{\mu^2}{Q^2}\right) + \lambda^3 \left(\frac{3}{2} b_0^3 f_1''(\lambda) \log^4 \frac{\mu^2}{Q^2} + \frac{7}{2} b_0 b_1 f_1''(\lambda) \log^3 \frac{\mu^2}{Q^2}\right. \\ &\left. + \frac{b_1^2}{2b_0} f_1''(\lambda) \log^2 \frac{\mu^2}{Q^2} + b_2 f_1''(\lambda) \log^2 \frac{\mu^2}{Q^2} + \frac{1}{6} b_0^3 f_2^{(3)}(\lambda) \log^3 \frac{\mu^2}{Q^2}\right) \\ &+ \lambda^2 \left(b_0^3 f_1'(\lambda) \log^4 \frac{\mu^2}{Q^2} + \frac{13}{3} b_0 b_1 f_1'(\lambda) \log^3 \frac{\mu^2}{Q^2} + \frac{3b_1^2}{2b_0} f_1'(\lambda) \log^2 \frac{\mu^2}{Q^2}\right. \\ &\left. + 3 b_2 f_1'(\lambda) \log^2 \frac{\mu^2}{Q^2} + \frac{b_3}{b_0} f_1'(\lambda) \log \frac{\mu^2}{Q^2} + b_0^3 f_2''(\lambda) \log^3 \frac{\mu^2}{Q^2} + b_0 b_1 f_2''(\lambda) \log^2 \frac{\mu^2}{Q^2}\right. \\ &\left. + \frac{1}{2} b_0^2 f_3''(\lambda) \log^2 \frac{\mu^2}{Q^2}\right) + \lambda \left(b_0^3 f_2'(\lambda) \log^3 \frac{\mu^2}{Q^2} + b_0^2 f_3'(\lambda) \log^2 \frac{\mu^2}{Q^2}\right. \\ &\left. + \frac{5}{2} b_1 b_0 f_2'(\lambda) \log^2 \frac{\mu^2}{Q^2} + b_0 f_4'(\lambda) \log \frac{\mu^2}{Q^2} + b_2 f_2'(\lambda) \log \frac{\mu^2}{Q^2} + b_1 f_3'(\lambda) \log \frac{\mu^2}{Q^2}\right).\end{aligned} \tag{81}$$

By varying the renormalization scale μ in the range $Q/2 \leq \mu \leq 2Q$, where $Q = m_Z$ we can estimate the uncertainty due to the truncation of the perturbative expansion.

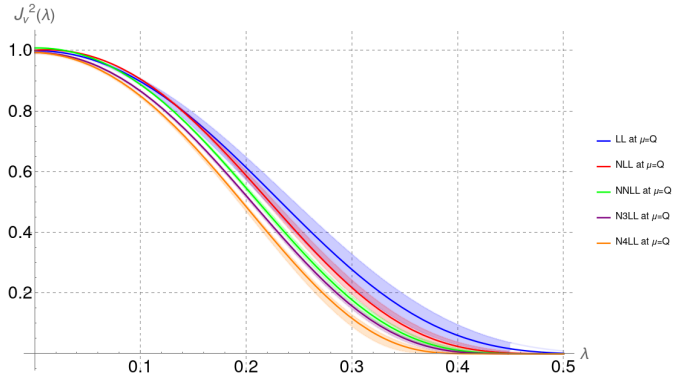

Figure 13: Plot of J_ν^2 eq. (57). Dependence on renormalization scale μ for LL, NLL, NNLL, $\mathrm{N^3LL}$ and $\mathrm{N^3LL}$ logarithmic accuracy.

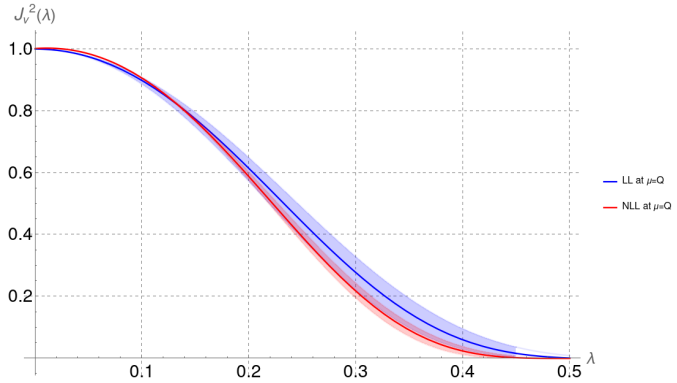

Figure 14: Scale variation of the Laplace transformed Thrust distribution eq. (57) for Leading Logarithm and Next-to-Leading Logarithm accuracy.

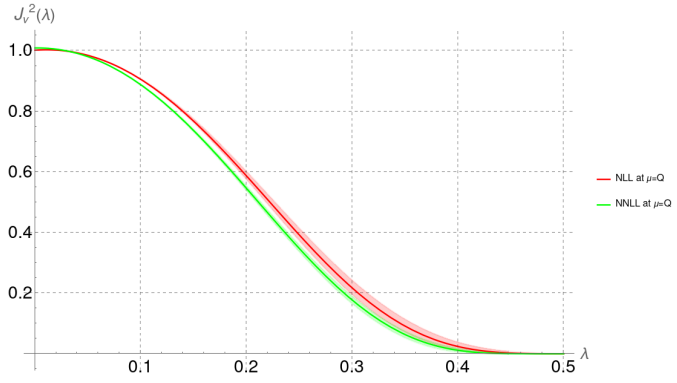

Figure 15: Scale variation of the Laplace transformed Thrust distribution eq. (57) for NLL and NNLL.

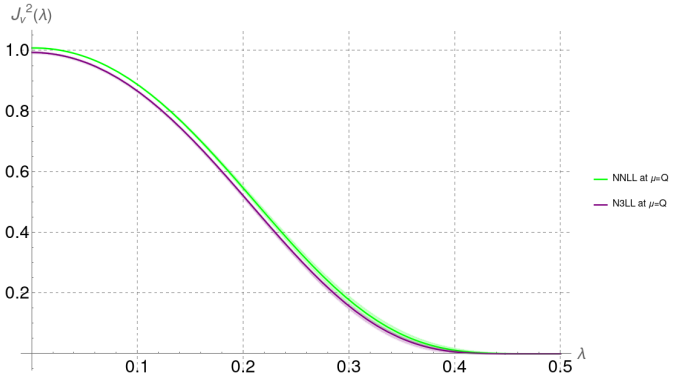

Figure 16: Scale variation of the Laplace transformed Thrust distribution eq. (57) for NNLL and N^{3}LL.

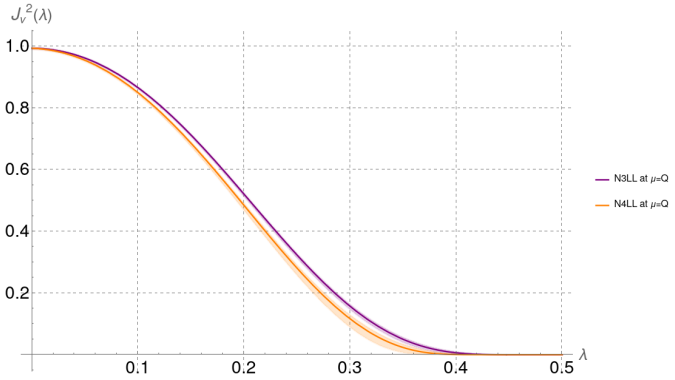

Figure 17: Scale variation of the Laplace transformed Thrust distribution eq. (57) for N^{3}LL and N^{4}LL.

We observe how the scale dependence decreases as we increase the logarithmic accuracy of the resummation. The N^{3}LL result is the most stable under scale variations, while N^{4}LL has some anomalous behavious, this indicates that the N^{4}LL result might not be fully reliable. In the following sections we will only use results up to N^{3}LL accuracy.

3.3 Inversion of the Laplace transform

In order to find the quark jet mass distribution $J^q(Q^2, k^2)$ or $R_T(\tau)$, we have to perform the inverse Laplace transform via the Mellin's inversion formula (or the Bromwich integral) given by the line integral:

$$J^q(Q^2, k^2) = \frac{1}{2\pi i} \lim_{T\to\infty} \int_{C-iT}^{C+iT} \mathrm{d}\nu e^{\nu k^2} \tilde{J}_\nu^q(Q^2), \tag{82}$$

where C is a real number such that it is at the right of all singularities of the integrand in the complex

plane and the function $\tilde{J}^q_\nu(Q^2)$ has to be bounded on the line.

Instead of working with the differential quark jet mass distribution J^q, it more convenient to deal with the mass fraction $R^q(w)$, which gives the fraction of jets with masses less than wQ^2 (cumulant distribution):

$$R^q(w) = \int_0^\infty J^q(Q^2, k^2)\Theta(wQ^2 - k^2)\mathrm{d}k^2. \tag{83}$$

Using the integral representation of the Heaviside step function eq. (52):

$$\Theta(wQ^2 - k^2) = \frac{1}{2\pi i}\lim_{T\to\infty}\int_{C-iT}^{C+iT}\frac{\mathrm{d}\nu}{\nu}e^{\nu(wQ^2-k^2)}, \tag{84}$$

we recognize the Laplace transform of the quark jet mass distribution eq. (51)

$$\begin{aligned}
R^q(w) &= \frac{1}{2\pi i}\lim_{T\to\infty}\int_{C-iT}^{C+iT}\frac{\mathrm{d}\nu}{\nu}e^{w\nu Q^2}\int_0^\infty J^q(Q^2,k^2)e^{-\nu k^2}\mathrm{d}k^2 \\
&= \frac{1}{2\pi i}\lim_{T\to\infty}\int_{C-iT}^{C+iT}\frac{\mathrm{d}\nu}{\nu}e^{w\nu Q^2}\tilde{J}^q_\nu(Q^2) \\
&= \frac{1}{2\pi i}\lim_{T\to\infty}\int_{C-iT}^{C+iT}\frac{\mathrm{d}\nu}{\nu}e^{w\nu Q^2}e^{\mathcal{F}(\alpha_s,\ln(\nu Q^2))} \\
&= \frac{1}{2\pi i}\lim_{T\to\infty}\int_{C'-iT}^{C'+iT}\frac{\mathrm{d}N}{N}e^{wN}e^{\mathcal{F}(\alpha_s,\ln N)},
\end{aligned} \tag{85}$$

where $N = \nu Q^2$ and $\mathcal{F}$ has the logarithms expansion:

$$\begin{aligned}
\mathcal{F}(\alpha_s, \ln N) = {} & f_1(b_0\alpha_s\ln N)\ln N + f_2(b_0\alpha_s\ln N) + f_3(b_0\alpha_s\ln N)\alpha_s \\
& + f_4(b_0\alpha_s\ln N)\alpha_s^2 + f_5(b_0\alpha_s\ln N)\alpha_s^3 + \mathcal{O}\big(\alpha_s^4\big).
\end{aligned} \tag{86}$$

Since the function $\mathcal{F}$ in the exponent varies more slowly with N than wN, we can introduce the integration variable $u = wN$ so that $\ln N = \ln u + \ln\frac{1}{w} = \ln u + L$ and Taylor expand with respect to $\ln u$ around 0, which is equivalent to expanding the original function $\mathcal{F}$ w.r.t $\ln N$ around $\ln N \approx \ln\frac{1}{w} \equiv L$:

$$\begin{aligned}
R^q(w) &= \frac{1}{2\pi i}\int_C\frac{\mathrm{d}u}{u}e^u e^{\mathcal{F}(\alpha_s,\ln u+L)} \\
&\overset{\text{Taylor}}{=} \int_C\frac{\mathrm{d}u}{2\pi i}e^{u-\ln u}e^{\mathcal{F}(\alpha_s,L)+\sum_{n=1}^\infty\frac{\mathcal{F}^{(n)}(\alpha_s,L)}{n!}\ln^n u} \\
&= e^{\mathcal{F}(\alpha_s,L)}\int_C\frac{\mathrm{d}u}{2\pi i}e^{u-\ln u}e^{\sum_{n=1}^\infty\frac{\mathcal{F}^{(n)}(\alpha_s,L)}{n!}\ln^n u},
\end{aligned} \tag{87}$$

where the integral is intended as before, along the line C to the right of all singularities of the integrand, and

$$\mathcal{F}^{(n)}(\alpha_s, L) = \frac{\partial^n \mathcal{F}(\alpha_s, \ln u + L)}{\partial (\ln u)^n}\bigg|_{\ln u=0}. \tag{88}$$

The n-th derivative of $\mathcal{F}$ w.r.t $\ln u$ evaluated at $\ln u = 0$ is at most of logarithmic order $\alpha_s^{n+k-1} L^k$ [1], so in order to achieve N^{4}LL accuracy we need to compute the first four derivatives of $\mathcal{F}$ w.r.t $\ln u$ and neglect the terms of order $\mathcal{O}\big(\alpha_s^4\big)$ that appear in the derivation. We obtain the following expressions:

$$\begin{aligned}\mathcal{F}^{(1)}(\alpha_s, L) = f_1(\lambda) + \lambda f_1'(\lambda) + \alpha_s b_0 f_2'(\lambda) + \alpha_s^2 b_0 f_3'(\lambda) + \alpha_s^3 b_0 f_4'(\lambda) \\ + \mathcal{O}\big(\alpha_s^n L^{n-3}\big),\end{aligned} \tag{89}$$

$$\begin{aligned}\mathcal{F}^{(2)}(\alpha_s, L) = 2\alpha_s b_0 f_1'(\lambda) + \alpha_s b_0 \lambda f_1''(\lambda) + \alpha_s^2 b_0^2 f_2''(\lambda) + \alpha_s^3 b_0^2 f_3''(\lambda) \\ + \mathcal{O}\big(\alpha_s^n L^{n-3}\big),\end{aligned} \tag{90}$$

$$\mathcal{F}^{(3)}(\alpha_s, L) = 3\alpha_s^2 b_0^2 f_1''(\lambda) + \alpha_s^2 b_0^2 \lambda f_1^{(3)}(\lambda) + \alpha_s^3 b_0^3 f_2^{(3)}(\lambda) + \mathcal{O}\big(\alpha_s^n L^{n-3}\big), \tag{91}$$

$$\mathcal{F}^{(4)}(\alpha_s, L) = 4\alpha_s^3 b_0^3 f_1^{(3)}(\lambda) + \alpha_s^3 b_0^3 \lambda f_1^{(4)}(\lambda) + \mathcal{O}\big(\alpha_s^n L^{n-3}\big), \tag{92}$$

Here $\lambda = \alpha_s b_0 L$ and derivative w.r.t $\ln u$ and then evaluated at $\ln u = 0$, or equivalently derivative w.r.t L gives the same result.

After recasting the expansion presented in eq. (87) using the expression $\gamma(\alpha_s, L) = f_1(\lambda) + \lambda f_1'(\lambda)$ from [1], and defining $\mathcal{F}_{res}^{(1)}(\alpha_s, L) \equiv \mathcal{F}^{(1)}(\alpha_s, L) - \gamma(\alpha_s, L)$, we proceed to expand the second exponential with respect to $\ln u$ around 0, following the approach outlined in [29]. This yields the subsequent expansion:

$$\begin{aligned}R^q(w) &= e^{\mathcal{F}(\alpha_s, L)} \int_C \frac{\mathrm{d}u}{2\pi i} e^{u - (1-\gamma(\alpha_s, L))\ln u} e^{\mathcal{F}_{res}^{(1)}(\alpha_s, L)\ln u + \sum_{n=2}^{\infty} \frac{\mathcal{F}^{(n)}(\alpha_s, L)}{n!} \ln^n u} \\ &= \int_C \frac{\mathrm{d}u}{2\pi i} e^{u - (1-\gamma(\alpha_s, L))\ln u} \bigg(1 + \mathcal{F}_{res}^{(1)} \ln u + \frac{1}{2}\Big(\mathcal{F}^{(2)} + (\mathcal{F}_{res}^{(1)})^2\Big)\ln^2 u \\ &+ \frac{1}{6}\Big(\mathcal{F}^{(3)} + 3\mathcal{F}^{(2)}\mathcal{F}_{res}^{(1)} + (\mathcal{F}_{res}^{(1)})^3\Big)\ln^3 u \\ &+ \frac{1}{24}\Big(\mathcal{F}^{(4)} + 3(\mathcal{F}^{(2)})^2 + 4\mathcal{F}^{(3)}\mathcal{F}_{res}^{(1)} + 6\mathcal{F}^{(2)}(\mathcal{F}_{res}^{(1)})^2 + (\mathcal{F}_{res}^{(1)})^4\Big)\ln^4 u \\ &+ \mathcal{O}\big(\ln^5 u\big)\bigg).\end{aligned} \tag{93}$$

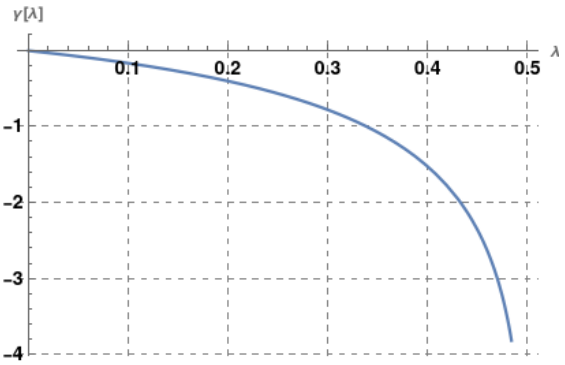

Figure 18: Plot of $\gamma(\lambda)$ in the range of interest $0 < \lambda < \frac{1}{2}$

Lastly, we utilize the following result to evaluate the integral presented in eq. (83):

$$\int_C \frac{\mathrm{d}u}{2\pi i} \ln^k u e^{u-(1-\gamma(\alpha_s,L))\ln u} = \frac{\mathrm{d}^k}{\mathrm{d}\gamma^k} \frac{1}{\Gamma(1-\gamma(\alpha_s,L))}, \tag{94}$$

where Γ is the Euler Γ-function, notice that for $k = 0$ the integral is the Hankel integral representation of the Γ-function:

$$\frac{1}{2\pi i} \int_C \mathrm{d}u e^u u^{-(1-\gamma(\alpha_s,L))} = \frac{1}{\Gamma(1-\gamma(\alpha_s,L))}. \tag{95}$$

The reciprocal of the Euler Γ-function is an entire function, meaning that it has no singularities in the complex plane, it's holomorphic everywhere. The above integral eq. (94) can be evaluated by differentiating with respect to $\gamma(\lambda)$ k times, and it is straightforward to see that each derivation inside the integral gives a factor of $\ln u$. Interchaning the order of derivation and integration is justified by the fact that the integral:

- is a contour integral whose contour doesn't depent on $\gamma(\lambda)$, and the function is holomorphic in the complex plane for each value of $\gamma(\lambda) \in (\infty, 0]$ (fig. 18)
- is dominated by the exponential factor $e^{u-(1-\gamma(\lambda))\ln u}$ as long as $\mathrm{Re}\{u\} > 0$.

$$\begin{aligned} R^q(w) = \frac{e^{\mathcal{F}(\alpha_s,L)}}{\Gamma(1-\gamma(\lambda))} \Bigg[& 1 + \mathcal{F}^{(1)}_{res}\psi_0 + \frac{1}{2}\Big(\mathcal{F}^{(2)} + (\mathcal{F}^{(1)}_{res})^2\Big)\big(\psi_0^2 - \psi_1\big) \\ & + \frac{1}{6}\Big(\mathcal{F}^{(3)} + 3\mathcal{F}^{(2)}\mathcal{F}^{(1)}_{res} + (\mathcal{F}^{(1)}_{res})^3\Big)\big(\psi_0^3 - 3\psi_0\psi_1 + \psi_2\big) \\ & + \frac{1}{24}\Big(\mathcal{F}^{(4)} + 3(\mathcal{F}^{(2)})^2 + 4\mathcal{F}^{(3)}\mathcal{F}^{(1)}_{res} + 6\mathcal{F}^{(2)}(\mathcal{F}^{(1)}_{res})^2 + (\mathcal{F}^{(1)}_{res})^4\Big) \\ & \big(\psi_0^4 - 6\psi_1 + 3\psi_1^3 + 4\psi_0\psi_2 - \psi_3\big) + \mathcal{O}\big(\ln^5 u\big)\Bigg], \end{aligned} \tag{96}$$

where ψ_n are the polygamma functions all evaluated at $(1-\gamma(\lambda))$, defined as:

$$\psi_n(z) = \frac{\mathrm{d}^{n+1}}{\mathrm{d}z^{n+1}} \ln\Gamma(z) = \frac{\mathrm{d}^n}{\mathrm{d}z^n}\frac{\Gamma'(z)}{\Gamma(z)} = \frac{\mathrm{d}^n}{\mathrm{d}z^n}\psi_0(z). \tag{97}$$

The expression eq. (96) can be verified against Eq.(56) in [29] and Eq.(4.28) in [5]. It is noteworthy that they share the same structure within the square brackets, the difference is that they don't include $(\mathcal{F}^{(1)}_{res})^2$ in the second term. This omission is due to the fact that $(\mathcal{F}^{(1)}_{res})^2$ is a term of order $\mathcal{O}\big(\alpha_s^2\big)$ and thus contributes to the N^{3}LL accuracy.

Substituting the expressions eqs. (89) to (92) into eq. (96) we obtain:

$$\begin{aligned}
R^q(w) = \frac{e^{\mathcal{F}(\alpha_s,L)}}{\Gamma(1-\gamma)}\Big[1 &+ \Big(\alpha_s^3 b_0 f_4'(\lambda) + \alpha_s^2 b_0 f_3'(\lambda) + \alpha_s b_0 f_2'(\lambda)\Big)\psi_0 \\
&+ \frac{1}{2}\Big(\alpha_s^3(2b_0^2 f_2'(\lambda)f_3'(\lambda) + b_0^2 f_3''(\lambda)) + \frac{1}{2}\alpha_s^2\big(b_0^2 f_2''(\lambda) + b_0^2 f_2'(\lambda)^2\big) \\
&+ \frac{1}{2}\alpha_s(b_0\lambda f_1''(\lambda) + 2b_0 f_1'(\lambda))\Big)\big(\psi_0^2 - \psi_1\big) \\
&+ \frac{1}{6}\Big(\alpha_s^3(b_0^3 f_2^{(3)}(\lambda) + b_0^3 f_2'(\lambda)^3 + 3b_0^3 f_2'(\lambda)f_2''(\lambda) + 3b_0^2\lambda f_1''(\lambda)f_3'(\lambda) \\
&+ 6b_0^2 f_1'(\lambda)f_3'(\lambda)) + \frac{1}{6}\alpha_s^2(b_0^2\lambda f_1^{(3)}(\lambda) + 3b_0^2\lambda f_1''(\lambda)f_2'(\lambda) + 3b_0^2 f_1''(\lambda) \\
&+ 6b_0^2 f_1'(\lambda)f_2'(\lambda))\Big)\big(\psi_0^3 - 3\psi_0\psi_1 + \psi_2\big) \\
&+ \frac{1}{24}\Big(\alpha_s^3(b_0^3\lambda f_1^{(4)}(\lambda) + 4b_0^3\lambda f_1^{(3)}(\lambda)f_2'(\lambda) \\
&+ 4b_0^3 f_1^{(3)}(\lambda) + 6b_0^3\lambda f_1''(\lambda)f_2''(\lambda) + 6b_0^3\lambda f_1''(\lambda)f_2'(\lambda)^2 + 12b_0^3 f_1''(\lambda)f_2'(\lambda) \\
&+ 12b_0^3 f_1'(\lambda)f_2''(\lambda) + 12b_0^3 f_1'(\lambda)f_2'(\lambda)^2) + \frac{1}{8}\alpha_s^2(b_0^2\lambda^2 f_1''(\lambda)^2 + 4b_0^2 f_1'(\lambda)^2 \\
&+ 4b_0^2\lambda f_1'(\lambda)f_1''(\lambda))\Big)\big(\psi_0^4 - 6\psi_1 + 3\psi_1^3 + 4\psi_0\psi_2 - \psi_3\big) + \mathcal{O}\big(\ln^5 u\big)\Big],
\end{aligned} \tag{98}$$

and reorganize as a power series of α_s:

$$\begin{aligned}
R^q(w) = \frac{e^{\mathcal{F}(\alpha_s,L)}}{\Gamma(1-\gamma)}\Big[1 &+ \alpha_s b_0\Big(\psi_0 f_2'(\lambda) + \frac{1}{2}(\psi_0^2 - \psi_1)(\lambda f_1''(\lambda) \\
&+ 2f_1'(\lambda))\Big) + \alpha_s^2\Big(\frac{1}{8}(\psi_0^4 - 6\psi_1 + 3\psi_1^3 + 4\psi_0\psi_2 - \psi_3)(b_0^2\lambda^2 f_1''(\lambda)^2 \\
&+ 4b_0^2 f_1'(\lambda)^2 + 4b_0^2\lambda f_1'(\lambda)f_1''(\lambda)) + \frac{1}{6}(\psi_0^3 - 3\psi_0\psi_1 + \psi_2)(b_0^2\lambda f_1^{(3)}(\lambda) \\
&+ 3b_0^2\lambda f_1''(\lambda)f_2'(\lambda) + 3b_0^2 f_1''(\lambda) + 6b_0^2 f_1'(\lambda)f_2'(\lambda)) + \frac{1}{2}(\psi_0^2 - \psi_1) \\
&(b_0^2 f_2''(\lambda) + b_0^2 f_2'(\lambda)^2) + b_0\psi_0 f_3'(\lambda)\Big) + \alpha_s^3\Big(\frac{1}{24}(\psi_0^4 - 6\psi_1 + 3\psi_1^3 + 4\psi_0\psi_2 \\
&- \psi_3)(b_0^3\lambda f_1^{(4)}(\lambda) + 4b_0^3\lambda f_1^{(3)}(\lambda)f_2'(\lambda) + 4b_0^3 f_1^{(3)}(\lambda) + 6b_0^3\lambda f_1''(\lambda)f_2''(\lambda)
\end{aligned} \tag{99}$$

$$
\begin{aligned}
&+ 6b_0^3\lambda f_1''(\lambda)f_2'(\lambda)^2 + 12b_0^3 f_1''(\lambda)f_2'(\lambda) + 12b_0^3 f_1'(\lambda)f_2''(\lambda) + 12b_0^3 f_1'(\lambda)f_2'(\lambda)^2)\\
&+ \frac{1}{2}(\psi_0^2 - \psi_1)(2b_0^2 f_2'(\lambda)f_3'(\lambda) + b_0^2 f_3''(\lambda)) + \frac{1}{6}(\psi_0^3 - 3\psi_0\psi_1\\
&+ \psi_2)(b_0^3 f_2^{(3)}(\lambda) + b_0^3 f_2'(\lambda)^3 + 3b_0^3 f_2'(\lambda)f_2''(\lambda) + 3b_0^2\lambda f_1''(\lambda)f_3'(\lambda)\\
&+ 6b_0^2 f_1'(\lambda)f_3'(\lambda)) + b_0\psi_0 f_4'(\lambda)\Big) + \mathcal{O}\big(\alpha_s^4\big)\Big].
\end{aligned}
$$

As observed in the previous section, to obtain the Thrust cross section, we simply multiply by 2 all the f_i eqs. (63) to (67). The final resummed expression $R_T(\tau)$ can be written as one exponential eq. (19),

$$
R_T(\tau) = \left(1 + \sum_{n=1}^{\infty} C_n \bar{\alpha}_s^n\right) \exp\big[L g_1(\lambda) + g_2(\lambda) + g_3(\lambda)\alpha_s + g_4(\lambda)\alpha_s^2 + g_5(\lambda)\alpha_s^3 + \mathcal{O}\big(\alpha_s^4\big)\big]. \quad (100)
$$

To do so, we observe that $\frac{1}{\Gamma(1-\gamma)} = \exp\{-\ln(\Gamma(1-\gamma))\}$ corrects f_2, while the expression in square parenthesis in eq. (99) can be seen as the expansion of an exponential for $\alpha_s \to 0$, the reason for this is that since we integrated an exponential function in eq. (85), we expect to find an exponential function as the result of the integration

$$
\begin{aligned}
\exp\big(\alpha_s g_3(\lambda) + \alpha_s^2 g_4(\lambda) + \alpha_s^3 g_5(\lambda) + \mathcal{O}\big(\alpha_s^4\big)\big) = 1 + \alpha_s g_3(\lambda) + \frac{1}{2}\alpha_s^2\big(g_3^2(\lambda) + 2g_4(\lambda)\big)\\
+ \frac{1}{6}\alpha_s^3\big(g_3^3(\lambda) + 6g_3(\lambda)g_4(\lambda) + 6g_5(\lambda)\big) + \mathcal{O}\big(\alpha_s^4\big).
\end{aligned} \quad (101)
$$

To obtain $g_3(\lambda)$, $g_4(\lambda)$ and $g_5(\lambda)$ we match eq. (99) with eq. (101) and obtain the following expressions in which all the Polygamma functions ψ_n are evaluated at $1-\gamma(\lambda)$ as before, and the functions f_i are twice the ones obtained in the previous section eqs. (63) to (67):

$$
\begin{aligned}
g_1(\lambda) &= f_1(\lambda), && (102)\\
g_2(\lambda) &= f_2(\lambda) - \ln\Gamma(1 - f_1(\lambda) - \lambda f_1'(\lambda)), && (103)\\
g_3(\lambda) &= f_3(\lambda) + \Big(\psi_0(1-\gamma(\lambda))f_2'(\lambda) + \frac{1}{2}(\psi_0^2 - \psi_1)(1-\gamma)(\lambda f_1''(\lambda) + 2f_1'(\lambda))\Big), && (104)\\
g_4(\lambda) &= f_4(\lambda) + \Big(\frac{1}{8}(\psi_0^4 - 6\psi_1 + 3\psi_1^3 + 4\psi_0\psi_2 - \psi_3)(1-\gamma(\lambda))(b_0^2\lambda^2 f_1''(\lambda)^2 && (105)\\
&\quad + 4b_0^2 f_1'(\lambda)^2 + 4b_0^2\lambda f_1'(\lambda)f_1''(\lambda)) + \frac{1}{6}(\psi_0^3 - 3\psi_0\psi_1 + \psi_2)(1-\gamma(\lambda))(b_0^2\lambda f_1^{(3)}(\lambda)\\
&\quad + 3b_0^2\lambda f_1''(\lambda)f_2'(\lambda) + 3b_0^2 f_1''(\lambda) + 6b_0^2 f_1'(\lambda)f_2'(\lambda)) + \frac{1}{2}(\psi_0^2 - \psi_1)(1-\gamma)\\
&\quad (b_0^2 f_2''(\lambda) + b_0^2 f_2'(\lambda)^2) + b_0\psi_0(1-\gamma(\lambda))f_3'(\lambda)\Big),
\end{aligned}
$$

$$
\begin{aligned}
g_5(\lambda) = f_5(\lambda) + \Big(& \frac{1}{24}(\psi_0^4 - 6\psi_1 + 3\psi_1^3 + 4\psi_0\psi_2 - \psi_3)(1-\gamma(\lambda)) \\
& (b_0^3\lambda f_1^{(4)}(\lambda) + 4b_0^3\lambda f_1^{(3)}(\lambda) f_2'(\lambda) + 4b_0^3 f_1^{(3)}(\lambda) + 6b_0^3\lambda f_1''(\lambda) f_2''(\lambda) \\
& + 6b_0^3\lambda f_1''(\lambda) f_2'(\lambda)^2 + 12b_0^3 f_1''(\lambda) f_2'(\lambda) + 12b_0^3 f_1'(\lambda) f_2''(\lambda) + 12b_0^3 f_1'(\lambda) f_2'(\lambda)^2) \\
& + \frac{1}{2}(\psi_0^2 - \psi_1)(1-\gamma(\lambda))(2b_0^2 f_2'(\lambda) f_3'(\lambda) + b_0^2 f_3''(\lambda)) + \frac{1}{6}(\psi_0^3 - 3\psi_0\psi_1 + \psi_2)(1-\gamma) \\
& (b_0^3 f_2^{(3)}(\lambda) + b_0^3 f_2'(\lambda)^3 + 3b_0^3 f_2'(\lambda) f_2''(\lambda) + 3b_0^2\lambda f_1''(\lambda) f_3'(\lambda) + 6b_0^2 f_1'(\lambda) f_3'(\lambda)) \\
& + b_0\psi_0(1-\gamma) f_4'(\lambda)\Big).
\end{aligned}
\tag{106}
$$

The procedure we just described extends the NLL [1] and NNLL [5] results for the analytical Laplace inversion to N^{3}LL and N^{4}LL accuracy.

The thrust differential distribution eq. (2) is obtained by taking the derivative of the thrust cross section $R_T(\tau)$ eq. (19) with respect to τ:

$$
\frac{1}{\sigma}\frac{\mathrm{d}\sigma}{\mathrm{d}\tau} = \frac{1}{\tau}\frac{\mathrm{d}R_T(\tau)}{\mathrm{d}\ln\tau}
\tag{107}
$$

Observe that resummation has cured the unphysical divergence for $\tau \to 0$ of the fixed order prediction (fig. 7). The fact that the thrust distribution vanishes at $\tau \to 0$ (fig. 19) has a simple physical interpretation [1]. At the parton model level the e^+e^- annihilation process produces a quark-antiquark pair. Since both the quark and the antiquark carry colour charge they are necessarily accompanied by their own bremsstrahlung (radiation of soft gluons) and the ensuing configuration has $\tau \neq 0$. The vanishing of the thrust distribution for $\tau \to 0$ thus corresponds to the impossibility of producing a bare charge in gauge theories.

We observe in fig. 19 that the peak of the distribution is closer to the experimental data as we increase the logarithmic accuracy, this is expected since the resummation of the logarithms is supposed to improve the accuracy of the prediction.

However, the peak also becomes lower while the tail of the distribution becomes higher, this means that if we set the value of the coupling to be $\alpha_s = 0.118$, there's too much radiation. To fix this, we would need to decrease the value of the coupling to have a better agreement, which then would lead us to extract a lower value of α_s with respect to the world average.

Increasing the coupling means to increase the intensity of the strong interaction, which in turn means that the quarks are more likely to radiate more particles, this is why the tail of the distribution is higher while the peak is lower for higher values of the coupling

We also observe that the tail of the distribution (Figure 20) is not well described by the resummed expression, this is as expected since the resummation tackles the problem of large logarithms in the $\tau \to 0$

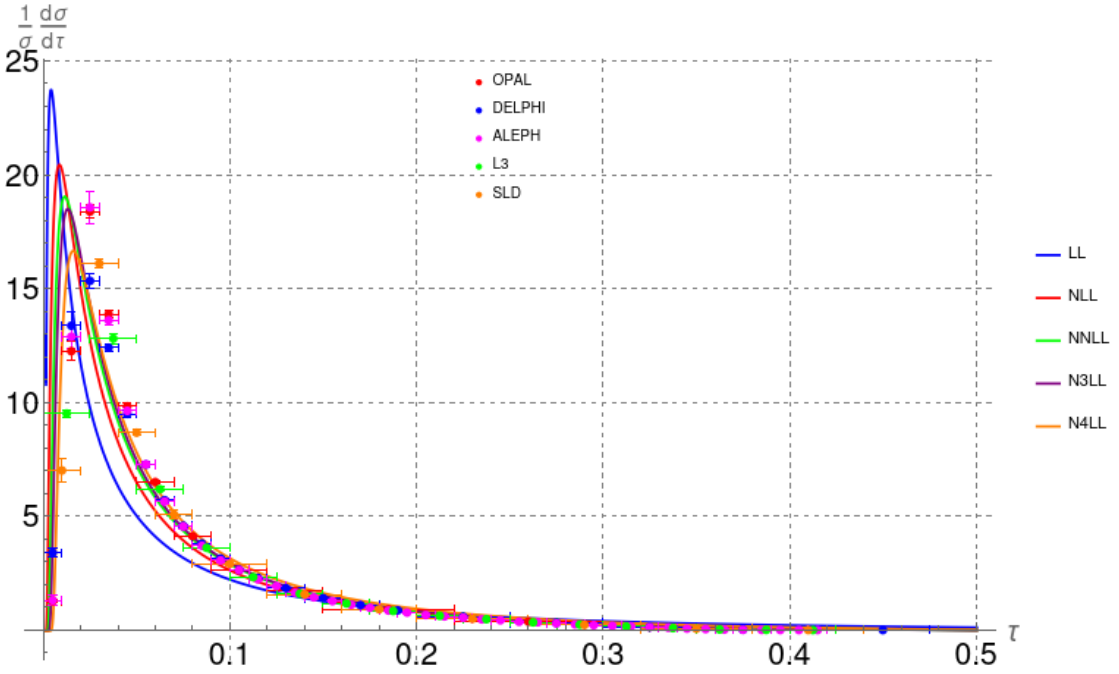

Figure 19: Plot of eq. (19) for different logarithmic accuracy orders, with coupling $\alpha_s(m_Z) = 0.118$.

region, for the tail of the distribution we would need to include the fixed order corrections. We'll see in the next section how to combine the resummed expression with the fixed order corrections to obtain a more accurate prediction in a greater range of τ.

3.4 Matching of resummation to fixed-order calculations

Having obtained a resummed expression such as eq. (100) for the shape cross sections at small values of τ, one can now match the resummed expression to the fixed-order NNLO calculations at large values of τ using the R-matching scheme [1]. The results presented in the previous sections allow us to compare the predictions at N^{3}LL accuracy with the fixed-order calculations at NNLO.

In the R-matching scheme, at N^{3}LL+NNLO accuracy the matching procedure is given by:

$$\begin{aligned} R_T(\tau) = (1 + C_1\bar{\alpha}_s + C_2\bar{\alpha}_s^2 + C_3\bar{\alpha}_s^3)\exp\{Lg_1(\lambda) + g_2(\lambda) + \alpha_s g_3(\lambda) + \alpha_s^2 g_4(\lambda)\} \\ + D_1(\tau)\bar{\alpha}_s + D_2(\tau)\bar{\alpha}_s^2 + D_3(\tau)\bar{\alpha}_s^3, \end{aligned} \tag{108}$$

where the coefficients C_i are determined by imposing the normalization $R_T(\tau_{max}) = 1$ of the fixed

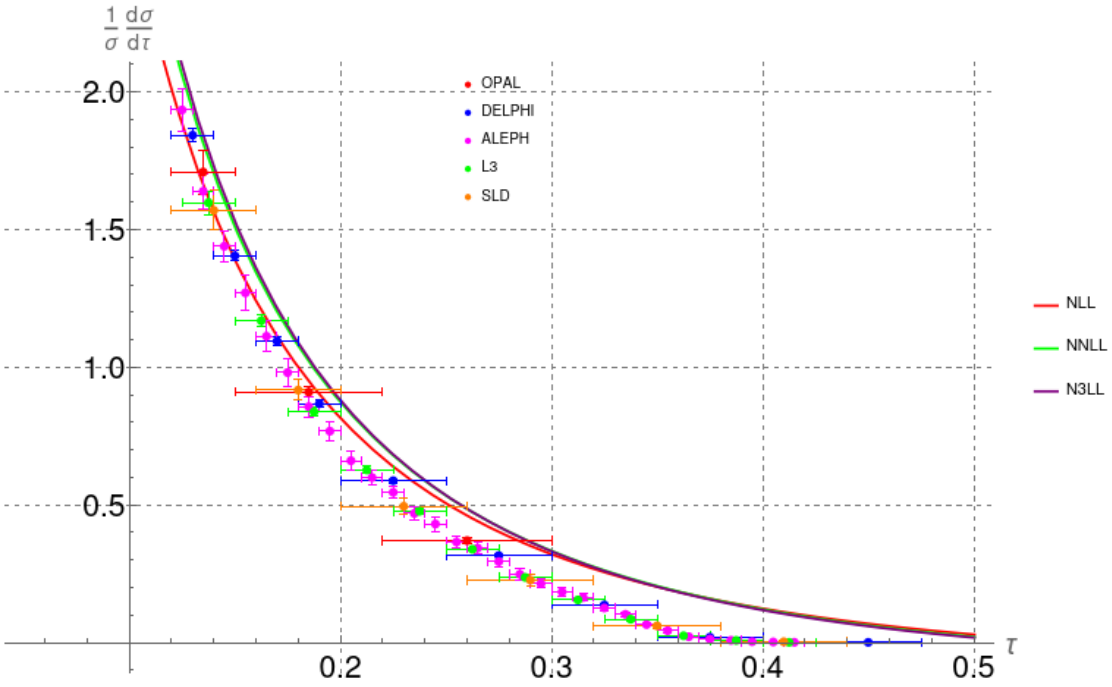

Figure 20: Zoom-in in the tail region of the resummed thrust differential distribution eq. (19) for different logarithmic accuracy orders, with fixed scale $\alpha_s = 0.118$.

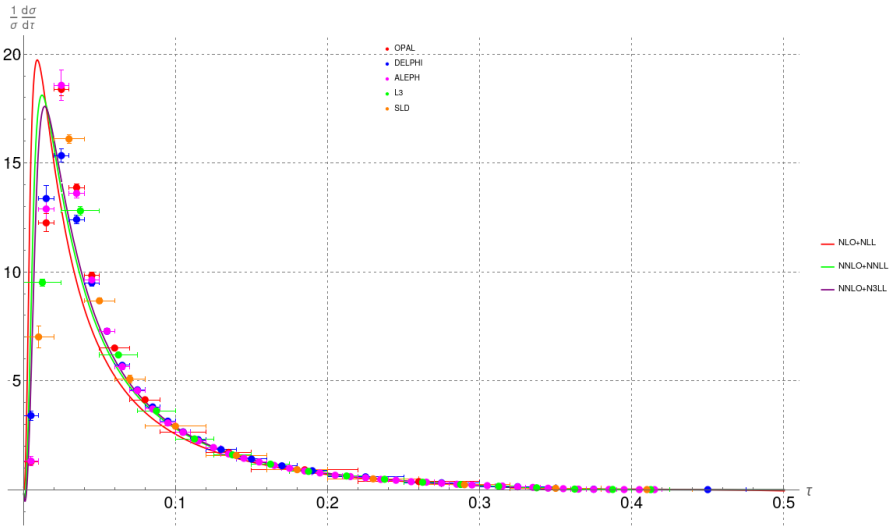

Figure 21: Plot of the matched Thrust distribution eq. (108) at NNLO+N^{3}LL accuracy.

order calculation order by order, while the remainder function D_i are determined by subtracting from the fixed order terms A, B and C the logarithmic terms already present in eq. (19) (see eq. (23)).

D_1 is analytical [1]:

$$D_1(\tau) = C_F\Big(-4\mathrm{Li}_2\left(\frac{t}{1-t}\right) + \frac{9t^2}{2} - 2\ln^2(1-t) + 6t(\ln(t)+1) \\ + 4\ln(1-t)\ln(t) + 3(1-2t)\ln(1-2t)\Big), \tag{109}$$

while D_2 and D_3 are extracted numerically from interpolating the fixed order results at NNLO given in [6], the results are shown in fig. 7.

By combining the resummed expression eq. (19) and the fixed order results at NNLO, we can obtain the matched results at N^{3}LL+NNLO accuracy, we also reproduced the NLO+NLL [1], [16] and NNLO+NNLL [5] accuracy already present in literature. The results are shown in fig. 21.

Resummation only slightly improves the fixed-order results at large values of τ as it includes some terms from higher orders in the perturbative expansion eq. (10), see table 2.

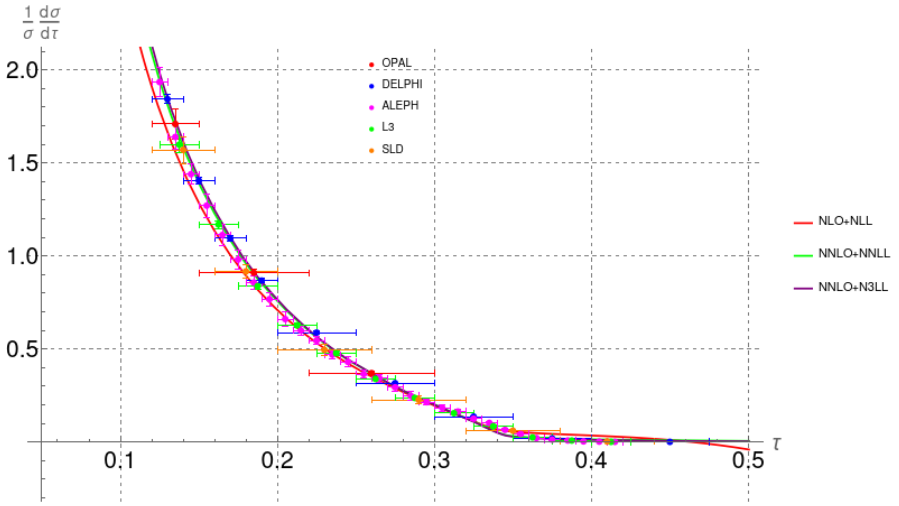

Figure 22: Plot of the matched Thrust distribution at NNLO+N^{3}LL and NNLO+NNLL accuracy in the tail region.

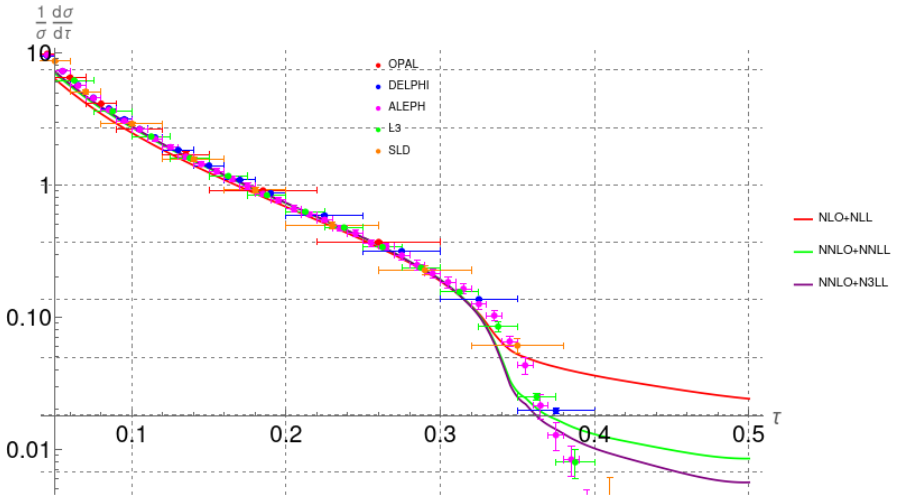

Figure 23: Log Plot of the matched Thrust distribution at NNLO+N^{3}LL and NNLO+NNLL accuracy in the tail region.

Chapter 4

Conclusions and Outlook

In this thesis, we have studied the resummation of QCD large infrared logarithms for the Thrust distribution in e^+e^- annihilation. The Thrust distribution is a classical precision observable in collider physics and it allows the extraction of the strong coupling constant α_s.

In the era of the LEP experiments(1989-2000) the calculations for certain classes of variables, such as event Thrust shape variable, were improved by resumming leading and next-to-leading logarithmic terms (NLL). These calculations, matched to fixed-order expressions, enlarged the kinematic range of applicability for α_s extractions and reduced the systematic theoretical uncertainty.

Our work aims to enhance these achievements by incorporating higher-order logarithmic terms in the resummation process and utilizing NNLO fixed-order calculations completed in 2007, which were unavailable during the LEP experiments.

Resummation tecniques are needed because in the kinematical region where the Thrust τ is close to 0, cancellations between real and virtual corrections are not complete due to kinematical constraints and large logarithms of the form $\alpha_s^n \log^m(\frac{1}{\tau})$ appear to spoil the convergence of the perturbative series. Therefore, resummation of these logarithms is needed to obtain a reliable theoretical prediction for the Thrust distribution in the region of small τ, then matching the resummed prediction with the fixed order calculation gives a prediction that is valid in a larger range of τ.

The theoretical prediction is made within perturbative QCD, expanded to a finite order in the coupling constant. The truncation of the perturbative series induces a theoretical uncertainty from omitting higher order terms. It can be quantified by the renormalisation scale dependence of the prediction, which is vanishing for an all-order prediction. The residual dependence on variations of the renormalisation scale is therefore an estimate of the theoretical error and we have observed that indeed the scale dependence

for the Laplace transformed thrust distribution at N^{3}LL accuracy is significantly reduced compared to the already improved N^{2}LL results. However, anomalies noted in N^{4}LL results suggest potential limitations in their reliability.

Initially, we calculated the resummation functions $f_i(\lambda)$ in Laplace space, where the natural exponentiation of the logarithms occurs. We were careful in ensuring consistency with prior findings and assembling necessary ingredients for resummation up to N^{4}LL accuracy from existing literature.

Subsequently, we performed the inverse Laplace transform of the resummed distribution following methodologies outlined by [1] and extended the results up to N^{4}LL accuracy. This has allowed us to obtain the resummed Thrust distribution in thrust space, which already gives us a shape closely resembling experimental data from LEP and SLAC. The predictions and data do not match completely yet because our prediction is calculated at parton (quarks and gluons) level and does not include hadronisation effects, while the experimental measurements are at the hadron (protons, pions, kaons, ...) level.

To refine our theoretical predictions further, we have matched the resummed expression to the fixed-order NNLO calculations at large values of τ using the R-matching scheme. The results presented in this thesis allow us to achieve NNLO+N^{3}LL accuracy. This represents a step towards achieving a more precise theoretical prediction for the Thrust distribution in e^+e^- annihilation and a more precise extraction of the strong coupling constant α_s, which is essential for the precision tests of the Standard Model and the search for new physics at the LHC.

Future endeavors will involve integrating a phenomenological model to address hadronization effects and conducting a fitting analysis with experimental data to accurately determine the strong coupling constant α_s. Additionally, it is also interesting to investigate if the analytical Laplace inversion used in the previous literature, which we reproduced and generalised to higher orders in this thesis gives us a reliable result. We observed that the peaks of the resummed Thrust distribution were too low compared to the experimental data, this would thus lead to a discrepancy in the extracted value of α_s relative to the world average.

Appendix A

Laplace transform in the large N limit

Using the methodology outlined in [24], we will demonstrate that the Mellin transform prescription is also applicable to the Laplace transform. in the large moment $\nu Q^2 = N$ limit, this fact was already known in the literature [30] and we'll show it here for completeness.

We are interested in solving the following integral

$$\int_0^1 \mathrm{d}z \, \frac{e^{-N(1-z)} - 1}{1-z} F(\alpha_s, \ln(1-z)) = \int_0^1 \frac{\mathrm{d}u}{u} \big(e^{-uN} - 1\big) F(\alpha_s, \ln u). \tag{110}$$

Start by considering

$$I_n(N) = \int_0^1 \frac{\mathrm{d}u}{u} \big(e^{-uN} - 1\big) \ln^n(u), \tag{111}$$

which can be evaluated as described in [31], using the following identity

$$\ln^n(u) = \lim_{\epsilon \to 0} \left(\frac{\partial}{\partial \epsilon}\right)^n u^\epsilon = \lim_{\epsilon \to 0} \left(\frac{\partial}{\partial \epsilon}\right)^n e^{\epsilon \ln u} \tag{112}$$

to replace the logarithm term in the integrand eq. (111) and straightforwardly integrate the resulting expression. We obtain

$$
\begin{aligned}
I_n(N) &= \lim_{\epsilon\to 0}\left(\frac{\partial}{\partial\epsilon}\right)^n \int_0^1 \mathrm{d}u\,\big(e^{-uN}-1\big)u^{\epsilon-1} \\
&= \lim_{\epsilon\to 0}\left(\frac{\partial}{\partial\epsilon}\right)^n \left\{-\frac{1}{\epsilon}+N^{-\epsilon}(\Gamma(\epsilon,0)-\Gamma(\epsilon,N))\right\} \\
&= \lim_{\epsilon\to 0}\lim_{N\to\infty}\left(\frac{\partial}{\partial\epsilon}\right)^n \left\{-\frac{1}{\epsilon}+N^{-\epsilon}\Gamma(\epsilon)\right\} + e^{-N+\mathcal{O}\left((\frac{1}{N})^2\right)}\mathcal{O}\left(\frac{1}{N}\right) \\
&= \lim_{\epsilon\to 0}\lim_{N\to\infty}\left(\frac{\partial}{\partial\epsilon}\right)^n \left\{\frac{1}{\epsilon}(N^{-\epsilon}\epsilon\Gamma(\epsilon)-1)\right\} + \mathcal{O}\left(\frac{e^{-N}}{N}\right) \\
&= \lim_{\epsilon\to 0}\lim_{N\to\infty}\left(\frac{\partial}{\partial\epsilon}\right)^n \left\{\frac{1}{\epsilon}(e^{-\epsilon\ln N}\Gamma(1+\epsilon)-1)\right\} + \mathcal{O}\left(\frac{e^{-N}}{N}\right),
\end{aligned}
\tag{113}
$$

where $\Gamma(\epsilon,0)=\Gamma(\epsilon)$, $\Gamma(\epsilon,N)$ is the incomplete Gamma function and $\epsilon\Gamma(\epsilon)=\Gamma(1+\epsilon)$

$$
\Gamma(\epsilon,N)=\int_N^\infty \mathrm{d}t\,t^{\epsilon-1}e^{-t}. \tag{114}
$$

The last equation in eq. (113) is the same as Eq. (68) obtained in [24] for the Mellin transform. Therefore, we can conclude that the Mellin transform prescription is also applicable to the Laplace transform in the large N limit.

Using the known expansion of the Gamma function for small ϵ

$$
\Gamma(1+\epsilon)=\exp\left\{-\gamma_E\epsilon+\sum_{n=2}^{\infty}(-1)^n\frac{\zeta(n)\epsilon^n}{n}\right\}, \tag{115}
$$

the term in curly brackets in eq. (115) can be expanded in power of ϵ and then derive. The result for $I_n(N)$ is thus a polynomial of degree $n+1$ in the large logarithm $\ln N$:

$$
\begin{aligned}
I_n(N) = {} & \frac{(-1)^n+1}{n+1}(\ln N+\gamma_E)^{n+1}+\frac{(-1)^{n-1}}{2}n\zeta(2)(\ln N+\gamma_E)^{n-1} \\
& +\sum_{k=0}^{n-2}a_{nk}(\ln N+\gamma_E)^k+\mathcal{O}\left(\frac{e^{-N}}{N}\right).
\end{aligned}
\tag{116}
$$

This result can be generalized using the following formal identity:

$$
e^{-\epsilon\ln N}\Gamma(1+\epsilon)=\Gamma\Big(1-\frac{\partial}{\partial\ln N}\Big)e^{\epsilon\ln N}, \tag{117}
$$

then we can perform the n-th derivative with respect to ϵ, and obtain

$$
I_n(N)=\Gamma\left(1-\frac{\partial}{\partial\ln N}\right)\frac{(-\ln N)^n+1}{n+1}+\mathcal{O}\left(\frac{e^{-N}}{N}\right). \tag{118}
$$

This expression can be regarded as a replacement for eq. (113) to compute the polynomial coefficients a_{nk} in eq. (116). Moreover, by observing that

$$\frac{(-\ln N)^n + 1}{n+1} = -\int_{\frac{1}{N}}^{1} \mathrm{d}u \, \frac{\ln^n(u)}{u}, \tag{119}$$

we obtain the all order generalization for of the prescriprion used in [1]:

$$e^{-uN} - 1 = -\Gamma\left(1 - \frac{\partial}{\partial \ln_N}\right)\Theta(u - \frac{1}{N}) + \mathcal{O}\left(\frac{e^{-N}}{N}\right) \tag{120}$$

$$= -\tilde{\Gamma}\left(1 - \frac{\partial}{\partial \ln_N}\right)\Theta(u - \frac{N_0}{N}) + \mathcal{O}\left(\frac{e^{-N}}{N}\right), \tag{121}$$

where

$$\tilde{\Gamma}(1-\epsilon) \equiv e^{\gamma_E \epsilon}\Gamma(1+\epsilon) = \exp\left\{\sum_{n=2}^{\infty}(-1)^n \frac{\zeta(n)\epsilon^n}{n}\right\}. \tag{122}$$

It is straightforward to show that the prescription can be applied to as follows:

$$\int_0^1 \frac{\mathrm{d}u}{u}\big(e^{-uN} - 1\big)F(\alpha_s, \ln u) = -\tilde{\Gamma}\left(1 - \frac{\partial}{\partial \ln_N}\right)\int_{\frac{N_0}{N}}^1 \frac{\mathrm{d}u}{u}F(\alpha_s, \ln u) + \mathcal{O}\left(\frac{e^{-N}}{N}\right), \tag{123}$$

and to evaluated the $\ln N$-contribution arising from the integration of any soft-gluon function F that has a generic perturbative expansion of the type

$$F(\alpha_s, \ln u) = \sum_{k=1}^{\infty}\alpha_s^k \sum_{n=0}^{2k-1} F_{kn} \ln^n u. \tag{124}$$

The result in eq. (123) can be used to obtain eq. (56) as shown in [24].

Appendix B

Equivalence between resummation formulae

Here we adapt the result in [24] to show the equivalence between the resummation formulae in eq. (24) and eq. (56) in the case of Thrust resummation.

It is straightforward to show that equation (90) in [24] becomes:

$$\begin{aligned}&\int_{N_0/N}^{1}\frac{\mathrm{d}u}{u}\frac{1}{2}\Big(\tilde{B}(\alpha_s(uQ^2))-B(\alpha_s(uQ^2))\Big)-\log\tilde{C}\bigg(\alpha_s(\mu^2),\frac{\mu^2}{Q^2}\bigg)=\\&\Gamma_2\bigg(\frac{\partial}{\partial\log N}\bigg)\bigg\{A(\alpha_s(\frac{N_0}{N}Q^2))-\frac{1}{2}\frac{\partial}{\partial\log N}B(\alpha_s(\frac{N_0}{N}Q^2))-2A(\alpha_s(\frac{N_0^2}{N^2}Q^2))\bigg\}.\end{aligned}\tag{125}$$

Observe that using the renormalization group equation eq. (27) and chain rule we can write the following relation:

$$\begin{aligned}\frac{\partial}{\partial\log N}B(\alpha_s(\frac{k}{N}))&=\frac{\partial B(\alpha_s)}{\partial\alpha_s}\frac{\partial\alpha_s(\frac{k}{N})}{\partial\frac{k}{N}}\frac{\partial\frac{k}{N}}{\partial\log N}=-\frac{\partial\alpha_s(\frac{k}{N})}{\partial\log\frac{k}{N}}\frac{\partial B(\alpha_s)}{\partial\alpha_s}\\&=-\beta(\alpha_s)\alpha_s\frac{\partial B(\alpha_s)}{\partial\alpha_s},\\\frac{\partial}{\partial\log N}A(\alpha_s(\frac{k}{N^2}))&=-2\beta(\alpha_s)\alpha_s\frac{\partial A(\alpha_s)}{\partial\alpha_s}.\end{aligned}\tag{126}$$

Define the differential operator $\partial(\alpha_s)$ as:

$$\partial_{\alpha_s}\equiv-\beta(\alpha_s)\alpha_s\frac{\partial}{\partial\alpha_s}.\tag{127}$$

Substituting the above relations in the previous equation, we obtain the equivalent of equation (92) in [24]:

$$\begin{aligned}&\int_{N_0/N}^{1}\frac{\mathrm{d}u}{u}\frac{1}{2}\Big(\tilde{B}(\alpha_s(uQ^2))-B(\alpha_s(uQ^2))\Big)-\log\tilde{C}\Big(\alpha_s(\mu^2),\frac{\mu^2}{Q^2}\Big)=\\&\Gamma_2(\partial_{\alpha_s})\Big\{A(\alpha_s(\frac{N_0}{N}Q^2))-\frac{1}{2}\partial_{\alpha_s}B(\alpha_s(\frac{N_0}{N}Q^2))\Big\}-2\Gamma(2\partial_{\alpha_s})A(\alpha_s(\frac{N_0^2}{N^2}Q^2)).\end{aligned}\tag{128}$$

Now by setting $N=N_0$ or applying $\frac{\partial}{\partial\log N}$ one obtains respectively the functions $\tilde{C}$ and $\tilde{B}$ as functions of A and B:

$$\tilde{C}(\alpha_s)=\exp\Big\{-\Gamma_2(\partial_{\alpha_s})\Big[A(\alpha_s)-\frac{1}{2}\partial_{\alpha_s}B(\alpha_s)\Big]-2\Gamma(2\partial_{\alpha_s})A(\alpha_s)\Big\}\Big|_{\alpha_s=\alpha_s(Q^2)},\tag{129}$$

$$\begin{aligned}\frac{\tilde{B}(\alpha_s)}{2}=\frac{B(\alpha_s)}{2}&+\partial_{\alpha_s}\Big\{\Gamma_2(\partial_{\alpha_s})\Big[A(\alpha_s)-\frac{1}{2}\partial_{\alpha_s}B(\alpha_s)\Big]\Big\}\Big|_{\alpha_s=\alpha_s\left(\frac{N_0}{N}Q^2\right)}\\&-4\partial_{\alpha_s}\{\Gamma_s(2\partial_{\alpha_s})A(\alpha_s)\}\Big|_{\alpha_s=\alpha_s\left(\frac{N_0^2}{N^2}Q^2\right)}.\end{aligned}\tag{130}$$

With eqs. (129) and (130) one can relate the two formulas in eq. (24) and eq. (56), *e.g.* $\log\tilde{C}$ can be obtained by inserting the expansion:

$$\begin{aligned}\Gamma_2(\epsilon)=&-\frac{1}{2}\zeta(2)-\frac{1}{3}\zeta(3)\epsilon-\frac{9}{16}\zeta(4)\epsilon^2-\Big(\frac{1}{6}\zeta(2)\zeta(3)+\frac{1}{5}\zeta(5)\Big)\epsilon^3\\&-\Big(\frac{1}{18}\zeta(3)^2-\frac{61}{128}\zeta(6)\Big)\epsilon^4+\mathcal{O}\big(\epsilon^5\big)\end{aligned}\tag{131}$$

in eq. (129), and up to N^{4}LL accuracy we have:

$$\begin{aligned}\log\tilde{C}\left(\alpha_s(\mu^2),\frac{\mu^2}{Q^2}\right) &= \frac{A_1}{\pi}(-\zeta(2)-1)\alpha_s + \Bigg(\frac{-2A_2\zeta(2)-2A_2+\pi b_0 B_1}{2\pi^2}\\ &+ \frac{A_1 b_0\left(3\zeta(2)\log\left(\frac{\mu^2}{Q^2}\right)+3\log\left(\frac{\mu^2}{Q^2}\right)-4\zeta(3)\right)}{3\pi}\Bigg)\alpha_s^2\\ &+ \Bigg(\frac{A_1}{3\pi}\Big(-27b_0^2\zeta(4)-3b_0^2\zeta(2)\log^2\left(\frac{\mu^2}{Q^2}\right)-3b_0^2\log^2\left(\frac{\mu^2}{Q^2}\right)\\ &+ 8b_0^2\zeta(3)\log\left(\frac{\mu^2}{Q^2}\right)+3b_1\zeta(2)\log\left(\frac{\mu^2}{Q^2}\right)+3b_1\log\left(\frac{\mu^2}{Q^2}\right)\\ &- 4b_1\zeta(3)\Big)-\frac{1}{6\pi^3}\Big(-12\pi A_2 b_0\zeta(2)\log\left(\frac{\mu^2}{Q^2}\right)\\ &- 12\pi A_2 b_0\log\left(\frac{\mu^2}{Q^2}\right)+16\pi A_2 b_0\zeta(3)+6A_3\zeta(2)+6A_3\\ &+ 6\pi^2 b_0^2 B_1\log\left(\frac{\mu^2}{Q^2}\right)-6\pi b_0 B_2-3\pi^2 b_1 B_1\Big)\Bigg)\alpha_s^3+\mathcal{O}\big(\alpha_s^4\big).\end{aligned} \tag{132}$$

For $\tilde{B}$ we'll have to use renormalization group equation to evolve the two scale $\frac{N_0}{N}Q^2$ and $\frac{N_0^2}{N^2}Q^2$ to a common scale Q^2. We note that $\tilde{B}$ corrects the B terms so it has to be expanded up to α_s^4 to achieve N^{4}LL accuracy while $\ln\tilde{C}$ corrects the f_i functions so they have to be expanded up to α_s^3 to achieve N^{4}LL accuracy, these corrections are necessary only for NNLL accuracy and beyond, consistent with the results in [1].

Appendix C

Constants and Ingredients for Resummation

The needed coefficients are often expressed in terms of the following parameters:

$$
\begin{aligned}
n_f &= 5 && \text{Number of active flavors,} \\
C_F &= \frac{4}{3} && \text{Quadratic Casimir operator for fundamental representation,} \\
C_A &= 3 && \text{Quadratic Casimir operator for adjoint representation,} \\
T_R &= \frac{1}{2} && \text{Trace normalization for fundamental representation.}
\end{aligned}
\tag{133}
$$

The renormalization group equation for the QCD coupling constant reads:

$$
\mu^2 \frac{\mathrm{d}\alpha_s}{\mathrm{d}\mu^2} = \beta(\alpha_s) = -\alpha_s^2\big(b_0 + b_1\alpha_s + b_2\alpha_s^2 + \dots\big), \tag{134}
$$

where the coefficients of the $\beta(\alpha_s)$ functions are [21]:

$$
\begin{aligned}
b_0 &= \frac{11C_A - 4n_f T_R}{12\pi} = \frac{33 - 2n_f}{12\pi}, \\
b_1 &= \frac{17C_A^2 - n_f T_R(10C_A + 6C_F)}{24\pi^2} = \frac{153 - 19n_f}{24\pi^2}, \\
b_2 &= \frac{325n_f^2}{3456\pi^3} - \frac{5033n_f}{1152\pi^3} + \frac{2857}{128\pi^3}, \\
b_3 &= \frac{1093n_f^3}{186624\pi^4} + n_f^2\left(\frac{809\zeta(3)}{2592\pi^4} + \frac{50065}{41472\pi^4}\right) + n_f\left(-\frac{1627\zeta(3)}{1728\pi^4} - \frac{1078361}{41472\pi^4}\right)
\end{aligned}
$$

$$
\begin{aligned}
&+\frac{891\zeta(3)}{64\pi^4}+\frac{149753}{1536\pi^4},\\
b_4 &= n_f^4\left(\frac{1205}{2985984\pi^5}-\frac{19\zeta(3)}{10368\pi^5}\right)\\
&+n_f^3\left(-\frac{24361\zeta(3)}{124416\pi^5}+\frac{115\zeta(5)}{2304\pi^5}+\frac{809}{1244160\pi}-\frac{630559}{5971968\pi^5}\right)\\
&+n_f^2\left(\frac{698531\zeta(3)}{82944\pi^5}-\frac{5965\zeta(5)}{1296\pi^5}-\frac{5263}{414720\pi}+\frac{25960913}{1990656\pi^5}\right)\\
&+n_f\left(-\frac{1202791\zeta(3)}{20736\pi^5}+\frac{1358995\zeta(5)}{27648\pi^5}+\frac{6787}{110592\pi}-\frac{336460813}{1990656\pi^5}\right)\\
&+\frac{621885\zeta(3)}{2048\pi^5}-\frac{144045\zeta(5)}{512\pi^5}-\frac{9801}{20480\pi}+\frac{8157455}{16384\pi^5}.
\end{aligned}
\tag{135}
$$

Numerically, for $n_f = 5$:

$$
\begin{aligned}
b_0 &= 0.875352 - 0.0530516 n_f = \frac{23}{12\pi} = 0.610094,\\
b_1 &= 0.645923 - 0.0802126 n_f = \frac{29}{12\pi^2} = 0.24486,\\
b_2 &= 0.719864 - 0.140904 n_f + 0.00303291 n_f^2 = \frac{9769}{3456\pi^3} = 0.0911647,\\
b_3 &= 1.17269 - 0.278557 n_f + 0.0162447 n_f^2 + 0.0000601247 n_f^3 = 0.193536,\\
b_4 &= 1.71413 - 0.594075 n_f + 0.0560618 n_f^2 - 0.000738048 n_f^3 - 5.87966\cdot 10^{-6} n_f^4 = 0.0493694.
\end{aligned}
\tag{136}
$$

The A coefficient in the resummation formula are given by:

$$A_1 = C_F, \tag{137}$$

$$A_2 = \frac{1}{2}C_A C_F\left(-\frac{1}{27}10 n_f T_R - \frac{\pi^2}{6}+\frac{67}{18}\right), \tag{138}$$

$$
\begin{aligned}
A_3 &= \left(-\frac{2051}{1296}-\frac{\pi^2}{18}\right)C_A C_F n_f + \left(-\frac{11\zeta(3)}{4}+\frac{11\pi^4}{720}-\frac{13\pi^2}{432}+\frac{15503}{2592}\right)C_A^2 C_F\\
&+\left(\frac{\zeta(3)}{2}-\frac{55}{96}\right)C_F^2 n_f + \left(\frac{25}{324}+\frac{\pi^2}{108}\right)C_F n_f^2,
\end{aligned}
\tag{139}
$$

$$
\begin{aligned}
A_4 &= \Big(-\frac{\zeta(3)^2}{16}+\frac{11\pi^2\zeta(3)}{32}-\frac{24461\zeta(3)}{864}+\frac{20513\pi^2}{5184}+\frac{1925\zeta(5)}{288}-\frac{253\pi^4}{1920}-\frac{313\pi^6}{90720}\\
&+\frac{4311229}{186624}\Big)C_F C_A^3 + \Big(\frac{7\pi^2\zeta(3)}{72}+\frac{43\zeta(3)}{144}+\frac{451\pi^4}{4320}+\frac{131\zeta(5)}{144}\\
&+T_R\left(-\frac{1}{72}11\pi^2\zeta(3)+\frac{685\zeta(3)}{48}-3\zeta(5)-\frac{11\pi^4}{144}-\frac{1123}{162}-\frac{12247\pi^2}{15552}\right)\\
&-\frac{64421\pi^2}{31104}-\frac{260731}{62208}\Big)C_F n_f C_A^2 + \Big(\Big(\Big(\frac{34\zeta(3)}{9}+\frac{11\pi^4}{720}+\frac{55\pi^2}{576}-\frac{7351}{1152}\Big)T_R - \frac{\pi^2\zeta(3)}{12}
\end{aligned}
\tag{140}
$$

$$+\frac{29\zeta(3)}{18}+\frac{5\zeta(5)}{8}-\frac{55\pi^2}{1152}-\frac{11\pi^4}{1440}-\frac{17033}{10368}\Big)n_f C_F^2$$
$$+\Big(\Big(-\frac{7\zeta(3)}{54}+\frac{\pi^4}{60}-\frac{481\pi^2}{1944}+\frac{1747}{3888}\Big)T_R^2+\Big(-\frac{143\zeta(3)}{108}+\frac{847\pi^2}{1296}+\frac{55}{486}\Big)T_R+\frac{803\pi^2}{3888}$$
$$-\frac{\zeta(3)}{144}-\frac{49\pi^4}{4320}+\frac{19889}{62208}\Big)n_f^2 C_F\Big)C_A+\frac{31\pi^6}{60480}+\Big(\Big(-\frac{7\zeta(3)}{27}+\frac{5\pi^2}{324}+\frac{130}{729}\Big)T_R^3$$
$$+\Big(\frac{13\zeta(3)}{108}-\frac{5}{486}-\frac{77\pi^2}{1296}\Big)T_R+\frac{\zeta(3)}{108}-\frac{1}{648}\Big)C_F n_f^3+\frac{\pi^2}{96}+\Big(\Big(-\frac{19\zeta(3)}{18}+\frac{215}{96}-\frac{5\pi^2}{144}$$
$$-\frac{\pi^4}{180}\Big)T_R^2+\frac{\pi^4}{720}+\frac{5\pi^2}{192}-\frac{5\zeta(3)}{18}+\frac{299}{2592}\Big)C_F^2 n_f^2+\frac{3\zeta(3)^2}{16}$$
$$+81\left(-\frac{\zeta(3)^2}{32}+\frac{\zeta(3)}{288}+\frac{55\zeta(5)}{576}-\frac{\pi^2}{576}-\frac{31\pi^6}{362880}\right)$$
$$+9\left(-\frac{5\zeta(3)^2}{32}+\frac{5\zeta(3)}{288}+\frac{275\zeta(5)}{576}-\frac{5\pi^2}{576}-\frac{31\pi^6}{72576}\right)+\Big(\Big(\frac{37\zeta(3)}{48}-\frac{5\zeta(5)}{4}+\frac{143}{576}\Big)C_F^3$$
$$+\frac{1}{3}\left(-\frac{\zeta(3)}{12}+\frac{\pi^2}{24}-\frac{5\zeta(5)}{12}\right)+\frac{1}{27}\left(\frac{\zeta(3)}{16}+\frac{5\zeta(5)}{16}-\frac{\pi^2}{32}\right)+3\left(\frac{7\zeta(3)}{288}+\frac{35\zeta(5)}{288}-\frac{7\pi^2}{576}\right)$$
$$+27\left(-\frac{\zeta(3)}{288}+\frac{\pi^2}{576}-\frac{5\zeta(5)}{288}\right)\Big)n_f-\frac{\zeta(3)}{48}-\frac{55\zeta(5)}{96},$$

$$A_5 = 14541.099. \tag{141}$$

The B coefficients are given by:

$$B_1 = -\frac{1}{2}\left(3C_F\right), \tag{142}$$

$$B_2 = C_A C_F\left(\frac{3\zeta(3)}{2}-\frac{57}{16}+\frac{11\pi^2}{24}\right)+C_F n_f\left(\frac{5}{8}-\frac{\pi^2}{12}\right)+C_F^2\left(-3\zeta(3)-\frac{3}{16}+\frac{\pi^2}{4}\right), \tag{143}$$

$$B_3 = C_A C_F n_f\Big(\Big(\frac{34\zeta(3)}{27}-\frac{485\pi^2}{432}-\frac{\pi^4}{720}+\frac{3683}{864}\Big)T_R+\frac{31\zeta(3)}{54}+\frac{131\pi^4}{4320}+\frac{5261}{1728}$$
$$-\frac{2657\pi^2}{2592}\Big)+C_A C_F^2\left(-\frac{\pi^2\zeta(3)}{12}-\frac{89\zeta(3)}{12}-\frac{15\zeta(5)}{4}+\frac{287\pi^2}{192}-\frac{23}{16}-\frac{17\pi^4}{360}\right) \tag{144}$$
$$+C_A^2 C_F\left(\frac{241\zeta(3)}{108}-\frac{5\zeta(5)}{4}+\frac{22841\pi^2}{5184}-\frac{5951}{432}-\frac{713\pi^4}{4320}\right)+C_F^2 n_f\Big(\Big(\frac{17\zeta(3)}{6}+\frac{23}{16}-$$
$$\frac{5\pi^2}{72}-\frac{29\pi^4}{1080}\Big)T_R-\frac{\zeta(3)}{4}+\frac{41\pi^4}{2160}+\frac{31}{64}-\frac{71\pi^2}{288}\Big)+C_F n_f^2\Big(\Big(\frac{2\zeta(3)}{9}+\frac{17}{72}-\frac{5\pi^2}{81}\Big)T_R^2+$$
$$\Big(-\frac{13\zeta(3)}{27}+\frac{193\pi^2}{648}-\frac{433}{432}\Big)T_R\Big)+\Big(\frac{\pi^2\zeta(3)}{6}-\frac{17\zeta(3)}{8}+\frac{15\zeta(5)}{2}-\frac{\pi^4}{20}-\frac{3\pi^2}{32}-\frac{29}{64}\Big)C_F^3,$$

$$B_4 = 3817.42. \tag{145}$$

By expanding in α_s the exponent of eq. (19) with eqs. (102) to (106) substituted, we can compare to the expression eq. (17) and obtain:

$$
\begin{aligned}
G_{12} &= -2A_1, \\
G_{11} &= -2B_1, \\
G_{23} &= -4\pi A_1 b_0, \\
G_{22} &= \frac{2}{3}\left(-2\pi^2 A_1^2 - 6A_2 - 3\pi b_0 B_1\right), \\
G_{21} &= \frac{2}{3}\left(-A_1\left(24A_1\zeta(3) - 3\pi^3 b_0 + 2\pi^2 B_1\right) - 6B_2\right), \\
G_{34} &= \frac{1}{3}(-28)\pi^2 A_1 b_0^2, \\
G_{33} &= \frac{4}{45}\left(-90\pi^3 A_1^2 b_0 - 90\pi^2 A_1 b_1 - 180\pi A_2 b_0 + 240A_1^3\zeta(3) - 30\pi^2 b_0^2 B_1\right), \\
G_{32} &= \frac{4}{45}\Big(-75\pi^3 A_1 b_0 B_1 - 1620\pi A_1^2 b_0\zeta(3) + 105\pi^4 A_1 b_0^2 + 360A_1^2 B_1\zeta(3) + 2\pi^4 A_1^3 - 60\pi^2 A_2 A_1 \\
&\quad - 90A_3 - 45\pi^2 b_1 B_1 - 90\pi b_0 B_2\Big), \\
G_{31} &= \frac{4}{45}\Big(-900\pi A_1 b_0 B_1\zeta(3) + 840\pi^2 A_1 b_0^2\zeta(3) + 45\pi^4 A_1 b_1 + 90\pi^3 A_2 b_0 + 180A_1 B_1^2\zeta(3) \\
&\quad + 2\pi^4 A_1^2 B_1 - 30\pi^2 A_1 B_2 - 30\pi^2 A_2 B_1 - 240\pi^2 A_1^3\zeta(3) + 2160A_1^3\zeta(5) - 720A_2 A_1\zeta(3) \\
&\quad - 15\pi^3 b_0 B_1^2 + 15\pi^4 b_0^2 B_1 - 90B_3\Big), \\
G_{45} &= -24\pi^3 A_1 b_0^3, \\
G_{44} &= 192\pi A_1^3 b_0\zeta(3) - \frac{332}{9}\pi^4 A_1^2 b_0^2 - \frac{140}{3}\pi^3 A_1 b_0 b_1 - 56\pi^2 A_2 b_0^2 + \frac{1}{45}(-32)\pi^4 A_1^4 - 4\pi^3 b_0^3 B_1, \\
G_{43} &= 256\pi A_1^2 b_0 B_1\zeta(3) - \frac{232}{9}\pi^4 A_1 b_0^2 B_1 - \frac{2656}{3}\pi^2 A_1^2 b_0^2\zeta(3) + \frac{32}{15}\pi^5 A_1^3 b_0 \\
&\quad - 16\pi^4 A_1^2 b_1 + 40\pi^5 A_1 b_0^3 - 48\pi^3 A_2 A_1 b_0 - 16\pi^3 A_1 b_2 - 48\pi A_3 b_0 - 32\pi^2 A_2 b_1 - \frac{64}{45}\pi^4 A_1^3 B_1 \\
&\quad + \frac{128}{3}\pi^2 A_1^4\zeta(3) - 512A_1^4\zeta(5) + 128A_2 A_1^2\zeta(3) - \frac{40}{3}\pi^3 b_0 b_1 B_1 - 16\pi^2 b_0^2 B_2, \\
G_{42} &= 112\pi A_1 b_0 B_1^2\zeta(3) - 464\pi^2 A_1 b_0^2 B_1\zeta(3) + \frac{32}{15}\pi^5 A_1^2 b_0 B_1 - \frac{40}{3}\pi^4 A_1 b_1 B_1 \\
&\quad - \frac{56}{3}\pi^3 A_1 b_0 B_2 - \frac{64}{3}\pi^3 A_2 b_0 B_1 - 416\pi^3 A_1^3 b_0\zeta(3) + 3648\pi A_1^3 b_0\zeta(5) - 288\pi^2 A_1^2 b_1\zeta(3) \\
&\quad + 480\pi^3 A_1 b_0^3\zeta(3) - 864\pi A_2 A_1 b_0\zeta(3) + \frac{56}{45}\pi^6 A_1^2 b_0^2 + \frac{140}{3}\pi^5 A_1 b_0 b_1 + 56\pi^4 A_2 b_0^2 \\
&\quad + 64\pi^2 A_1^3 B_1\zeta(3) - 768A_1^3 B_1\zeta(5) + 64A_1^2 B_2\zeta(3) + 128A_2 A_1 B_1\zeta(3) - \frac{16}{15}\pi^4 A_1^2 B_1^2 \\
&\quad + 512A_1^4\zeta(3)^2 + \frac{1}{945}(-464)\pi^6 A_1^4 + \frac{16}{15}\pi^4 A_2 A_1^2 - \frac{32}{3}\pi^2 A_3 A_1 - \frac{16}{3}\pi^2 A_2^2 \\
&\quad - 16A_4 - 4\pi^4 b_0^2 B_1^2 + 4\pi^5 b_0^3 B_1 - 8\pi^3 b_2 B_1 - 16\pi^2 b_1 B_2 - 24\pi b_0 B_3,
\end{aligned}
$$

$$
\begin{aligned}
G_{41} = &-120\pi A_1^3 b_0 \gamma^6 + \frac{64}{3}\pi^2 A_1^4 \gamma^5 + \frac{368}{3}\pi^2 A_1^2 b_0^2 \gamma^5 - 16 A_1^2 A_2 \gamma^5 - 56\pi A_1^2 b_0 B_1 \gamma^5 + \frac{460}{3}\pi^3 A_1^3 b_0 \gamma^4 \\
&+ \frac{40}{3}\pi^2 A_1^3 B_1 \gamma^4 - 480 A_1^4 \zeta(3)\gamma^4 - \frac{32}{9}\pi^4 A_1^4 \gamma^3 - \frac{1840}{9}\pi^4 A_1^2 b_0^2 \gamma^3 + \frac{80}{3}\pi^2 A_1^2 A_2 \gamma^3 \\
&+ \frac{280}{3}\pi^3 A_1^2 b_0 B_1 \gamma^3 - 1280\pi A_1^3 b_0 \zeta(3)\gamma^3 - 320 A_1^3 B_1 \zeta(3)\gamma^3 - \frac{2}{3}\pi^5 A_1^3 b_0 \gamma^2 - \frac{8}{3}\pi^4 A_1^3 B_1 \gamma^2 \\
&+ \frac{800}{3}\pi^2 A_1^4 \zeta(3)\gamma^2 + \frac{7360}{3}\pi^2 A_1^2 b_0^2 \zeta(3)\gamma^2 - 320 A_1^2 A_2 \zeta(3)\gamma^2 - 1120\pi A_1^2 b_0 B_1 \zeta(3)\gamma^2 \\
&- 1920 A_1^4 \zeta(5)\gamma^2 + \frac{92}{9}\pi^6 A_1^2 b_0^2 \gamma - \frac{4}{3}\pi^4 A_1^2 A_2 \gamma - \frac{14}{3}\pi^5 A_1^2 b_0 B_1 \gamma - \frac{1600}{3}\pi^3 A_1^3 b_0 \zeta(3)\gamma \\
&+ \frac{800}{3}\pi^2 A_1^3 B_1 \zeta(3)\gamma + 3840\pi A_1^3 b_0 \zeta(5)\gamma - 1920 A_1^3 B_1 \zeta(5)\gamma - 2\pi^7 A_1 b_0^3 - \frac{16}{45}\pi^4 A_1 B_1^3 \\
&+ \frac{28}{45}\pi^5 A_1 b_0 B_1^2 - \frac{8}{3}\pi^4 b_1 B_1^2 + 128\pi A_1^3 b_0 \zeta(3)^2 - 128 A_1^3 B_1 \zeta(3)^2 - \frac{1}{15}\pi^7 A_1^3 b_0 \\
&+ 24\pi^3 A_3 b_0 + 16\pi^4 A_2 b_1 + 8\pi^5 A_1 b_2 - \frac{2}{135}\pi^6 A_1^3 B_1 + \frac{56}{45}\pi^6 A_1 b_0^2 B_1 + \frac{32}{45}\pi^4 A_1 A_2 B_1 \\
&- \frac{16}{3}\pi^2 A_3 B_1 + \frac{20}{3}\pi^5 b_0 b_1 B_1 + \frac{16}{45}\pi^4 A_1^2 B_2 + 8\pi^4 b_0^2 B_2 - \frac{16}{3}\pi^2 A_2 B_2 - 8\pi^3 b_0 B_1 B_2 \\
&- \frac{16}{3}\pi^2 A_1 B_3 - 16 B_4 + \frac{344}{45}\pi^4 A_1^4 \zeta(3) + 16\pi b_0 B_1^3 \zeta(3) - 64 A_2^2 \zeta(3) + \frac{752}{9}\pi^4 A_1^2 b_0^2 \zeta(3) \\
&+ 448\pi^2 A_2 b_0^2 \zeta(3) + 32\pi^2 A_1^2 B_1^2 \zeta(3) - 48\pi^2 b_0^2 B_1^2 \zeta(3) + 32 A_2 B_1^2 \zeta(3) - \frac{224}{3}\pi^2 A_1^2 A_2 \zeta(3) \\
&- 128 A_1 A_3 \zeta(3) + \frac{1120}{3}\pi^3 A_1 b_0 b_1 \zeta(3) + 32\pi^3 b_0^3 B_1 \zeta(3) - \frac{304}{3}\pi^3 A_1^2 b_0 B_1 \zeta(3) \\
&- 256\pi A_2 b_0 B_1 \zeta(3) - 160\pi^2 A_1 b_1 B_1 \zeta(3) - 224\pi A_1 b_0 B_2 \zeta(3) + 64 A_1 B_1 B_2 \zeta(3) \\
&- 64\pi^2 A_1^4 \zeta(5) - 896\pi^2 A_1^2 b_0^2 \zeta(5) - 384 A_1^2 B_1^2 \zeta(5) + 768 A_1^2 A_2 \zeta(5) + 1152\pi A_1^2 b_0 B_1 \zeta(5).
\end{aligned}
\tag{146}
$$

Bibliography

[1] S. Catani, L. Trentadue, G. Turnock, and B. Webber, "Resummation of large logarithms in e+e- event shape distributions," *Nuclear Physics B*, vol. 407, no. 1, pp. 3–42, 1993, ISSN: 0550-3213. DOI: https://doi.org/10.1016/0550-3213(93)90271-P. [Online]. Available: https://www.sciencedirect.com/science/article/pii/055032139390271P.

[2] R. K. Ellis, D. A. Ross, and A. E. Terrano, "The Perturbative Calculation of Jet Structure in e+ e- Annihilation," *Nucl. Phys. B*, vol. 178, pp. 421–456, 1981. DOI: 10.1016/0550-3213(81)90165-6.

[3] A. Gehrmann-De Ridder, T. Gehrmann, E. W. N. Glover, and G. Heinrich, "Second-order QCD corrections to the thrust distribution," *Phys. Rev. Lett.*, vol. 99, p. 132 002, 2007. DOI: 10.1103/PhysRevLett.99.132002. arXiv: 0707.1285 [hep-ph].

[4] G. Dissertori, A. G.-D. Ridder, T. Gehrmann, E. Glover, G. Heinrich, and H. Stenzel, "First determination of the strong coupling constant using nnlo predictions for hadronic event shapes in e+e−annihilations," *Journal of High Energy Physics*, vol. 2008, no. 02, pp. 040–040, Feb. 2008, ISSN: 1029-8479. DOI: 10.1088/1126-6708/2008/02/040. [Online]. Available: http://dx.doi.org/10.1088/1126-6708/2008/02/040.

[5] P. F. Monni, T. Gehrmann, and G. Luisoni, "Two-Loop Soft Corrections and Resummation of the Thrust Distribution in the Dijet Region," *JHEP*, vol. 08, p. 010, 2011. DOI: 10.1007/JHEP08(2011)010. arXiv: 1105.4560 [hep-ph].

[6] S. Weinzierl, "Event shapes and jet rates in electron-positron annihilation at nnlo," *Journal of High Energy Physics*, vol. 2009, no. 06, pp. 041–041, Jun. 2009, ISSN: 1029-8479. DOI: 10.1088/1126-6708/2009/06/041. [Online]. Available: http://dx.doi.org/10.1088/1126-6708/2009/06/041.

[7] "Measurement of event shape distributions and moments in $e^+e^- \to \mathrm{hadrons}$ at 91-209 gev and a determination of α_s," *The European Physical Journal C*, vol. 40, no. 3, Apr. 2005, ISSN: 1434-6052. DOI: 10.1140/epjc/s2005-02120-6. [Online]. Available: http://dx.doi.org/10.1140/epjc/s2005-02120-6.

[8] P. Abreu *et al.*, "Consistent measurements of alpha(s) from precise oriented event shape distributions," *Eur. Phys. J. C*, vol. 14, pp. 557–584, 2000. DOI: 10.1007/s100520000354. arXiv: hep-ex/0002026.

[9] DELPHI Collaboration, *Consistent measurements of alpha(s) from precise oriented event shape distributions.* HEPData (collection), https://doi.org/10.17182/hepdata.13245, 2000.

[10] A. Heister *et al.*, "Studies of QCD at e+ e- centre-of-mass energies between 91-GeV and 209-GeV," *Eur. Phys. J. C*, vol. 35, pp. 457–486, 2004. DOI: 10.1140/epjc/s2004-01891-4.

[11] ALEPH Collaboration, *Studies of QCD at e+ e- centre-of-mass energies between 91-GeV and 209-GeV.* HEPData (collection), https://doi.org/10.17182/hepdata.12794, 2004.

[12] P. Achard, O. Adriani, M. Aguilar-Benitez, *et al.*, "Studies of hadronic event structure in e+e- annihilation from 30 to 209gev with the l3 detector," *Physics Reports*, vol. 399, no. 2-3, pp. 71–174, Sep. 2004, ISSN: 0370-1573. DOI: 10.1016/j.physrep.2004.07.002. [Online]. Available: http://dx.doi.org/10.1016/j.physrep.2004.07.002.

[13] K. Abe, I. Abt, C. J. Ahn, *et al.*, "Measurement of of $\alpha_s(M_Z^2)$ from hadronic event observables at the Z_0 resonance," *Physical Review D*, vol. 51, no. 3, pp. 962–984, Feb. 1995, ISSN: 0556-2821. DOI: 10.1103/physrevd.51.962. [Online]. Available: http://dx.doi.org/10.1103/PhysRevD.51.962.

[14] S. Catani, "Higher-order qcd corrections in hadron collisions: Soft-gluon resummation and exponentiation," *Nuclear Physics B - Proceedings Supplements*, vol. 54, no. 1–2, pp. 107–113, Mar. 1997, ISSN: 0920-5632. DOI: 10.1016/s0920-5632(97)00024-8. [Online]. Available: http://dx.doi.org/10.1016/S0920-5632(97)00024-8.

[15] S. Catani, *Soft-gluon resummation: A short review*, 1997. arXiv: hep-ph/9709503 [hep-ph].

[16] S. Catani, G. Turnock, B. Webber, and L. Trentadue, "Thrust distribution in e+e- annihilation," *Physics Letters B*, vol. 263, no. 3, pp. 491–497, 1991, ISSN: 0370-2693. DOI: https://doi.org/10.1016/0370-2693(91)90494-B. [Online]. Available: https://www.sciencedirect.com/science/article/pii/037026939190494B.

[17] G. F. Sterman, "Summation of Large Corrections to Short Distance Hadronic Cross-Sections," *Nucl. Phys. B*, vol. 281, pp. 310–364, 1987. DOI: 10.1016/0550-3213(87)90258-6.

[18] F. Bloch and A. Nordsieck, "Note on the radiation field of the electron," *Phys. Rev.*, vol. 52, pp. 54–59, 2 Jul. 1937. DOI: 10.1103/PhysRev.52.54.

[19] T. Kinoshita, "Mass singularities of Feynman amplitudes," *J. Math. Phys.*, vol. 3, pp. 650–677, 1962. DOI: 10.1063/1.1724268.

[20] T. D. Lee and M. Nauenberg, "Degenerate Systems and Mass Singularities," *Phys. Rev.*, vol. 133, G. Feinberg, Ed., B1549–B1562, 1964. DOI: 10.1103/PhysRev.133.B1549.

[21] F. Herzog, B. Ruijl, T. Ueda, J. A. M. Vermaseren, and A. Vogt, "The five-loop beta function of yang-mills theory with fermions," *Journal of High Energy Physics*, vol. 2017, no. 2, Feb. 2017, ISSN: 1029-8479. DOI: 10.1007/jhep02(2017)090. [Online]. Available: http://dx.doi.org/10.1007/JHEP02(2017)090.

[22] W. R. Inc., *Mathematica, Version 13.3*, Champaign, IL, 2023.

[23] P. D. Group, R. L. Workman, V. D. Burkert, *et al.*, "Review of Particle Physics," *Progress of Theoretical and Experimental Physics*, vol. 2022, no. 8, p. 083C01, Aug. 2022, ISSN: 2050-3911. DOI: 10.1093/ptep/ptac097. eprint: https://academic.oup.com/ptep/article-pdf/2022/8/083C01/49175539/ptac097.pdf. [Online]. Available: https://doi.org/10.1093/ptep/ptac097.

[24] S. Catani, D. d. Florian, M. Grazzini, and P. Nason, "Soft-gluon resummation for higgs boson production at hadron colliders," *Journal of High Energy Physics*, vol. 2003, no. 07, pp. 028–028, Jul. 2003, ISSN: 1029-8479. DOI: 10.1088/1126-6708/2003/07/028. [Online]. Available: http://dx.doi.org/10.1088/1126-6708/2003/07/028.

[25] U. Aglietti, G. Ricciardi, and G. Ferrera, "Threshold resummed spectra in B —> X(u) l nu decays in NLO. I," *Phys. Rev. D*, vol. 74, p. 034 004, 2006. DOI: 10.1103/PhysRevD.74.034004. arXiv: hep-ph/0507285.

[26] T. Becher and M. D. Schwartz, "A precise determination of α_s from lep thrust data using effective field theory," *Journal of High Energy Physics*, vol. 2008, no. 07, pp. 034–034, Jul. 2008, ISSN: 1029-8479. DOI: 10.1088/1126-6708/2008/07/034. [Online]. Available: http://dx.doi.org/10.1088/1126-6708/2008/07/034.

[27] W.-L. Ju, Y. Xu, L. L. Yang, and B. Zhou, "Thrust distribution in higgs decays up to the fifth logarithmic order," *Physical Review D*, vol. 107, no. 11, Jun. 2023, ISSN: 2470-0029. DOI: 10.1103/physrevd.107.114034. [Online]. Available: http://dx.doi.org/10.1103/PhysRevD.107.114034.

[28] A. Chakraborty, T. Huber, R. N. Lee, *et al.*, *The $Hb\bar{b}$ vertex at four loops and hard matching coefficients in scet for various currents*, 2022. arXiv: 2204.02422 [hep-ph]. [Online]. Available: https://arxiv.org/abs/2204.02422.

[29] U. Aglietti and G. Ricciardi, "Approximate NNLO threshold resummation in heavy flavor decays," *Phys. Rev. D*, vol. 66, p. 074 003, 2002. DOI: 10.1103/PhysRevD.66.074003. arXiv: hep-ph/0204125.

[30] S. Catani, B. Webber, and G. Marchesini, "Qcd coherent branching and semi-inclusive processes at large χ," *Nuclear Physics B*, vol. 349, no. 3, pp. 635–654, 1991, ISSN: 0550-3213. DOI: https://doi.org/10.1016/0550-3213(91)90390-J. [Online]. Available: https://www.sciencedirect.com/science/article/pii/055032139190390J.

[31] S. Catani and L. Trentadue, "Resummation of the qcd perturbative series for hard processes," *Nuclear Physics B*, vol. 327, no. 2, pp. 323–352, 1989, ISSN: 0550-3213. DOI: https://doi.org/10.1016/0550-3213(89)90273-3. [Online]. Available: https://www.sciencedirect.com/science/article/pii/0550321389902733.